HW-76300

UC-25, Metals, Ceramics,
and Materials
(TID-4500, 19th Ed.)

CERAMICS RESEARCH AND DEVELOPMENT OPERATION

QUARTERLY REPORT

OCTOBER–DECEMBER, 1962

HANFORD ATOMIC PRODUCTS OPERATION
RICHLAND, WASHINGTON

Work performed under Contract No. AT(45-1)-1350 between the
Atomic Energy Commission and General Electric Company

Printed by/for the U. S. Atomic Energy Commission

Printed in USA. Price $2.50 Available from the
Office of Technical Services
Department of Commerce
Washington 25, D.C.

DISCLAIMER

INTRODUCTION

This report is the first of a new series to be issued by the recently organized Ceramics Research and Development Operation, Reactor and Fuels Laboratory, Hanford Laboratories. The Ceramics Research and Development Component (E. A. Evans, Manager) comprises the following groups:

Ceramics Research	D. R. deHalas, Manager
Advance Fuel Development	K. Drumheller, Manager
Fabrication Development	R. D. Widrig, Manager
Fuels Testing and Analysis	W. E. Roake, Manager
Special Projects	L. E. Mills, Manager

The work reported in this and subsequent reports is a continuation of reactor fuels studies previously discussed in reports issued by the Fuels Development and the Plutonium Metallurgy Operations. Previous reports in those series are:

Fuels Development	Plutonium Metallurgy	Date
HW-74378 (Secret)	HW-74718 (Secret)	July-September, 1962
HW-74377 (Secret)	HW-74162 (Secret)	April-June, 1962
HW-72347 (Secret)	HW-73318 (Unclassified)	January-March, 1962
HW-72346 (Secret)	HW-72161 (Secret)	October-December, 1961

SUMMARY OF CONTENTS

Page

CERAMICS RESEARCH

Plutonium Sulfides - Y. B. Katayama 2.1

Pu_2S_3 melted congruently at 1725 ± 10 C under vacuum or argon and was stable to 2300 C in argon. Pu_2S_3 was not attacked by boiling, demineralized water.

Plutonium Mononitride - D. F. Carroll 2.1

PuN melted congruently at 2750 ± 75 C under nitrogen (1 atm), but dissociated at 2600 degrees under argon or helium.

PuO_2-Carbon Reaction - R. E. Skavdahl 2.2

Plutonium carbides and oxides of various compositions were formed by inert gas sintering of pressed mixtures of PuO_2 and graphite powder.

Plutonium Carbide - J. B. Burnham and R. E. Skavdahl . . . 2.3

Spontaneous lattice expansion of PuC at about 0.02% per month occurred over periods extending to 15 months, with no apparent saturation.

PuO_2-MgO Phase Studies - D. F. Carroll 2.4

PuO_2 and MgO are immiscible in all proportions and form no compounds stable at room temperature.

UO_2-ThO_2 Phase Studies - J. A. Christensen. 2.5

ThO_2 was soluble in UO_2 in all proportions, although the solution was not ideal as shown by minima in both melting point versus composition and lattice parameter versus composition curves.

Properties of Sintered ThO_2-PuO_2 - M. D. Freshley and H. M. Mattys 2.6

Small additions of PuO_2 enhance the sinterability of ThO_2. Melting points of (Th, Pu)O_2 solid solutions are constant below 25 wt% ThO_2. Lattice parameters of the solid solution obey Vegard's Law.

UO_2 Cermets - D. W. Brite and K. R. Sump 2.10

A series of tungsten-UO_2 cermets was fabricated by high-energy-rate impaction. The tungsten matrix was uniform and continuous at UO_2 concentrations as great as 50 wt%.

UN-Tungsten Cermet - D. W. Brite and K. R. Sump 2.10

A 50 wt% uranium mononitride-tungsten cermet was fabricated by impaction. The impacted density, 16.3 g/cc, was 99.0% of the theoretical density.

Uranium Monosulfide - D. W. Brite, K. R. Sump, and J. L. Bates 2.15

Uranium monosulfide impacted to 99% TD showed improvements in physical properties over sintered US.

Electron Microscopy of UO_2-Tungsten Cermet - J. L. Daniel 2.15

A UO_2-50 wt% cermet was examined at temperatures to 1500 C by reflection electron microscopy.

Microstructure of Sintered, Impacted UO_2 - D. W. Brite and K. R. Sump 2.15

The effects of variations in sintering rate, time, and temperature on the microstructure of the sintered UO_2 are illustrated in a series of photomicrographs.

Thermal Expansion of UO_2 - J. A. Christensen 2.20

An equation relating the specific volume of UO_2 to temperatures between zero and 3100 C was derived.

Molten UO_2 - J. A. Christensen 2.21

UO_2 heated to 3100 C in closed tungsten capsules retained an O/U ratio of 2.00 and reacted little with the tungsten.

Preparation of Samples for In-Reactor UO_2 Melting Studies - J. A. Christensen and L. A. Pember 2.23

Random distribution of 1 vol% tungsten shot (-100+200 mesh) in sintered UO_2 was achieved.

Hardness of UO_2 - J. L. Bates 2.23

Hardness of a (100) crystal face of UO_2 showed four-fold rotational symmetry. The (100) plane was identified as the only active slip plane at room temperature.

Release of Sorbed Gases by Ionizing Radiation - H. J. Anderson 2.27

Gas desorption equivalent to 900 C vacuum annealing was obtained by vacuum irradiation of UO_2 at room temperature in a Co^{60} gamma field of 8.9×10^5 R/hr.

Evaluation of UO_2 Analyses - H. J. Anderson 2.28

The reliability of analytical techniques for commercially fused UO_2 was evaluated by checking the vendor's results for density, stoichiometry, and carbon and nitrogen content.

Determination of Pore Size Distribution in UO_2 - H. J. Anderson 2.28

Development of a more precise measurement of the contact angle between mercury and UO_2 yielded a 30 percent correction in pore size determination.

UO_2 Specimens for Basic Research - H. J. Anderson. 2.28

UO_2 single crystals of various shapes were prepared for sites in Germany, France, and the United States.

High Temperature Electron Microscopy - J. O. McPartland. . 2.29

Specimens examined by reflection electron microscopy were heated to temperatures greater than 1400 C with an auxiliary electron gun.

FUELS DEVELOPMENT

Impaction of UO_2-PuO_2 - D. W. Brite, K. R. Sump, W. T. Ross, and L. G. Merker 3.1

Urania - 2.5 wt% plutonia powder was densified by impact, using a hooded Dynapak machine, to provide a ceramic material suitable for fuel in vibrationally compacted fuel elements.

Fuel Element Rejuvenation - R. C. Smith 3.4

A one-foot-long fuel element designed to test the feasibility of fuel rejuvenation was fabricated and sent to NRTS for irradiation.

Hot Isostatic Pressing - J. J. Hauth 3.6

UO_2 rods clad in thin stainless steel were fabricated by swaging and hot isostatic pressing, in cooperation with BMI.

Vibrational Compaction Studies - J. J. Hauth 3.11

Transverse excitation applied to the top of vertically suspended cladding simplifies coupling of vibrational energy to thin-wall cladding tubes.

Hot Vibrational Compaction - J. J. Hauth and D. R. Burroughs 3.11

Higher densities achievable by vibrational compaction at elevated temperatures are directly related to the thermal expansion characteristics of the cladding and core materials.

PRTR Fuel Fabrication - C. H Bloomster 3.13

Fabrication of UO_2-PuO_2 fuel elements for a full PRTR core loading proceeded on schedule. Forty-two elements have been produced, and successful operation has been demonstrated to a maximum exposure of 600 Mwd/ton at tube powers up to 1150 kw.

Plutonium Distribution in Incrementally Loaded PRTR Fuel Rods - R. E. Bardsley and C. H. Bloomster. 3.13

To minimize plutonium segregation in mixed-oxide fuel rods, the number of increments loaded in a rod was doubled. A process for continuous fuel loading is being developed. Preliminary investigation of nondestructive tests for determining segregation revealed two promising methods.

EBWR Plutonium Fuel Loading - R. E. Sharp 3.16

A cooperative HL-ANL program was initiated to irradiate plutonium fuel elements in the Experimental Boiling Water Reactor. Fuel criteria were established and material procurement initiated. Design of a facility for vibrational compaction of the material is in progress.

Extended Surface Plutonium Fuels - C. H. Bloomster 3.17

A roll-cladding process developed for Zircaloy-clad, Pu-Zr fuel elements eliminates external contamination.

Special Fuel Element Fabrication - C. H. Bloomster, L. C. Lemon, and W. T. Ross 3.18

Special fuel fabrication activities included (1) completion of 219 Al-Pu rods and 40 flux monitor foils for physics tests, (2) 33 percent completion of 1000 Pu-Al rods for physics tests, (3) development of a process to make depleted UO_2-0.90 wt% PuO_2 pellets of 91-94 percent theoretical density for physics experiments, (4) casting and partial extrusion of 14 Al - 8 wt% Pu - 2 wt% Ni billets for corrosion test fuel elements, and (5) fabrication of 71 Al-clad, coextruded, thin-walled tubular fuel elements containing Al-Pu and Al-U^{235} alloy cores.

Fuel Preparation Facilities - L. P. Murphy 3.21

Laboratory facilities for UO_2 powder preparation were modified.

Facility Hazards Analysis - W. J. Bailey, J. B. Burnham, and L. G. Merker 3.21

The final draft of a hazards analysis for the Plutonium Fabrication Pilot Plant is being assembled for publication.

FUELS TESTING AND ANALYSIS

Irradiation of a Large Diameter Fuel Rod - G. R. Horn, M. K. Millhollen, and W. J. Flaherty. 4.1

Postirradiation examination of a failed 2.33-inch diameter fuel rod revealed evidence of a severe transverse flux gradient, reduction of coolant flow, and bowing of the rod.

High Temperature Irradiation Testing of UO_2-Tungsten Cermet - G. R. Horn, W. J. Flaherty, and D. W. Brite . . 4.4

Short-term irradiation of high-energy-rate impact formed 50 wt% UO_2-W cermet produced no reaction between the components. UO_2 sublimed only from exposed surfaces.

Irradiation of UO_2 Single Crystal Pellets - G. R. Horn 4.9

Relatively greater thermal conductivity of large grain UO_2 was demonstrated by lack of structure change in 1/2-inch diameter single, bi- and tri-crystal pellets irradiated to generate approximately 760,000 Btu/(hr)(ft^2).

Low Temperature Irradiation Sintering of Swaged UO_2 - W. J. Flaherty 4.10

Ceramographic examination of irradiated, cold-swaged UO_2 revealed sintering between point contact at bulk fuel temperature of only 300–400 C.

Burst Tests of Cold-Swaged PRTR Fuel Rods - W. J. Flaherty, and L. E. Mills 4.10

Cold-swaged, Zircaloy-clad UO_2 PRTR fuel rods burst at pressures (7820 and 7880 psi, at 550 F) three times greater than those expected in PRTR rods after 10,000 Mwd/ton_U exposure.

Phoenix Fuel Experiment - M. D. Freshley 4.12

Al-Pu alloy specimens containing 6.33, 16.33 and 27.17 percent Pu^{240} were irradiated for investigation of reactivity change.

Irradiation of Prototypic UO_2-PuO_2 Fuel Elements, M. D. Freshley 4.13

Comparative irradiation tests of uniformly and variably enriched fuel rods revealed evidence of dissolution of impurity nitrogen by the Zircaloy cladding of the higher heat flux rods. Fuel performance was comparable in all rods.

Irradiation Performance of MgO-PuO_2 and ZrO_2-PuO_2 Fuels - M. D. Freshley and D. F. Carroll 4.15

No redistribution of PuO_2 particles in MgO occurred during irradiation of immiscible mixtures of MgO-PuO_2 pellets, even in columnar grain growth regions. Unusual microstructures were developed during irradiation of ZrO_2-PuO_2 pellets.

PuO_2 Segregation in Incrementally Loaded PRTR Fuel Rods - M. D. Freshley 4.20

Approximately the same degree of in-reactor sintering was found in irradiated, swaged UO_2-PuO_2 PRTR fuel rods containing 80 or 160 UO_2 and PuO_2 increments. The equiaxed grain growth that occurred is typical of 0.565-inch diameter fuel rods irradiated to generate 300,000 to 400,000 Btu/(hr)(ft^2).

Extended Surface PRTR Fuel Element Wear Pads - W. J. Flaherty, M. D. Freshley, M. K. Millhollen, and R. E. Sharp 4.23

Encouraging alleviation of fuel element process tube wear and fretting corrosion was achieved by additions of extended surface, clip-on fuel element wear pads.

Postirradiation Examination of a MgO-PuO_2 PRTR Fuel Element - M. D. Freshley 4.25

Postirradiation examination of a failed, swaged MgO-PuO_2 PRTR fuel element revealed regions of anomalously high PuO_2 content, one of which probably coincided with the point of failure. A ductile split propagated from the point of original brittle failure associated with an external layer of massive zirconium hydride and severe internal corrosion.

Inspection of PRTR Fuel Elements - M. K. Millhollen, W. J. Flaherty, and M. D. Freshley 4.28

Four PRTR fuel elements were removed from service because of mechanical damage found during postdecontamination inspection.

Irradiation of Uranium-Plutonium Oxide - W. J. Bailey and T. D. Chikalla 4.29

PuO_2 content has a marked effect on structure changes during irradiation of low density UO_2-PuO_2 fuel, but little effect in high density pellets. High density pellets incorporating mixed crystal (U, Pu)O_2 developed more extensive grain growth and released more fission gas than did pellets made from mixtures of UO_2 and PuO_2. Fuel capsules performed adequately to 10,000 Mwd/ton UO_2-PuO_2.

Short Duration Irradiations of UO_2 and UO_2-PuO_2 - W. J. Bailey and T. D. Chikalla 4.44

Four specimens irradiated in the MTR will be destructively examined for additional information on in-reactor sintering and the effect of plutonium content on the stability of UO_2.

Fission Fragment Migration in UO_2 - J. L. Bates, J. A. Christensen, and W. E. Roake 4.45

Drillings taken along the diameter of an irradiated UO_2 fuel core confirmed earlier findings of gross fission fragment relocation during irradiations, but revealed no plutonium migration.

In-Reactor Testing Devices - W. J. Bailey and S. H. Woodcock 4.45

Three test devices for in-reactor fuel evaluation are described.

SUMMARY OF CONTENTS

Page

CERAMICS RESEARCH

Plutonium Sulfides - Y. B. Katayama 2.1

Pu_2S_3 melted congruently at 1725 ± 10 C under vacuum or argon and was stable to 2300 C in argon. Pu_2S_3 was not attacked by boiling, demineralized water.

Plutonium Mononitride - D. F. Carroll 2.1

PuN melted congruently at 2750 ± 75 C under nitrogen (1 atm), but dissociated at 2600 degrees under argon or helium.

PuO_2-Carbon Reaction - R. E. Skavdahl 2.2

Plutonium carbides and oxides of various compositions were formed by inert gas sintering of pressed mixtures of PuO_2 and graphite powder.

Plutonium Carbide - J. B. Burnham and R. E. Skavdahl . . . 2.3

Spontaneous lattice expansion of PuC at about 0.02% per month occurred over periods extending to 15 months, with no apparent saturation.

PuO_2-MgO Phase Studies - D. F. Carroll 2.4

PuO_2 and MgO are immiscible in all proportions and form no compounds stable at room temperature.

UO_2-ThO_2 Phase Studies - J. A. Christensen. 2.5

ThO_2 was soluble in UO_2 in all proportions, although the solution was not ideal as shown by minima in both melting point versus composition and lattice parameter versus composition curves.

Properties of Sintered ThO_2-PuO_2 - M. D. Freshley and H. M. Mattys 2.6

Small additions of PuO_2 enhance the sinterability of ThO_2. Melting points of (Th, Pu)O_2 solid solutions are constant below 25 wt% ThO_2. Lattice parameters of the solid solution obey Vegard's Law.

UO_2 Cermets - D. W. Brite and K. R. Sump 2.10

A series of tungsten-UO_2 cermets was fabricated by high-energy-rate impaction. The tungsten matrix was uniform and continuous at UO_2 concentrations as great as 50 wt%.

UN-Tungsten Cermet - D. W. Brite and K. R. Sump 2.10

A 50 wt% uranium mononitride-tungsten cermet was fabricated by impaction. The impacted density, 16.3 g/cc, was 99.0% of the theoretical density.

Uranium Monosulfide - D. W. Brite, K. R. Sump, and J. L. Bates 2.15

Uranium monosulfide impacted to 99% TD showed improvements in physical properties over sintered US.

Electron Microscopy of UO_2-Tungsten Cermet - J. L. Daniel 2.15

A UO_2-50 wt% cermet was examined at temperatures to 1500 C by reflection electron microscopy.

Microstructure of Sintered, Impacted UO_2 - D. W. Brite and K. R. Sump 2.15

The effects of variations in sintering rate, time, and temperature on the microstructure of the sintered UO_2 are illustrated in a series of photomicrographs.

Thermal Expansion of UO_2 - J. A. Christensen 2.20

An equation relating the specific volume of UO_2 to temperatures between zero and 3100 C was derived.

Molten UO_2 - J. A. Christensen 2.21

UO_2 heated to 3100 C in closed tungsten capsules retained an O/U ratio of 2.00 and reacted little with the tungsten.

Preparation of Samples for In-Reactor UO_2 Melting Studies - J. A. Christensen and L. A. Pember 2.23

Random distribution of 1 vol% tungsten shot (-100+200 mesh) in sintered UO_2 was achieved.

Hardness of UO_2 - J. L. Bates 2.23

Hardness of a (100) crystal face of UO_2 showed four-fold rotational symmetry. The (100) plane was identified as the only active slip plane at room temperature.

Release of Sorbed Gases by Ionizing Radiation - H. J. Anderson 2.27

Gas desorption equivalent to 900 C vacuum annealing was obtained by vacuum irradiation of UO_2 at room temperature in a Co^{60} gamma field of 8.9×10^5 R/hr.

Evaluation of UO_2 Analyses - H. J. Anderson 2.28

The reliability of analytical techniques for commercially fused UO_2 was evaluated by checking the vendor's results for density, stoichiometry, and carbon and nitrogen content.

Determination of Pore Size Distribution in UO_2 - H. J. Anderson 2.28

Development of a more precise measurement of the contact angle between mercury and UO_2 yielded a 30 percent correction in pore size determination.

UO_2 Specimens for Basic Research - H. J. Anderson. 2.28

UO_2 single crystals of various shapes were prepared for sites in Germany, France, and the United States.

High Temperature Electron Microscopy - J. O. McPartland. . 2.29

Specimens examined by reflection electron microscopy were heated to temperatures greater than 1400 C with an auxiliary electron gun.

FUELS DEVELOPMENT

Impaction of UO_2-PuO_2 - D. W. Brite, K. R. Sump, W. T. Ross, and L. G. Merker 3.1

Urania - 2.5 wt% plutonia powder was densified by impact, using a hooded Dynapak machine, to provide a ceramic material suitable for fuel in vibrationally compacted fuel elements.

Fuel Element Rejuvenation - R. C. Smith 3.4

A one-foot-long fuel element designed to test the feasibility of fuel rejuvenation was fabricated and sent to NRTS for irradiation.

Hot Isostatic Pressing - J. J. Hauth 3.6

UO_2 rods clad in thin stainless steel were fabricated by swaging and hot isostatic pressing, in cooperation with BMI.

Vibrational Compaction Studies - J. J. Hauth 3.11

Transverse excitation applied to the top of vertically suspended cladding simplifies coupling of vibrational energy to thin-wall cladding tubes.

Hot Vibrational Compaction - J. J. Hauth and D. R. Burroughs 3.11

Higher densities achievable by vibrational compaction at elevated temperatures are directly related to the thermal expansion characteristics of the cladding and core materials.

PRTR Fuel Fabrication - C. H Bloomster 3.13

Fabrication of UO_2-PuO_2 fuel elements for a full PRTR core loading proceeded on schedule. Forty-two elements have been produced, and successful operation has been demonstrated to a maximum exposure of 600 Mwd/ton at tube powers up to 1150 kw.

Plutonium Distribution in Incrementally Loaded PRTR Fuel Rods - R. E. Bardsley and C. H. Bloomster 3.13

To minimize plutonium segregation in mixed-oxide fuel rods, the number of increments loaded in a rod was doubled. A process for continuous fuel loading is being developed. Preliminary investigation of nondestructive tests for determining segregation revealed two promising methods.

EBWR Plutonium Fuel Loading - R. E. Sharp 3.16

A cooperative HL-ANL program was initiated to irradiate plutonium fuel elements in the Experimental Boiling Water Reactor. Fuel criteria were established and material procurement initiated. Design of a facility for vibrational compaction of the material is in progress.

Extended Surface Plutonium Fuels - C. H. Bloomster 3.17

A roll-cladding process developed for Zircaloy-clad, Pu-Zr fuel elements eliminates external contamination.

Special Fuel Element Fabrication - C. H. Bloomster, L. C. Lemon, and W. T. Ross 3.18

Special fuel fabrication activities included (1) completion of 219 Al-Pu rods and 40 flux monitor foils for physics tests, (2) 33 percent completion of 1000 Pu-Al rods for physics tests, (3) development of a process to make depleted UO_2-0.90 wt% PuO_2 pellets of 91-94 percent theoretical density for physics experiments, (4) casting and partial extrusion of 14 Al - 8 wt% Pu - 2 wt% Ni billets for corrosion test fuel elements, and (5) fabrication of 71 Al-clad, coextruded, thin-walled tubular fuel elements containing Al-Pu and Al-U^{235} alloy cores.

Fuel Preparation Facilities - L. P. Murphy 3.21

Laboratory facilities for UO_2 powder preparation were modified.

Facility Hazards Analysis - W. J. Bailey, J. B. Burnham, and L. G. Merker 3.21

The final draft of a hazards analysis for the Plutonium Fabrication Pilot Plant is being assembled for publication.

FUELS TESTING AND ANALYSIS

Irradiation of a Large Diameter Fuel Rod - G. R. Horn, M. K. Millhollen, and W. J. Flaherty. 4.1

Postirradiation examination of a failed 2.33-inch diameter fuel rod revealed evidence of a severe transverse flux gradient, reduction of coolant flow, and bowing of the rod.

High Temperature Irradiation Testing of UO_2-Tungsten Cermet - G. R. Horn, W. J. Flaherty, and D. W. Brite . . 4.4

Short-term irradiation of high-energy-rate impact formed 50 wt% UO_2-W cermet produced no reaction between the components. UO_2 sublimed only from exposed surfaces.

Irradiation of UO_2 Single Crystal Pellets - G. R. Horn 4.9

Relatively greater thermal conductivity of large grain UO_2 was demonstrated by lack of structure change in 1/2-inch diameter single, bi- and tri-crystal pellets irradiated to generate approximately 760,000 Btu/(hr)(ft^2).

Low Temperature Irradiation Sintering of Swaged UO_2 - W. J. Flaherty 4.10

Ceramographic examination of irradiated, cold-swaged UO_2 revealed sintering between point contact at bulk fuel temperature of only 300-400 C.

Burst Tests of Cold-Swaged PRTR Fuel Rods - W. J. Flaherty, and L. E. Mills 4.10

Cold-swaged, Zircaloy-clad UO_2 PRTR fuel rods burst at pressures (7820 and 7880 psi, at 550 F) three times greater than those expected in PRTR rods after 10,000 Mwd/ton_U exposure.

Phoenix Fuel Experiment - M. D. Freshley 4.12

Al-Pu alloy specimens containing 6.33, 16.33 and 27.17 percent Pu^{240} were irradiated for investigation of reactivity change.

Irradiation of Prototypic UO_2-PuO_2 Fuel Elements, M. D. Freshley 4.13

Comparative irradiation tests of uniformly and variably enriched fuel rods revealed evidence of dissolution of impurity nitrogen by the Zircaloy cladding of the higher heat flux rods. Fuel performance was comparable in all rods.

Irradiation Performance of MgO-PuO_2 and ZrO_2-PuO_2 Fuels - M. D. Freshley and D. F. Carroll 4.15

No redistribution of PuO_2 particles in MgO occurred during irradiation of immiscible mixtures of MgO-PuO_2 pellets, even in columnar grain growth regions. Unusual microstructures were developed during irradiation of ZrO_2-PuO_2 pellets.

PuO_2 Segregation in Incrementally Loaded PRTR Fuel Rods - M. D. Freshley 4.20

Approximately the same degree of in-reactor sintering was found in irradiated, swaged UO_2-PuO_2 PRTR fuel rods containing 80 or 160 UO_2 and PuO_2 increments. The equiaxed grain growth that occurred is typical of 0.565-inch diameter fuel rods irradiated to generate 300,000 to 400,000 Btu/(hr)(ft^2).

Extended Surface PRTR Fuel Element Wear Pads - W. J. Flaherty, M. D. Freshley, M. K. Millhollen, and R. E. Sharp 4.23

Encouraging alleviation of fuel element process tube wear and fretting corrosion was achieved by additions of extended surface, clip-on fuel element wear pads.

Postirradiation Examination of a MgO-PuO_2 PRTR Fuel Element - M. D. Freshley 4.25

Postirradiation examination of a failed, swaged MgO-PuO_2 PRTR fuel element revealed regions of anomalously high PuO_2 content, one of which probably coincided with the point of failure. A ductile split propagated from the point of original brittle failure associated with an external layer of massive zirconium hydride and severe internal corrosion.

Inspection of PRTR Fuel Elements - M. K. Millhollen, W. J. Flaherty, and M. D. Freshley 4.28

Four PRTR fuel elements were removed from service because of mechanical damage found during postdecontamination inspection.

Irradiation of Uranium-Plutonium Oxide - W. J. Bailey and T. D. Chikalla 4.29

PuO_2 content has a marked effect on structure changes during irradiation of low density UO_2-PuO_2 fuel, but little effect in high density pellets. High density pellets incorporating mixed crystal (U, Pu)O_2 developed more extensive grain growth and released more fission gas than did pellets made from mixtures of UO_2 and PuO_2. Fuel capsules performed adequately to 10,000 Mwd/ton UO_2-PuO_2.

Short Duration Irradiations of UO_2 and UO_2-PuO_2 - W. J. Bailey and T. D. Chikalla 4.44

Four specimens irradiated in the MTR will be destructively examined for additional information on in-reactor sintering and the effect of plutonium content on the stability of UO_2.

Fission Fragment Migration in UO_2 - J. L. Bates, J. A. Christensen, and W. E. Roake 4.45

Drillings taken along the diameter of an irradiated UO_2 fuel core confirmed earlier findings of gross fission fragment relocation during irradiations, but revealed no plutonium migration.

In-Reactor Testing Devices - W. J. Bailey and S. H. Woodcock 4.45

Three test devices for in-reactor fuel evaluation are described.

LIST OF FIGURES

Figure Number	Title	Page
2.1	Lattice Parameter Change in PuC as a Function of Time	2.3
2.2	Phase Relationships for the UO_2-ThO_2 System	2.5
2.3	Density of ThO_2-PuO_2 Mixtures Sintered in Helium 1650 C for 6 Hours	2.6
2.4	Melting Point of (Th, Pu)O_2 Solid Solution	2.7
2.5	Lattice Parameter of (Th, Pu)O_2 Solid Solution	2.8
2.6	PuO_2-Zr Cermet	2.9
2.7	Microstructures of UO_2-W Cermets	2.11
2.8	Impacted Discs of UO_2-W Cermets	2.12
2.9	Microstructure of Micronized UO_2-W Cermet	2.13
2.10	UN-W Cermet	2.13
2.11	Microstructures of UO_2 Cermets	2.14
2.12	Microstructures of Sintered and Impacted US	2.16
2.13	UO_2-50 wt% W Cermet (Reflection Electron Microscopy)	2.17
2.14	Microstructures of Impacted and Sintered UO_2	2.18
2.15	Effect of Sintering Conditions on Density of Impacted and Sintered UO_2	2.20
2.16	Thermal Expansion of UO_2	2.21
2.17	UO_2 After Heating to 3000 C in a Closed Tungsten Vessel	2.22
2.18	Uranium Dioxide Heated to 3000 C in a Closed Tungsten Vessel	2.24
2.19	Dispersion of Tungsten Spheres in Sintered UO_2	2.25
2.20	Hardness of UO2 (100) Plane as a Function of Knoop Indentor Orientation	2.26
2.21	Slip Lines and Etch Pits Formed Near Microhardness Identor Marks on UO_2 Single Crystal Surfaces are (111) Planes	2.27

Figure Number	Title	Page
3.1	Impaction of UO_2-PuO_2	3.2
3.2	Capsule Assembly and Impacted Can Containing PuO_2-UO_2 and Axial Cross Section of Impacted Can	3.3
3.3	Fuel Rejuvenation Test Element	3.4
3.4	Rejuvenation Fuel Rod	3.5
3.5	Hot Isostatically Pressed UO_2:	
	A. 70 wt% Fused (-100 +200 mesh), 30 wt% Micronized	3.7
	B. 70 wt% Fused (-65 +100 mesh), 30 wt% Micronized	3.8
	C. 70 wt% Fused (-35+65 mesh), 30 wt% Micronized	3.9
	D. 70 wt% Fused (-20 mesh), 20 wt% Micronized	3.10
3.6	Hot Vibrational Compaction by Transverse Excitation	3.12
3.7	Comparative Autoradiographs: 150-Increment Rod Vibrated Continuously During Loading and 80-Increment Rod Loaded Without Vibration	3.14
3.8	Autoradiographs and Eddy Current Test Results for Incrementally Loaded PuO_2-UO_2 Fuel Rods	3.15
3.9	Roll-Clad, Zircaloy-Clad, Zr-Pu Fuel Plate	3.17
3.10	High Exposure Aluminum-Plutonium Elements (0.563-Inch OD) for PCTR	3.19
3.11	Flux Monitor Foil for PCTR	3.19
3.12	Aluminum-Plutonium Fuel Elements for Light-Water Experiments in the PRP-CF	3.20
3.13	Plutonium Fuel Elements for Aluminum Alloy Corrosion Tests	3.20
3.14	Equipment for Powder Preparation	3.22

Figure Number	Title	Page
4.1	Sections of Irradiated, Large-Diameter (2.33-Inch OD) UO_2 Fuel Rod	4.2
4.2	Separator Plates Between Gas Plenum and Fuel in Irradiated 2.33-Inch-Diameter Fuel Rod	4.3
4.3	Microstructure of Impacted UO_2–50 wt% Tungsten Cermet Before Irradiation	4.5
4.4	Components of Tungsten-Clad, UO_2-Tungsten Cermet Irradiation Capsule	4.6
4.5	UO_2-Tungsten Cermet Test Capsule After Irradiation	4.6
4.6	Cross Section of Irradiated, Tungsten-Clad, UO_2–Tungsten Cermet	4.7
4.7	Microstructure of UO_2–50 wt% Tungsten Cermet	4.8
4.8	Irradiated High Density UO_2 Pellets	4.9
4.9	Low Temperature, In-Reactor Sintering of UO_2	4.11
4.10	PRTR Fuel Rod Burst Test Specimens	4.12
4.11	Gas Release from Irradiated Swage-Compacted UO_2-PuO_2	4.14
4.12	Irradiated MgO–13.5 wt% PuO_2 Sintered Pellet Showing Uniform Distribution of PuO_2	4.17
4.13	Irradiated MgO–13.5 wt% PuO_2 Sintered Pellet Showing Uniform Distribution of PuO_2	4.18
4.14	Irradiated MgO–13.5 wt% PuO_2 Sintered Pellet Showing Uniform Distribution of PuO_2 in the Columnar Grain Growth Region of the MgO Matrix	4.18
4.15a	Irradiated ZrO_2–10.4 wt% PuO_2 High Density (91 % TD) Sintered Pellets	4.19
4.15b	Irradiated ZrO_2–10.4 wt% PuO_2 High Density (91% TD) Sintered Pellets	4.20
4.16	Autoradiographs of Segments of Irradiated, Incrementally Loaded, and Swage-Compacted UO_2-PuO_2 PRTR Fuel Rods	4.21
4.17	Longitudinal Sections of Irradiated, Swage-Compacted UO_2-PuO_2 Fuel Rods	4.22

Figure Number	Title	Page
4.18	Extended Surface, Clip-on Wear Pads (Insert) Installed on PRTR Mark I Fuel Element	4.24
4.19	Cross Sections of Cladding from $MgO-PuO_2$ PRTR Fuel Element	4.26
4.20	Polished Cross Section of Zircaloy Cladding from $MgO-PuO_2$ Fuel Element	4.27
4.21	Irradiated UO_2–0.0259 mole % PuO_2 (GEH-14-22)	4.31
4.22	Irradiated UO_2–0.187 mole % PuO_2 (GEH-14-65)	4.32
4.23	Irradiated UO_2–0.187 mole % PuO_2 (GEH-14-66)	4.33
4.24	Irradiated UO_2–1.46 mole % PuO_2 (GEH-14-68)	4.35
4.25	Irradiated UO_2–0.0259 mole % PuO_2 (GEH-14-20)	4.36
4.26	Irradiated UO_2–0.0259 mole % PuO_2 (GEH-14-91)	4.37
4.27	Irradiated UO_2–2.57 mole % PuO_2 (GEH-14-85)	4.38
4.28	Irradiated UO_2–4.13 mole % PuO_2 (GEH-14-86)	4.39
4.29	Fission Fragment Distribution in Irradiated UO_2; Comparison of Scratch Sampling with Drill Sampling	4.46
4.30	Proposed Equipment to Operate Fuel Elements at High Specific Power and Discharge Them During Reactor Operation Without Reducing Coolant Flow ("Icarus" Experiment)	4.47
4.31	Proposed Equipment for Measurement of High Temperatures in an Operating Fuel Element ("Helios" Experiment)	4.48
4.32	Proposed Equipment for Visual Observation and Recording of High Temperature Fuel Region of an Operating Fuel Element ("Argus" Experiment)	4.49

CERAMICS RESEARCH

Plutonium Sulfides - Y. B. Katayama

Pu_2S_3 melts congruently at 1725 ± 10 C under a 10^{-2} torr pressure. X-ray diffraction analysis of a sample after melting and resolidification showed only the Pu_2S_3 lines, but on heating to 2000 C in this vacuum, some Pu_2O_2S was formed. In argon, however, Pu_2S_3 was stable to 2300 C, the maximum temperature attained. Temperatures were measured in a tungsten ribbon furnace with a calibrated brightness pyrometer.

Corrosion samples of Pu_2S_3 exposed to boiling demineralized water showed no sign of chemical instability.

The reaction of plutonium chips with sulfur at 300 C for 20 hours yielded PuS with traces of Pu_2O_2S and some unreacted elemental plutonium.

Plutonium Mononitride - D. F. Carroll

Plutonium nitride appeared to dissociate and volatize rapidly at 2600 ± 75 C under one atmosphere of either argon or helium. No distinct melting point was observed.

Under one atmosphere of nitrogen, congruent melting occurred at 2750 ± 75 C. X-ray diffraction analyses of the specimens melted in nitrogen show them to be stoichiometric PuN. Atmospheres were gettered with zirconium chips at 650 C. Temperatures were measured in a tungsten ribbon furnace with a calibrated brightness pyrometer.

Solubility measurements were made of PuN in concentrated HCl, HF, HNO_3, H_3PO_4, and H_2SO_4 at 32 C. In HCl and H_3PO_4, PuN samples were completely dissolved in less than 3 minutes, resulting in a clear green and a clear blue solution indicative of Pu^{+3}. In HF, HNO_3 and H_2SO_4, dissolution was not complete after 24 hours, although some reaction had occurred.

PuO_2-Carbon Reactions - R. E. Skavdahl

Plutonium carbides and oxides of various compositions were formed by carbon reduction of PuO_2. Samples were prepared by mixing PuO_2 powder with the amount of powdered carbon calculated to yield the desired product. The mixed samples were pressed into pellets and sintered in two lots at about 1300 to 1400 C for 6 hours in flowing helium. Results are summarized in Table 2.1.

TABLE 2.1

PuO_2-CARBON REACTION PRODUCTS

Sample	Initial wt % Carbon	Desired Product	wt % Carbon In Reaction Product
1	1.91	$PuO_{1.56}$	1.1
2	1.66	$PuO_{1.62}$	1.0
3	1.31	$PuO_{1.70}$	0.60
4	1.22	$PuO_{1.72}$	0.80
5	11.20	PuC (46 at. % C)	6.0
6	13.40	Pu_2C_3	8.6
7	15.10	PuC_2	10.2

Samples 1 through 4 were processed together; residual carbon contents all correspond to a range of 40-45 percent completion of the reduction reaction.

Samples 5 through 7 were treated in a second run and had residual carbon contents corresponding to 75-85 percent completion of reaction. X-ray analysis showed that Sample 5 contained a large quantity of Pu_2C_3, intermediate quantities of both α-Pu_2O_3 and β-Pu_2O_3, and no detectable amount of PuO or PuC.

The presence of Pu_2O_3 combined with the absence of PuO in Sample 5 suggests that the formation of PuC by carbon reduction of PuO_2 may proceed by the following route:

$$PuO_2 \xrightarrow{+C} \alpha\text{-}Pu_2O_3 \xrightarrow{+C} \beta\text{-}Pu_2O_3 \xrightarrow{+C} Pu_2C_3 \xrightarrow{+\beta\text{-}Pu_2O_3} PuC.$$

Plutonium Carbides - J. B. Burnham and R. E. Skavdahl

Plutonium carbides of varying carbon content exhibited spontaneous expansion with time. Lattice parameter versus time for samples sealed in double glass capillaries (Figure 2.1) indicates that the rate of damage may increase with time.

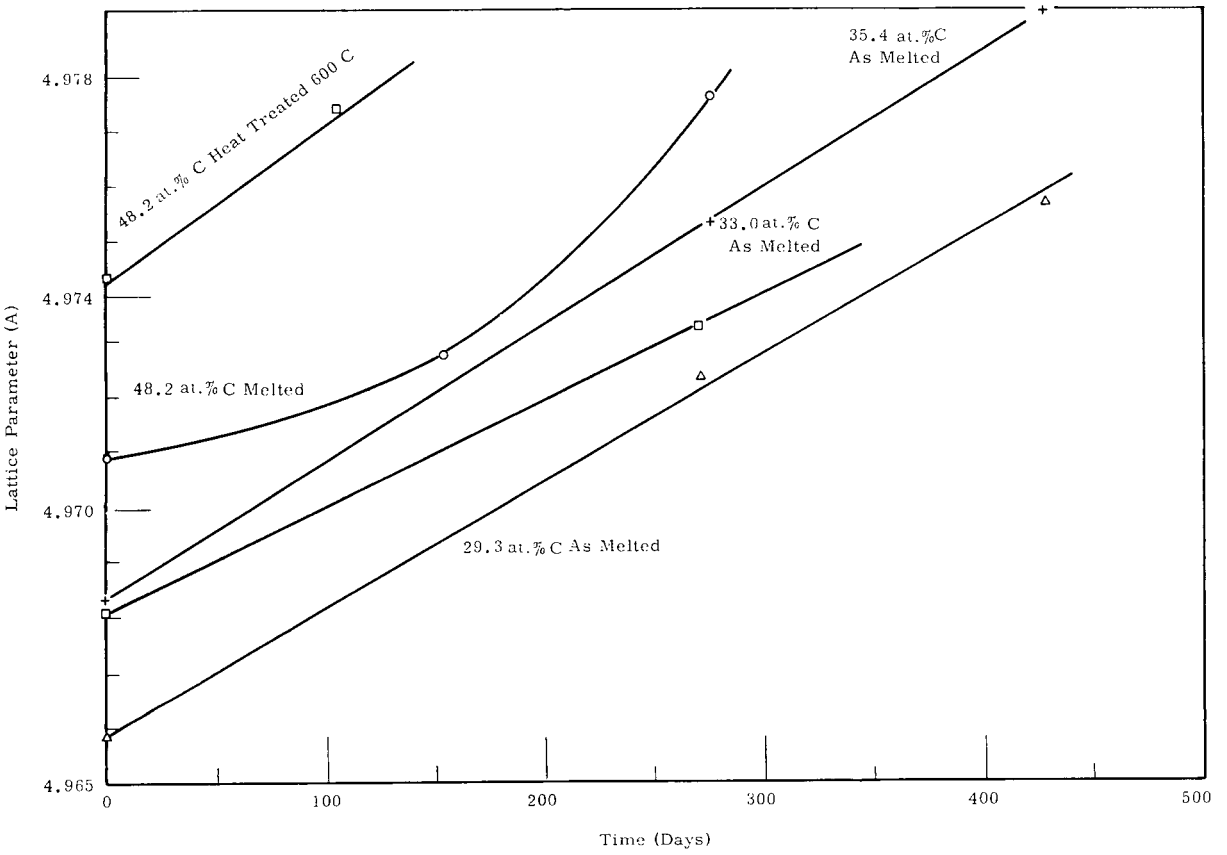

FIGURE 2.1

Lattice Parameter Change in PuC as a Function of Time

The dilation is not caused by atmospheric contamination since a 5 day exposure of the samples to nitrogen contaminated with 1/2 percent oxygen caused no change in lattice parameter. The most probable damage mechanism is the creation of Frenkel defects[1] and/or residual helium

(1) Kinchin, G. H. and R. S. Pease. "The Displacement of Atoms in Solids by Radiation", The Physical Society Reports on Progress in Physics, Vol. 18:2-51. 1955.

atoms by alpha decay of plutonium. The calculated density of helium atoms is 3×10^{-6} helium atoms/PuC molecule, which is probably not great enough to explain all of the growth.

The cumulative expansion data are shown in Table 2.2.

TABLE 2.2

LATTICE EXPANSION OF PLUTONIUM CARBIDES WITH TIME

Atom Percent Carbon	$\Delta a/a_o$	Total Time(days)	$\Delta a/a$/100 days
29.1	1.92×10^{-3}	426	0.46×10^{-3}
33.0	1.13×10^{-3}	279	0.41×10^{-3}
35.4	2.27×10^{-3}	426	0.53×10^{-3}
48.2	1.33×10^{-3}	276	0.49×10^{-3}
48.2	1.51×10^{-3}	273	0.55×10^{-3}

No correlation between growth rate and carbon content was apparent. Theoretically, the highly defected, carbon-poor PuC (35.4 at. % C) should expand at a lower rate than the carbon-rich variety (48.2 at. % C). The fact that it does not implies that the mobility of vacancies is very low at room temperature.

PuO_2-MgO Phase Studies - D. F. Carroll

PuO_2 and MgO are immiscible in all proportions and form no compounds that are stable at room temperature, as shown by X-ray diffraction analyses of samples representing 17 different PuO_2-MgO compositions. The samples were mechanically mixed, pressed, and sintered in helium at 1600 C for 20 hours.

The sinterability of PuO_2-MgO was independent of composition and green density. Some PuO_2 reduction was indicated by the presence of α-Pu_2O_3 reflections in the diffraction patterns for PuO_2-rich compositions.

UO_2-ThO_2 Phase Studies - J. A. Christensen

A continuous series of UO_2-ThO_2 solid solutions is formed at ThO_2 concentrations between 2 and 95 wt %, as evidenced by the absence of extraneous X-ray diffraction lines in this compositional range and the apparently continuous nature of the liquidus.

Significant departure from ideal solid solubility does occur, however, as shown by the minimum and the departure from Vegard's Law apparent in a plot of lattice parameter versus composition (Figure 2.2).

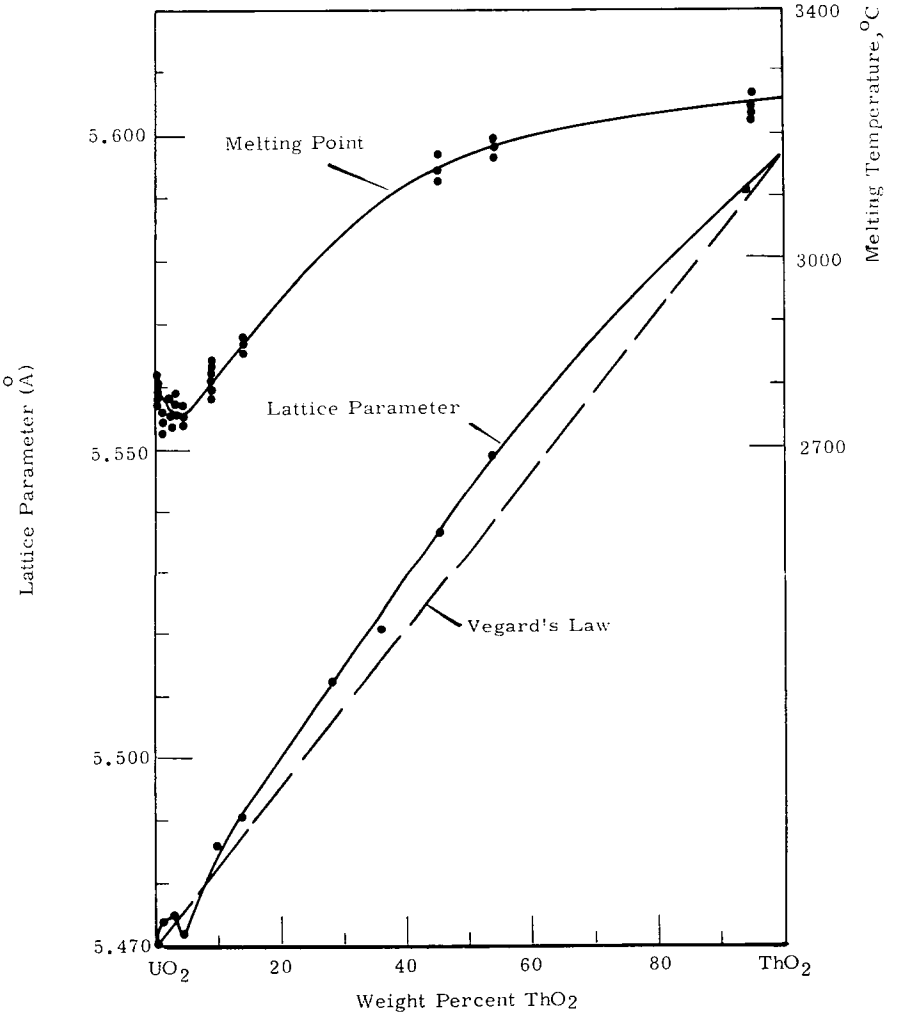

FIGURE 2.2

Phase Relationships for the UO_2-ThO_2 System

Lattice parameters were measured by extrapolation of the Nelson-Riley function and are precise to ± 0.001A. The minimum occurred between 2 and 4 wt % ThO_2, the same composition range in which a minimum in the liquidus was previously observed.(1)

Properties of Sintered ThO_2-PuO_2 - M. D. Freshley and H. M. Mattys

The sinterability, melting points, and lattice parameters of ThO_2-PuO_2 mixtures were investigated in preparation for in-reactor evaluation. Such a fuel would be useful in a reactor complex based on crossed uranium-thorium fuel cycles. ThO_2 enriched with 2, 5, 10, 15, and 20 wt % PuO_2 will be irradiated, in the form of high-density sintered pellets, at different core temperatures to different exposures.

Sintering studies showed that achievable sintered densities of (Th, Pu)O_2 compacts increase with increasing PuO_2 content between 2 wt % and 50 at. % PuO_2 (Figure 2.3). At PuO_2 concentrations greater than 50 wt % PuO_2, the apparent density is lower because of cracking.

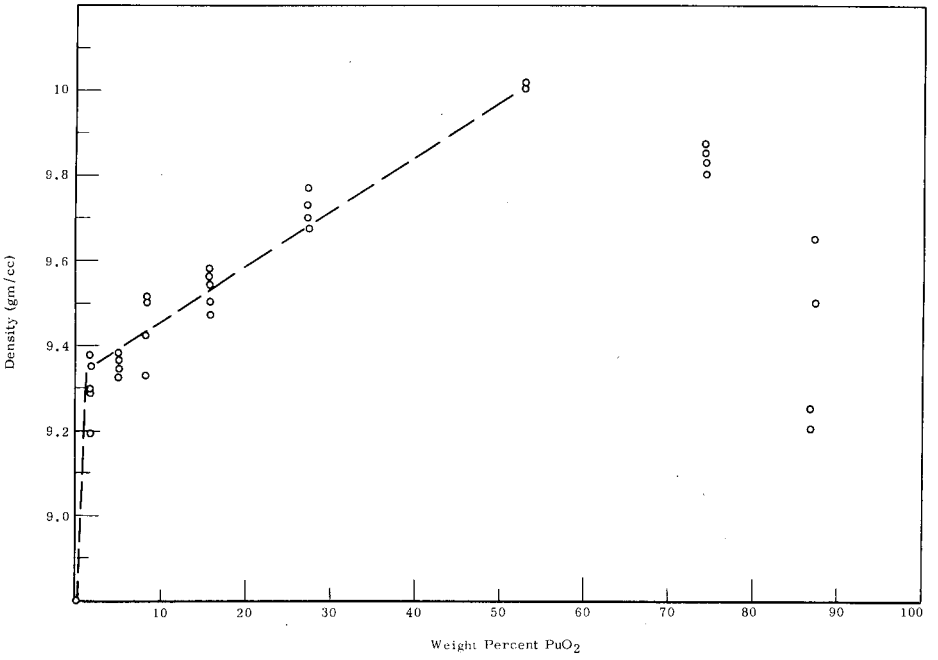

FIGURE 2.3

Density of ThO_2-PuO_2 Mixtures Sintered in Helium 1650 C for 6 Hours

(1) Cadwell, J. J. Fuels Development Operation Quarterly Progress Report, July, August, September, 1962, HW-74378. October, 1962. (SECRET)

Small additions of PuO_2 enhance the sinterability of ThO_2 in the same way as do small additions of CaO. Sintered densities of ThO_2 were 88% TD with 220 ppm added CaO, and 95% TD with approximately 0.1% CaO. Similar ThO_2 containing 8 wt% PuO_2 was sintered to 94% TD regardless of CaO content.

The sintering tests were performed at 1650 C for 6 hours in helium. ThO_2-PuO_2 mixtures were prepared by blending and wet ball milling ThO_2 and plutonium oxalate, followed by calcination for 2 hours in air at 500 C to convert the plutonium oxalate to PuO_2. The mixed powders were double pressed without binder to 60% TD before sintering.

The melting points of PuO_2 and of (Th, Pu)O_2 solid solutions were measured in helium on a tungsten ribbon filament. The melting point of specimens containing less than approximately 25 wt% ThO_2 is constant, as shown in Figure 2.4. Similar behavior in UO_2-ThO_2 systems was

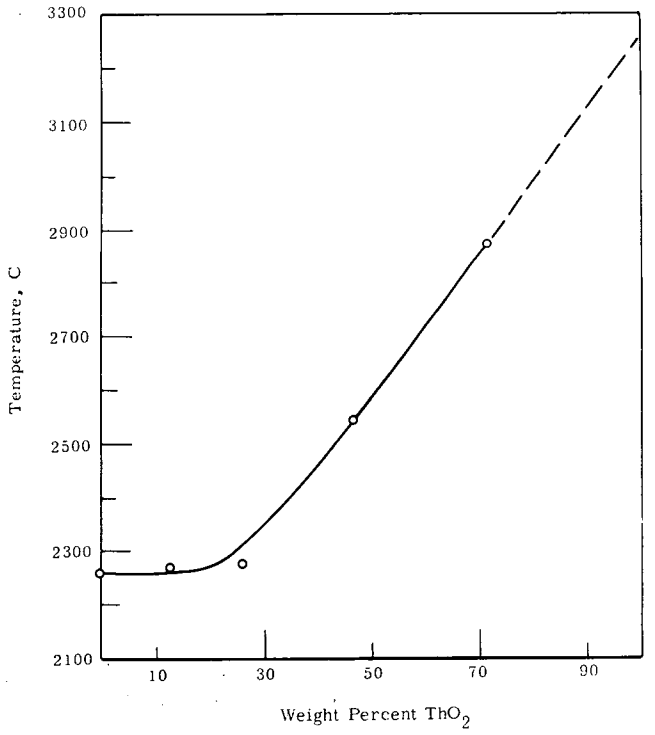

FIGURE 2.4
Melting Point of (Th, Pu)O_2 Solid Solution

earlier reported.[1] An apparent melting point of 2260 C was obtained for pure PuO_2, in agreement with Chikalla, et al.[2] Extrapolation of the curve indicates a melting point greater than 3200 C for pure ThO_2.

The lattice parameters of (Th, Pu)O_2 solid solutions were determined by X-ray diffraction. The lattice parameter changes linearly from 5.6010 A (ThO_2) to 5.3960 A (PuO_2) in accordance with Vegard's Law, as shown in Figure 2.5. X-ray diffraction patterns of PuO_2-rich pellets sintered in helium revealed traces of α-Pu_2O_3. A low-intensity peak corresponding to β-Pu_2O_3 was also recorded. The unexpected coexistence of β-Pu_2O_3 and the PuO_2-rich phase indicates a nonequilibrium condition.

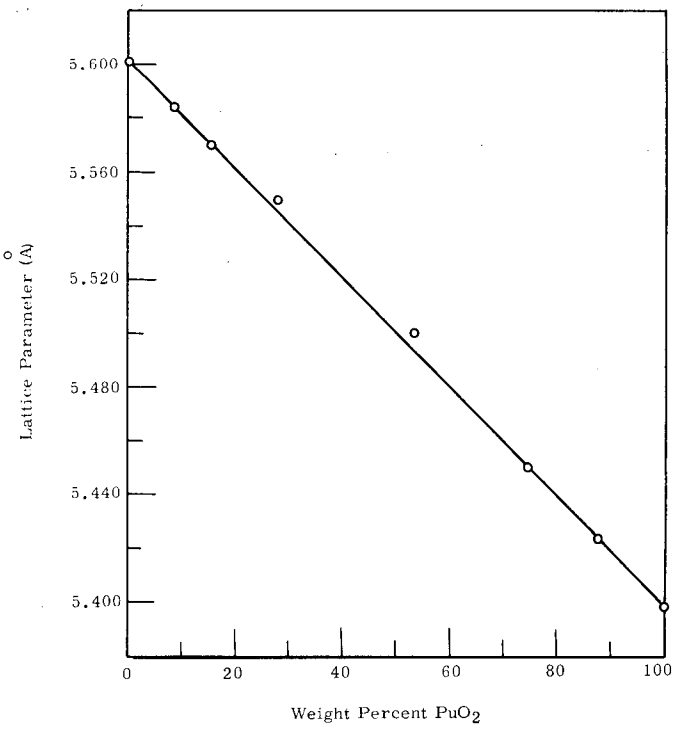

FIGURE 2.5

Lattice Parameter of (Th, Pu)O_2 Solid Solution

(1) Lambertson, W. A., M. H. Mueller, and F. H. Gunzell, Jr., "Uranium Oxide Equilibrium Systems: IV, UO_2-ThO_2", Journal of the American Ceramic Society, Vol. 36, No. 11:397. November 1, 1953.

(2) Chikalla, T. D., C. E. McNeilly, and R. E. Skavdahl. The Plutonium Oxygen System, HW-74802. September, 1962.

Page 2.9 deleted from copies intended for public release because of patent considerations. (Includes Figure 2.6)

UO_2 Cermets - D. W. Brite and K. R. Sump

In an impacted, UO_2-50 wt% tungsten cermet, a uniform and continuous tungsten matrix was produced. Contact between UO_2 particles, apparent at UO_2 concentrations greater than 50 wt%, increases with increasing UO_2 concentration, as shown in Figure 2.7

The cermets were formed by impaction, at 1200 C and 280,000 psi, of mixtures of tungsten powder (< 10μ diameter particles) and fused UO_2 (-65+200 mesh). Machinable discs (Figure 2.8) containing 50, 60, 70, 80, 90, and 95 wt% UO_2 were produced, with densities which varied from 96.0 percent TD (50 wt% UO_2) to 98.4 percent TD (95 wt% UO_2).

A UO_2-50 wt% tungsten cermet having a density of 13.48 g/cm^3 (96.3 percent TD) was formed from a mixture of similar tungsten powder and micronized UO_2 (Figure 2.9). The mixture was impacted at 1200 C and 400,000 psi, using a modified Bridgman anvil technique.

UN-Tungsten Cermet - D. W. Brite and K. R. Sump

Under impaction conditions of 1200 C and 400,000 psi, a UN-50 wt% tungsten cermet having a density of 16.28 g/cm^3 (99.0 percent TD) was formed (Figure 2.10).

A series of UO_2 cermets, comprising 35 vol% metallic constituent and -65+200 mesh fused UO_2, was formed by impaction at 1200 C and 250,000 psi. The compositions and densities of the cermets are shown in the following table.

Metallic Constituent	Cermet Density
Molybdenum	10.44 g/cc (97.6% TD)
18-8 Stainless Steel	9.69 g/cc (97.9% TD)
Nickel-20 Chromium	9.65 g/cc (95.8% TD)

Microstructures of the cermets are shown in Figure 2.11

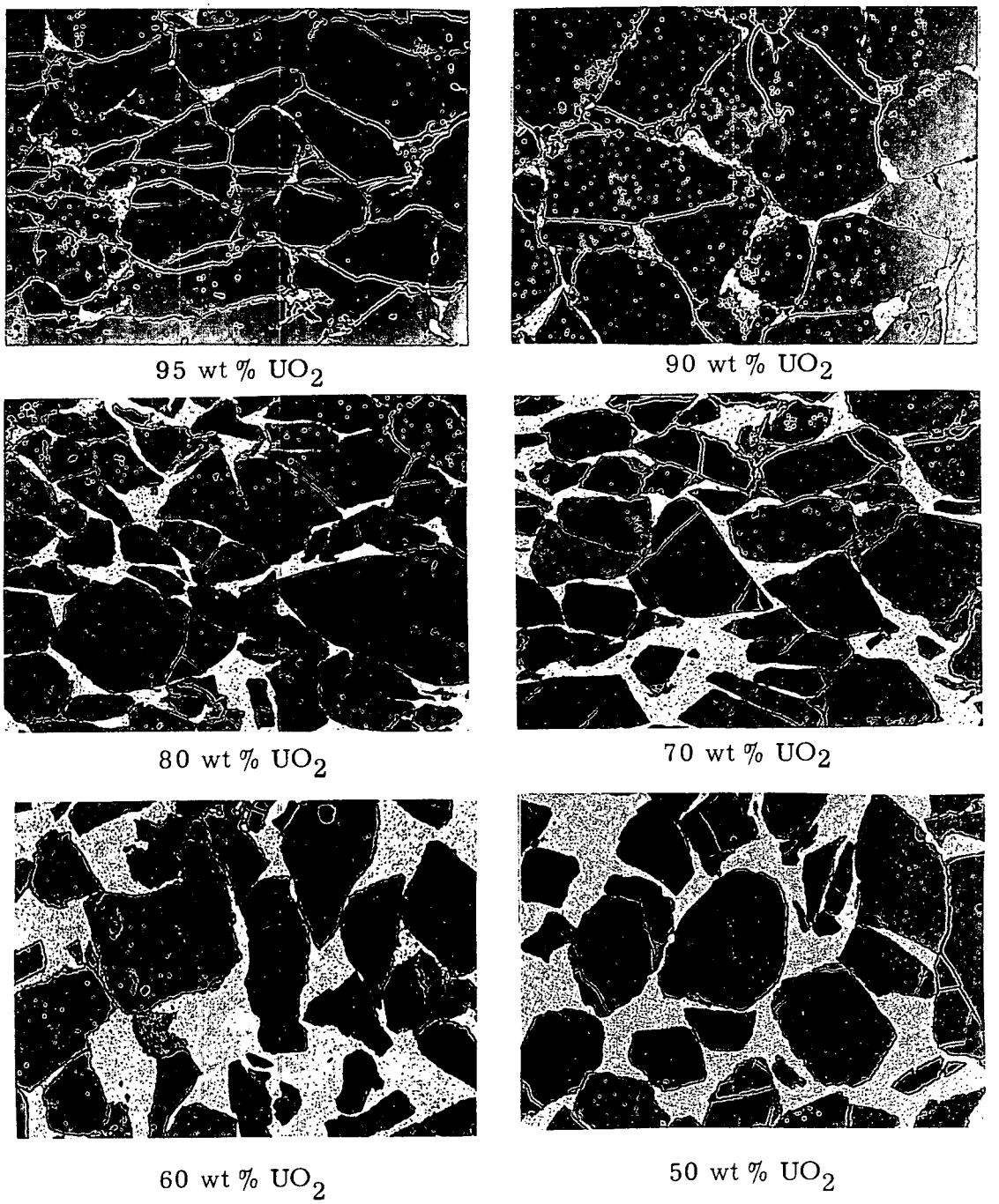

As-Polished, 100X

FIGURE 2.7

Microstructure of UO_2-W Cermets

AEC-GE RICHLAND, WASH.

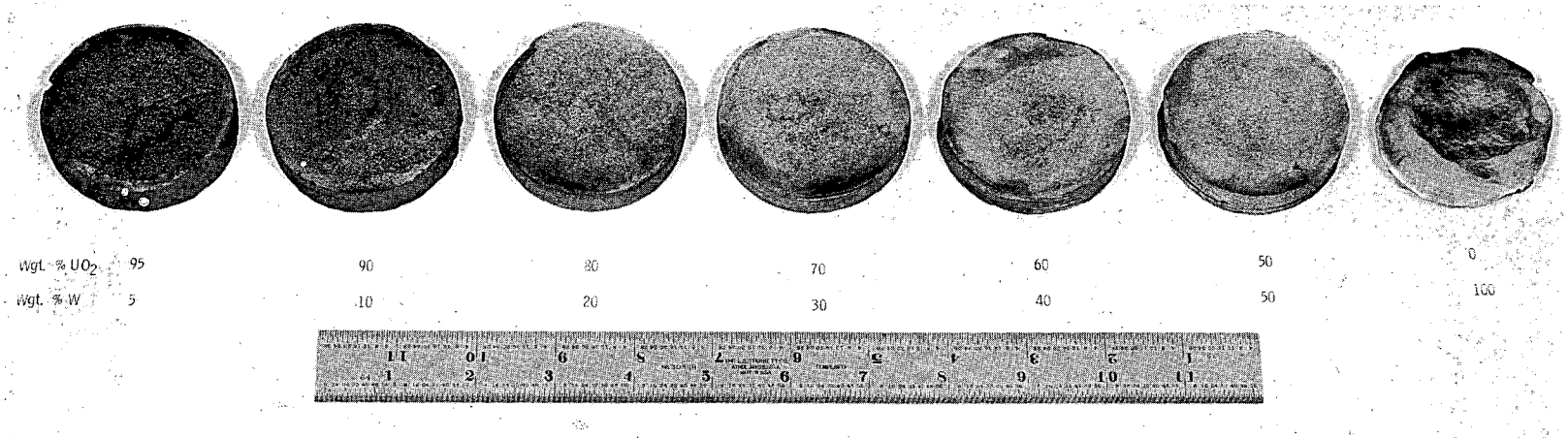

FIGURE 2.8

Impacted Discs of UO_2-W Cermets

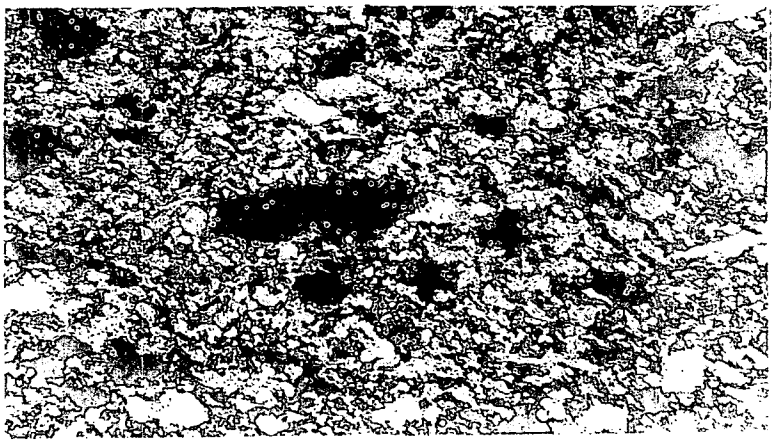

Polished, 100X

FIGURE 2.9

Microstructure of Micronized UO_2-W Cermet

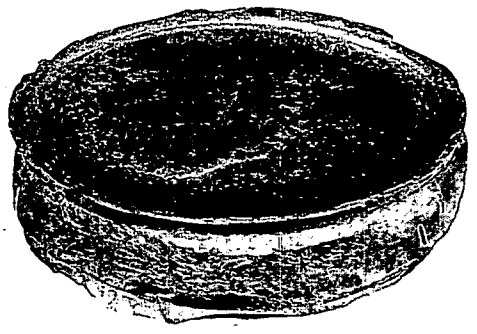

Impacted, 1.5X

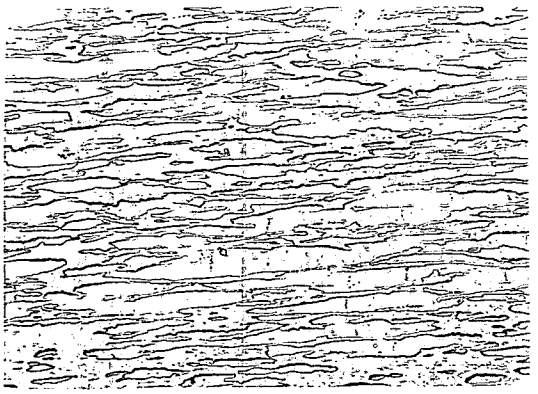

Polished, 100X

FIGURE 2.10

UN-W Cermet

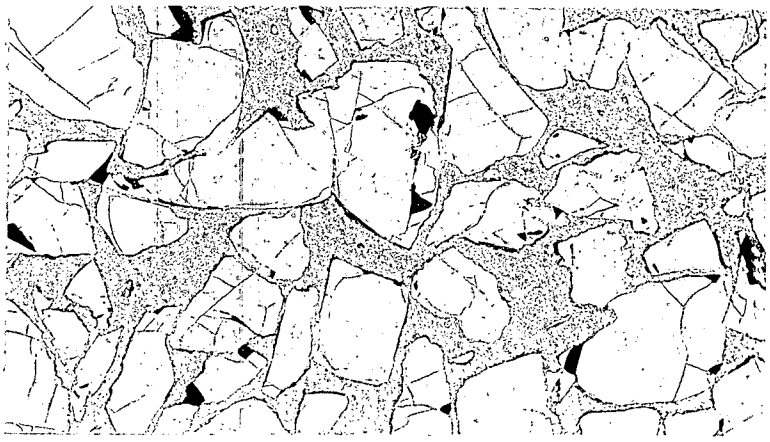

35 vol % Molybdenum

35 vol % Stainless Steel (18-8)

35 vol % NiCr (80-20)

Polished 100X

FIGURE 2.11

Microstructures of UO_2 Cermets

Uranium Monosulfide* - D. W. Brite, K. R. Sump, and J. L. Bates

Uranium monosulfide powder was impacted to 10.81 g/cm^3 (99.5 percent TD). The highest density previously obtained by conventional methods is reported to be approximately 90 percent TD. The US powder (-65 mesh) was heated under vacuum in a stainless steel capsule at 1200 C for 20 minutes before impaction at 400,000 psi, using Bridgman anvils. The impacted US (Figure 2.12) has a metallic appearance and is less susceptible to spalling and crumbling than lower density samples of sintered US.

Electron Microscopy of UO_2-Tungsten Cermet - J. L. Daniel

Reflection electron microscopy was used to study impacted UO_2-50 wt % tungsten cermets at elevated temperatures. At 900 C, the UO_2 in a nonsintered compact developed a continuous surface covering of small crystals while the tungsten remained unchanged (Figure 2.13). At the same temperature, a specimen previously sintered in H_2 at 1750 C for 12 hours developed a dense growth of larger crystallites on the tungsten phase only. At 1500 C, both sintered and nonsintered specimens displayed distinctive crystal growth on both the UO_2 and the tungsten.

Microstructure of Sintered, Impacted UO_2 - D. W. Brite and K. R. Sump

The grain size of impacted and sintered UO_2 can be controlled over a wide range by varying the heating rate, temperature and soaking time during postimpaction sintering. Figure 2.14 shows the effects of these variables on the microstructure of UO_2 impacted to 92.7% TD before sintering. Figure 2.15, reproduced from a previous report,[1] shows the effects of sintering conditions on the density of the same material.

---

* The uranium monosulfide used in these studies was obtained from the Ceramics Research group at Argonne National Laboratory.

(1) Cadwell, J. J. Fuels Development Operation Quarterly Progress Report, July, August, September, 1962, HW-74378. October, 1962. (SECRET)

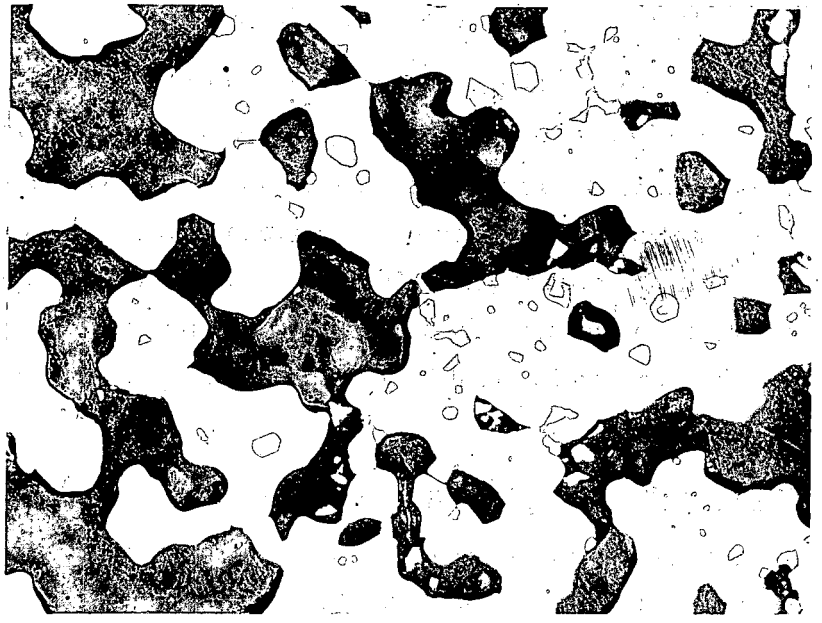

Sintered 250X

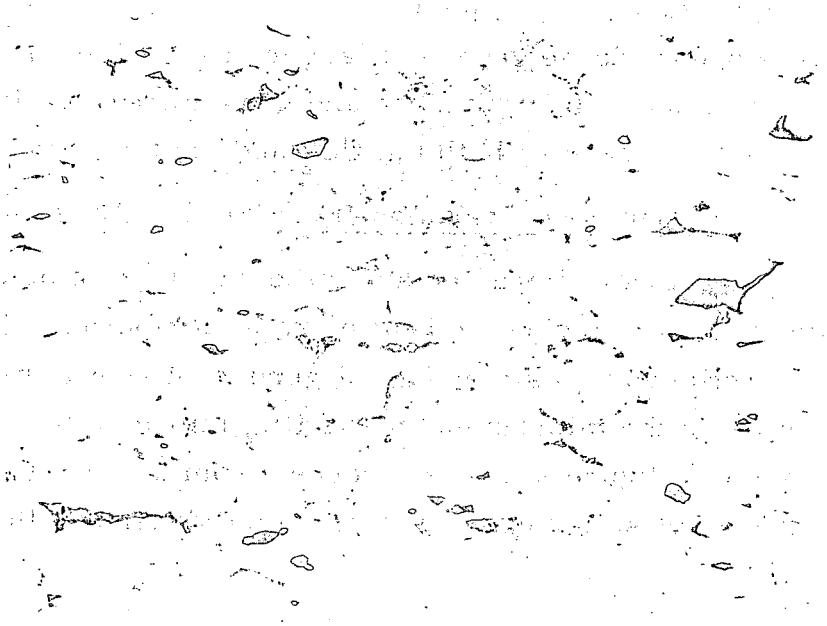

Impacted US 250X

FIGURE 2.12

Microstructures of Sintered and Impacted US

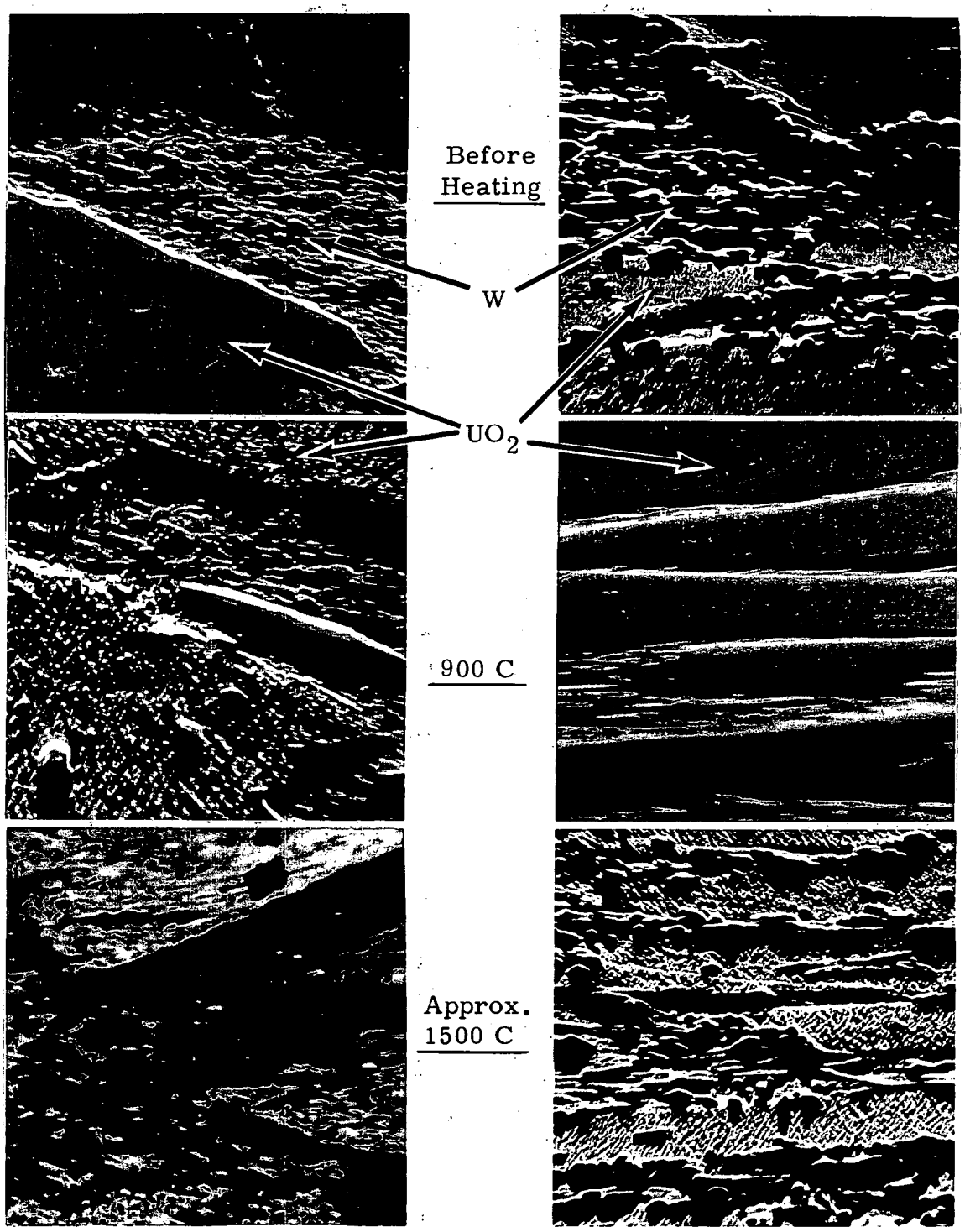

FIGURE 2.13

UO_2-50 wt % Tungsten Cermet (Reflection Electron Microscopy)

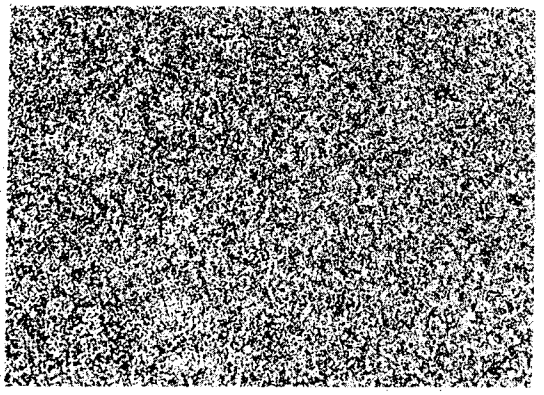

Before Sintering - 92.7% TD

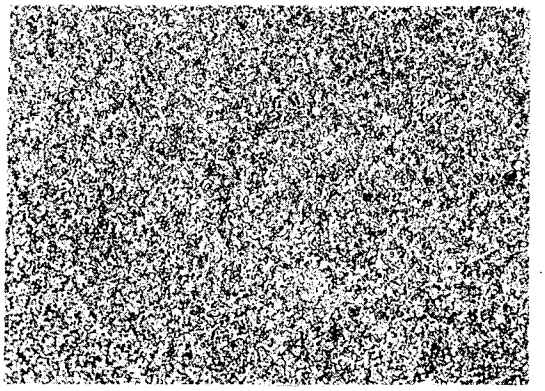

1400 C, 1 hr, 75 C/hr, 96.2% TD

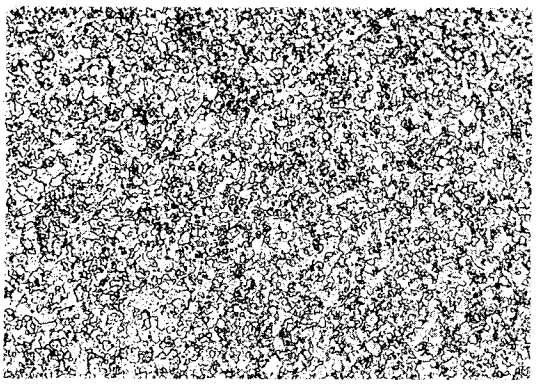

1400 C, 4 hr, 75 C/hr, 97.1% TD

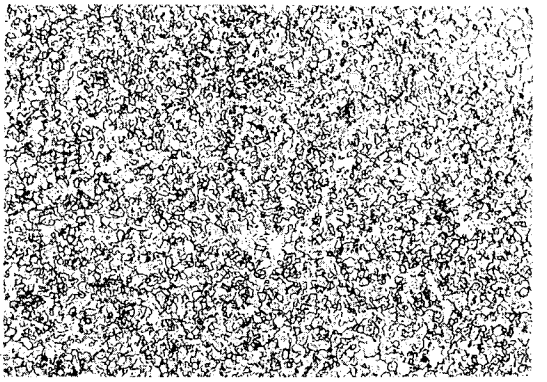

1400 C, 12 hr, 75 C/hr, 97.7% TD

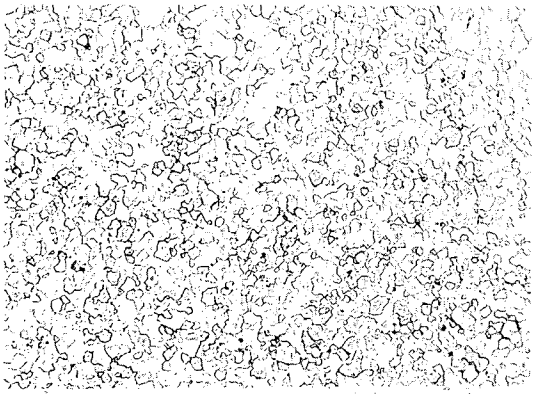

1600 C, 1 hr, 75 C/hr, 98.2% TD

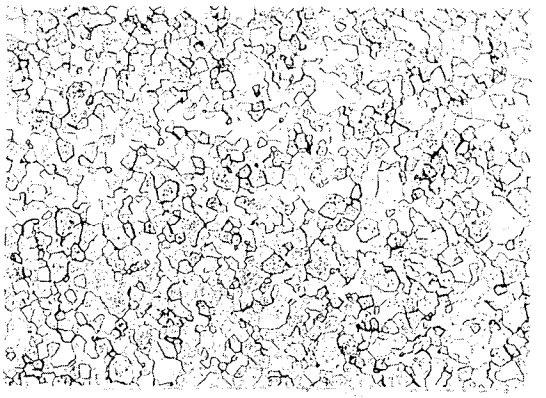

1600 C, 4 hr, 75 C/hr, 98.3% TD

Polished, Etched, 250X

FIGURE 2.14

Microstructures of Impacted and Sintered UO_2

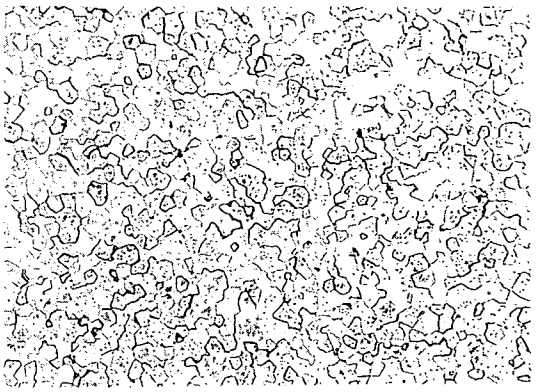

1600 C, 12 hr, 75 C/hr, 98.7% TD

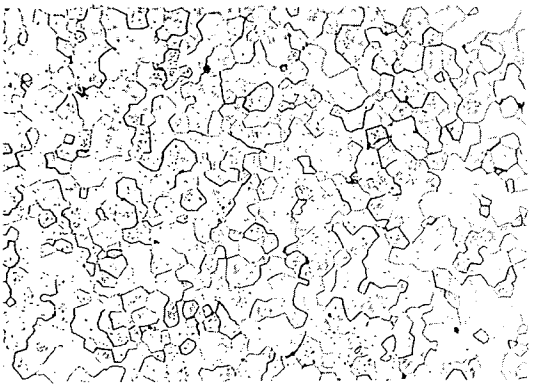

1750 C, 4 hr, 225 C/hr, 98.4 TD

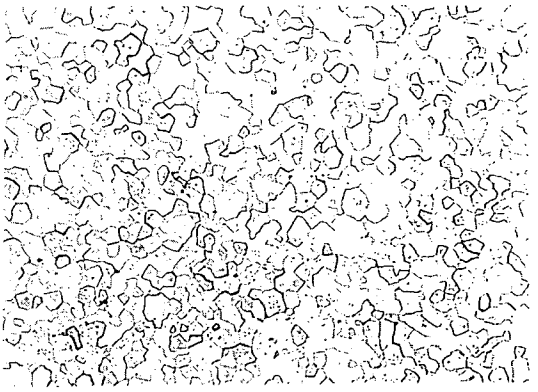

1750 C, 1 hr, 75 C/hr, 98.9% TD

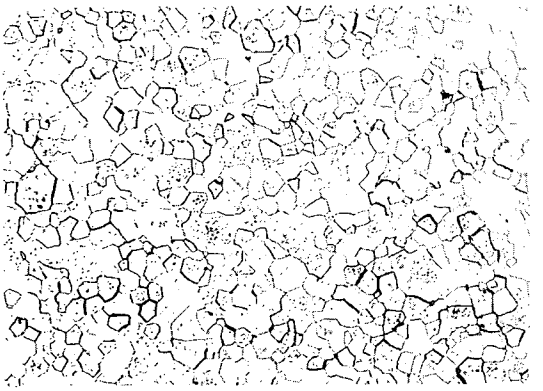

1750 C, 4 hr, 150 C/hr, 99.1% TD

1750 C, 4 hr, 75 C/hr, 99.3% TD

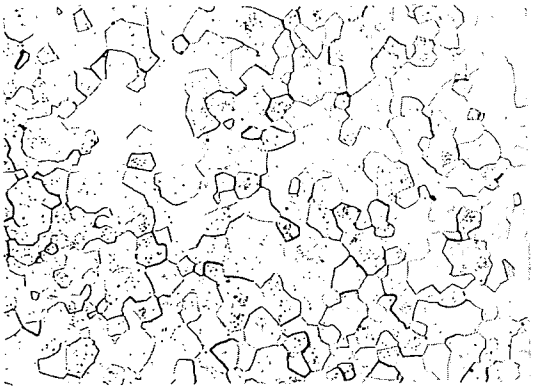

1750 C, 12 hr, 75 C/hr, 99.2% TD

Polished, Etched, 250X

FIGURE 2.14 (contd)

Microstructures of Impacted and Sintered UO_2

AEC-GE RICHLAND, WASH.

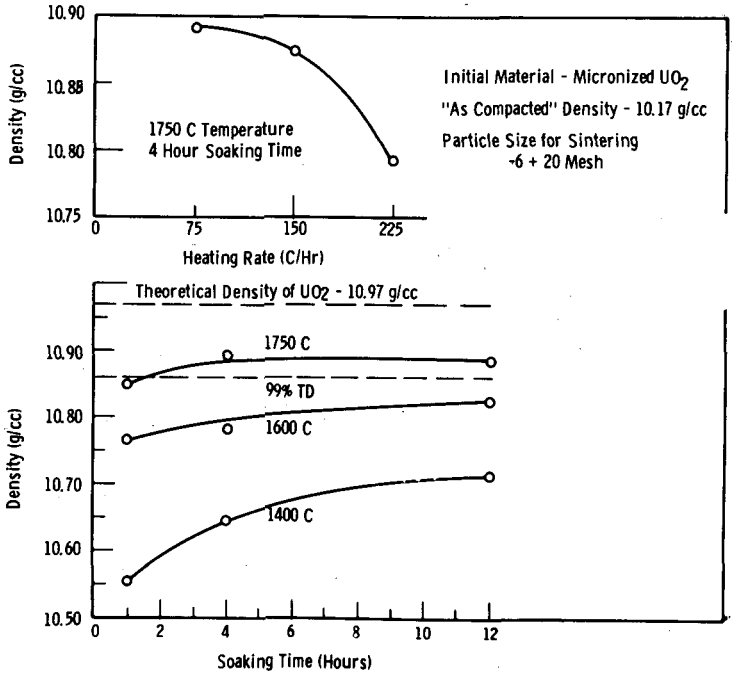

FIGURE 2.15

Effect of Sintering Conditions on Density of Impacted and Sintered UO_2

Thermal Expansion of UO_2 - J. A. Christensen

The specific volume of single crystal $UO_{2.00}$ between 0 C and the melting point (2800 C) is described by:

$$V_T = V_o (1 + 9 \times 10^{-6} T + 6 \times 10^{-9} T^2 + 3 \times 10^{-12} T^3)$$

where

T = temperature (° C)

V_T = specific volume (g cm^{-3}) at temperature T

V_o = specific volume at 0 C.

This equation and the data from which it was derived are shown in Figure 2.16. These data were obtained by high temperature radiography of UO_2 at temperatures to 3100 C.[1]

(1) Cadwell, J. J. Fuels Development Operation Quarterly Progress Report, April, May, June, 1962, HW-74377. July, 1962. (SECRET)

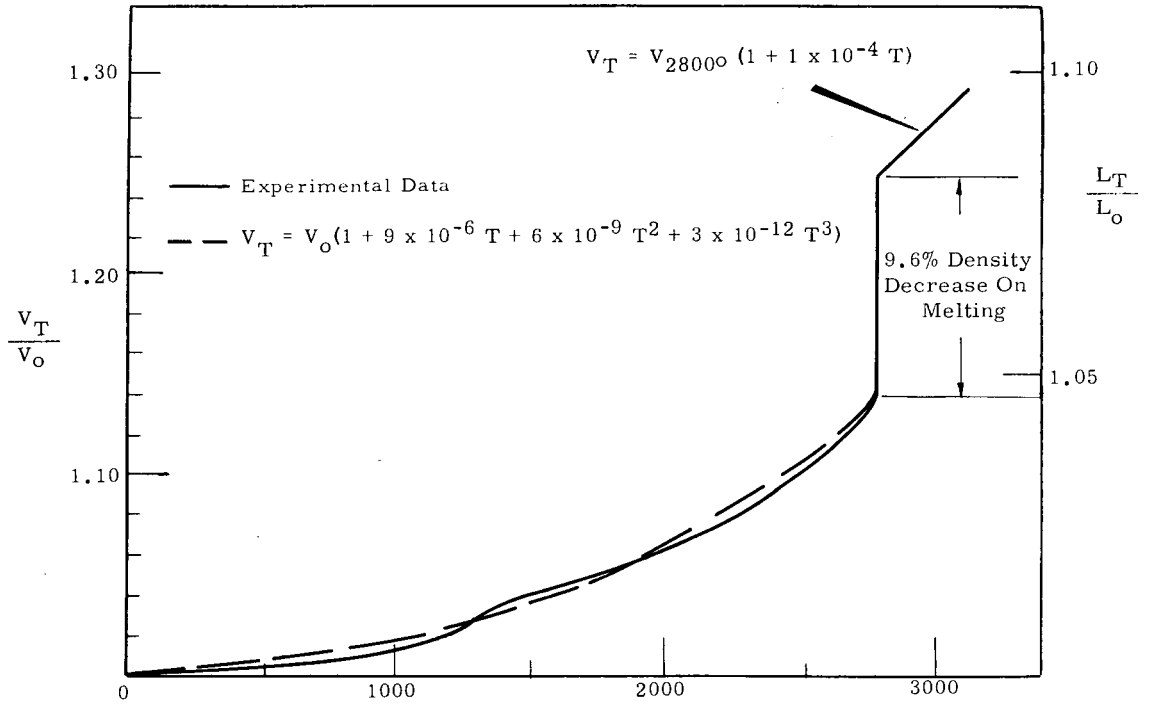

FIGURE 2.16
Thermal Expansion of UO_2

Molten UO_2 - J. A. Christensen

Single crystal UO_2 heated to 3100 C in closed tungsten capsules, in vacuum or under argon, retained an O/U ratio of 2.00 and reacted only slightly with the tungsten. Reaction was restricted to a limited portion of the UO_2-W interface and was less extensive than is typical of W-UO_2 couples heated to only 2800 C in an open system. The most serious UO_2-W interaction which occurred is shown in Figure 17a. Metallic appearing inclusions (Figure 17b) randomly scattered throughout the resolidified UO_2 may be either elemental uranium or impurities (e.g., UC or UN).

The illustrated specimen was heated in an evacuated capsule at 2700, 2800, 2900, and 3000 C with about 8 minute arrests at each temperature. A normalizing quench from 3000 degrees in flowing argon cooled the UO_2 to below 500 C in less than twenty seconds. The UO_2 lattice

Tungsten - UO_2 Interface

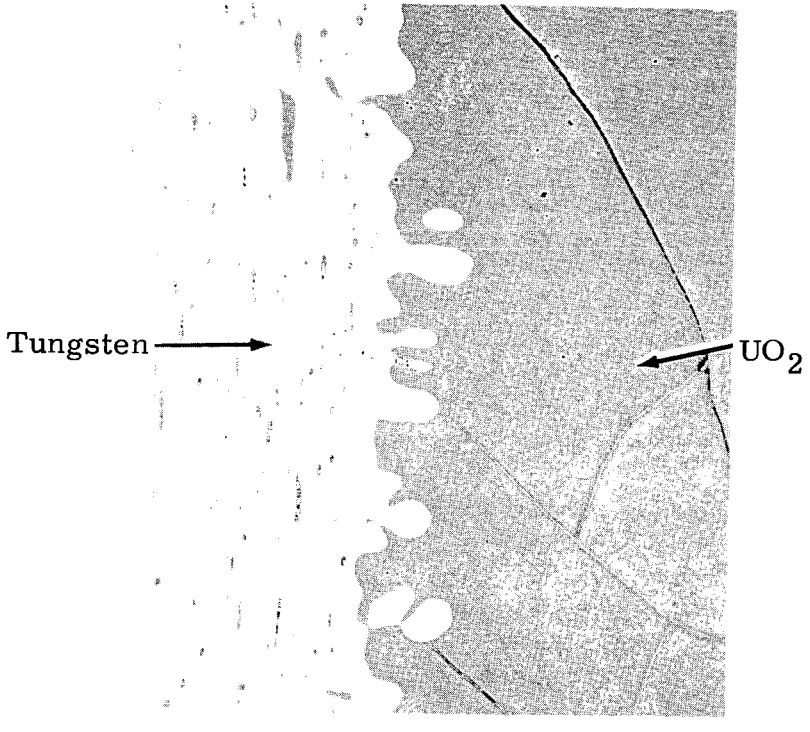

a (500 X)

Region of Most Extensive W-UO_2 Reaction

Typical UO_2 Microstructure

b (500 X)

Small, Metallic-Appearing Inclusions

FIGURE 2.17

UO_2 After Heating to 3000 C in a Closed Tungsten Vessel

parameter was changed less than 0.001 A by the heating treatment indicating no change in stoichiometry. Four additional specimens subjected to similar heating cycles are being examined.

Each of the five capsules was radiographed at temperatures above and below the melting point to determine the volume change during melting. Typical radiographs of a capsule (Figure 2.18) show the silhouette of the UO_2 liquid meniscus at 3000 C, and the deep shrinkage cavity which formed during solidification. The macrograph on the right more clearly shows the solidification pipe and the cracks formed during rapid cooling of the solid. The specific volume of the UO_2 in this capsule increased 9.5% during melting.

Preparation of Samples for In-Reactor UO_2 Melting Studies - J. A. Christensen and L. A. Pember

Tungsten spheres distributed in UO_2 will serve as in-reactor temperature markers for additional determinations of radii of initial molten regions in irradiated UO_2.[2] A random distribution of 1 vol % tungsten (-100 +200 mesh spheres) in sintered UO_2 was obtained by wet mulling the mixture, pressing and sintering in 1700 C hydrogen for twelve hours (Figure 2.19). A uranium dioxide density of 10.5 g/cm^3 was attained.

Hardness of UO_2 - J. L. Bates

The hardness of a (100) crystal face of UO_2 showed a symmetrical, four-fold variation with Knoop indentor orientation (Figure 2.20), with an average variation between maxima and minima of approximately 7.5%. Previous measurements revealed a two-fold symmetry on the (110) and (213) planes.[1, 2] Both results are compatible with the symmetry of the Knoop indentor and the crystal planes examined.

---

(1) Cadwell, J. J. Fuels Development Operation Quarterly Progress Report, July, August, September, 1962, HW-74378. October, 1962. (SECRET)

(2) Cadwell, J. J. Fuels Development Operation Quarterly Progress Report, July, August, September, 1962, HW-74377. July, 1962. (SECRET)

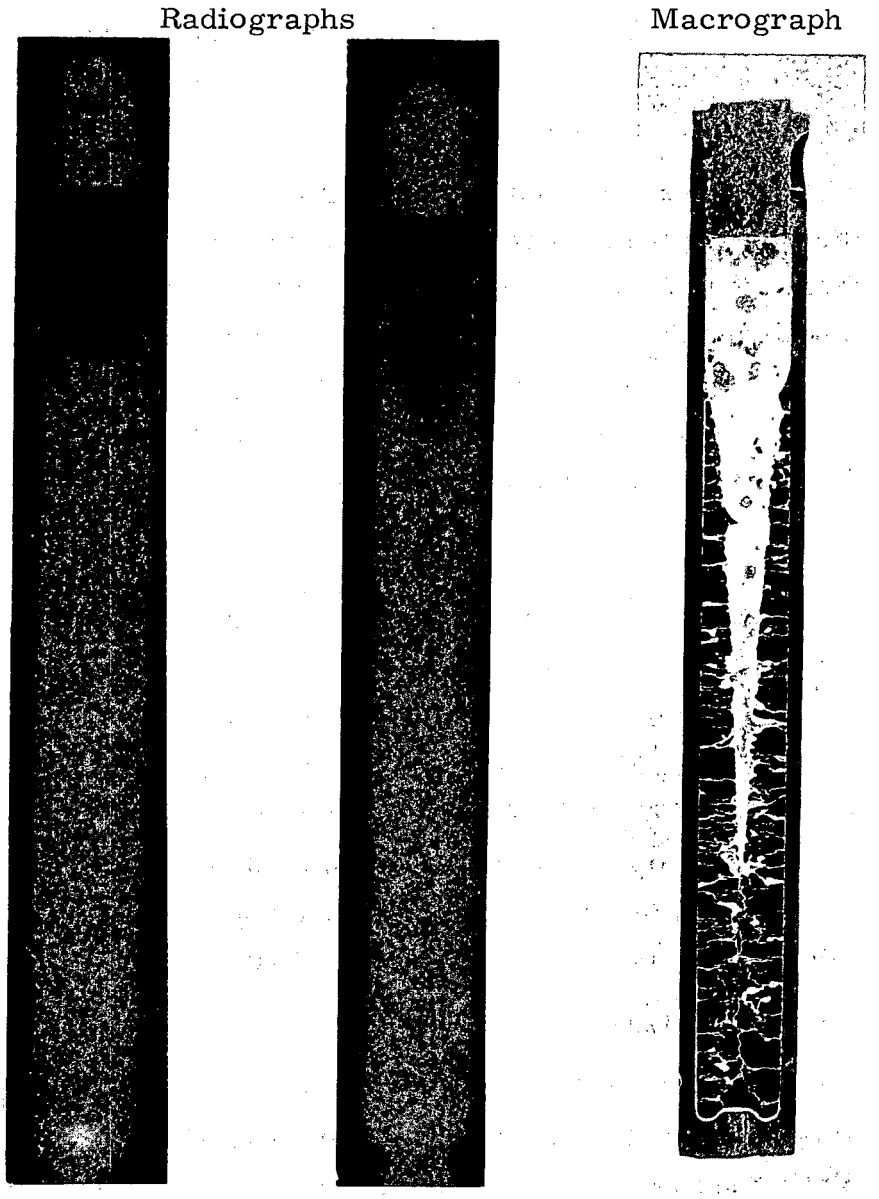

FIGURE 2.18

Uranium Dioxide Heated to 3000 C in a Closed Tungsten Vessel. (Radiograph at left was made with UO_2 at 3000 C to measure density of $UO_{2(\ell)}$.)

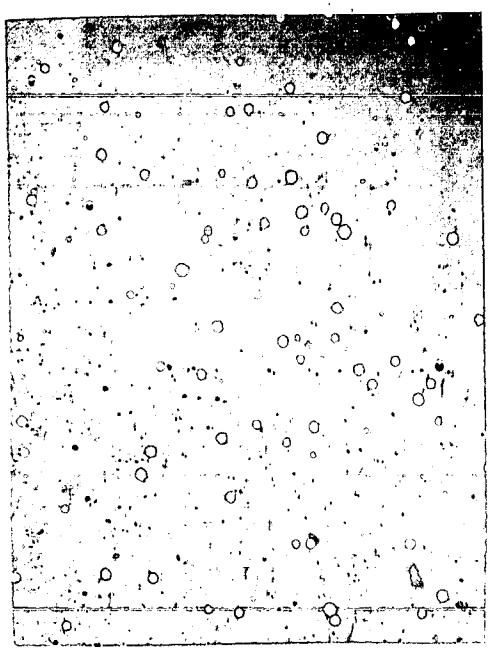

10X

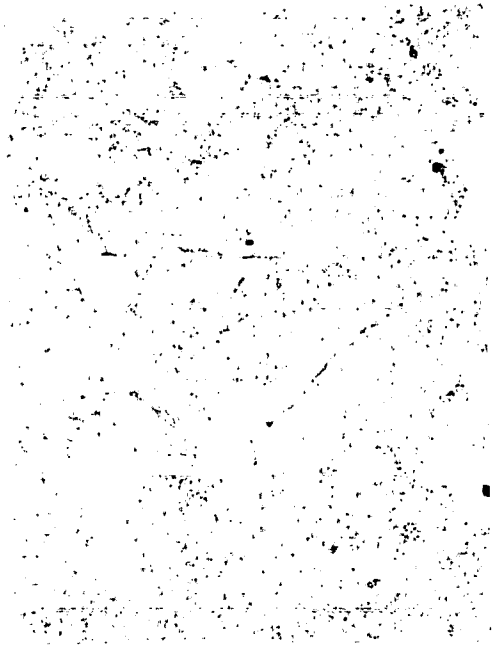

100X

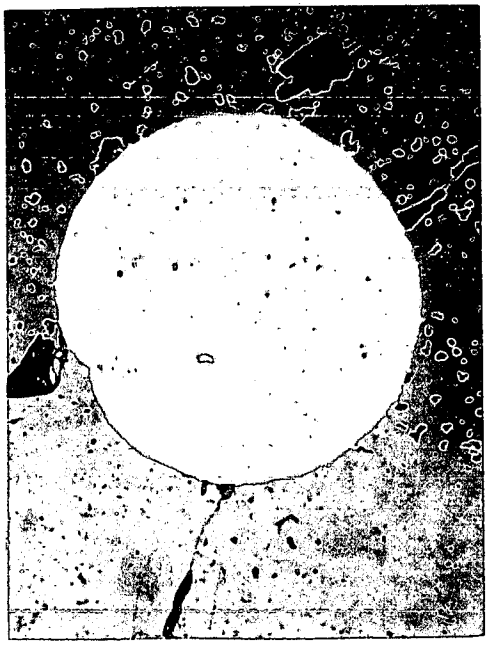

750X

FIGURE 2.19

Dispersion of Tungsten Spheres in Sintered UO_2

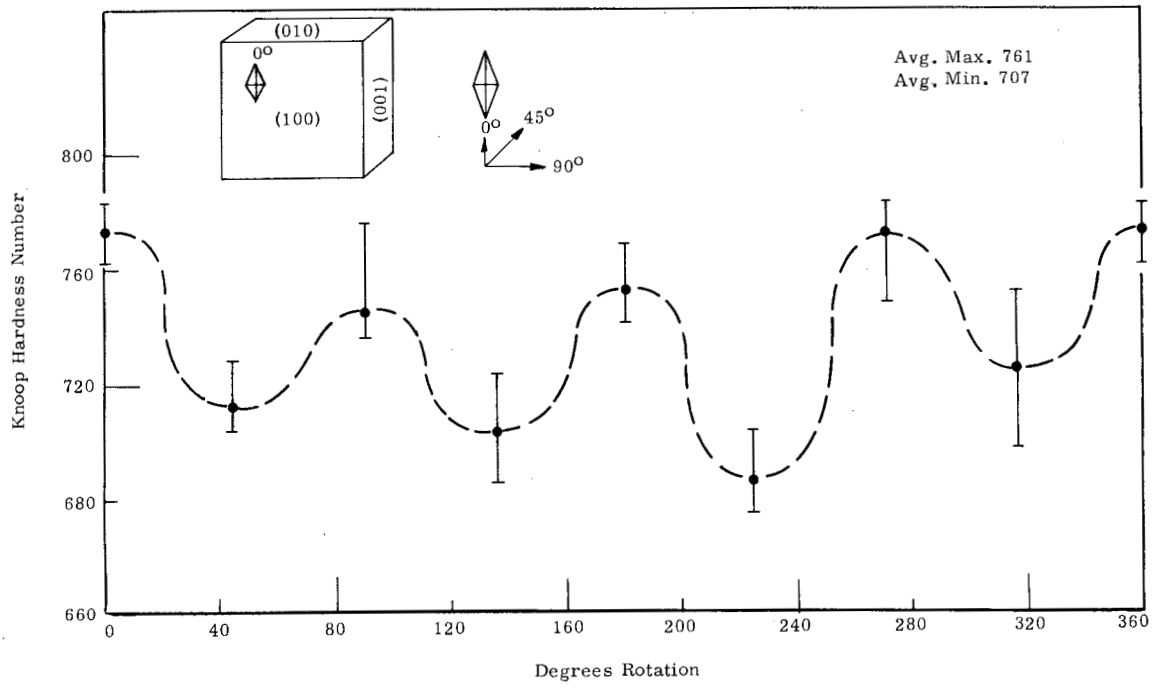

FIGURE 2. 20

Hardness of UO_2 (100) Plane as a Function of Knoop Indentor Orientation

The maxima occurred when the long dimension of the Knoop indentor was parallel to the intersection of (100) planes. The minima were observed when the long dimension was parallel to intersections of (100) with (111) planes. This is consistent with other hardness measurements which have shown the (100) plane to be harder than the (111) plane.

Active room temperature slip systems were deduced from the directions of slip lines and the distributions of etch pits formed adjacent to hardness impressions (Figure 2. 21). The (100) plane was the only active slip plane observed.

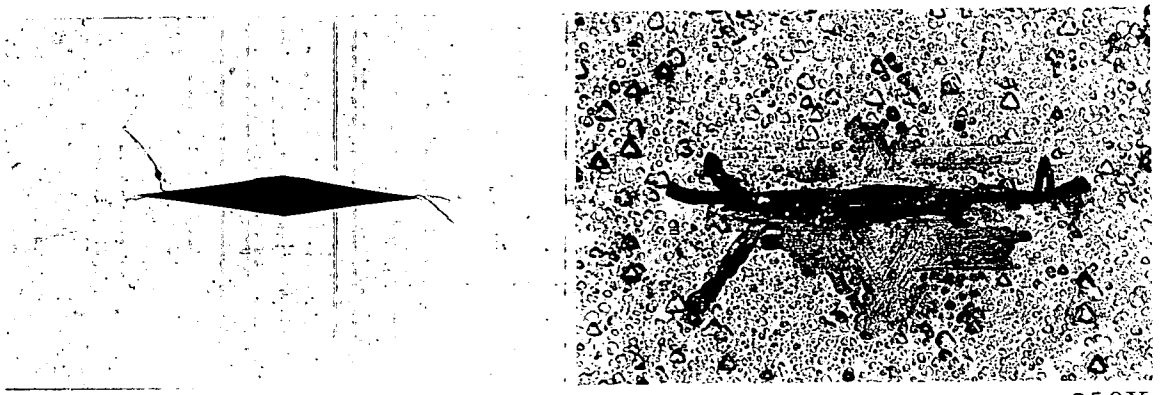

Unetched 250X Etched 250X

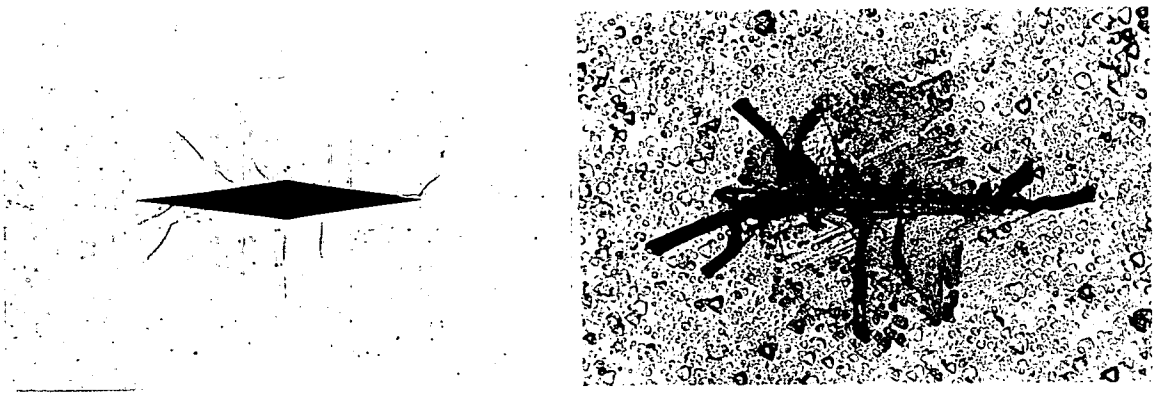

Unetched 250X Etched 250X

FIGURE 2.21

Slip Lines and Etch Pits Formed Near Microhardness Indentor Marks on UO_2 Single Crystal. Crystal Surfaces are (111) Planes.

Release of Sorbed Gases from UO_2 by Ionizing Radiation - H. J. Anderson

Extensive gas desorption from fused uranium dioxide resulted from irradiation at room temperature with ionizing radiation from a Co^{60} source. Specimens were sealed in pyrex capsules under vacuum, or in helium at pressures of approximately 0.3 atmospheres, and irradiated in an 8.9×10^5 R/hr field for periods up to 200 hours.

Exposures of 100 to 200 hours caused a release of sorbed gases comparable to that which normally occurs during vacuum annealing at

800 C to 1000 C. The released gases were principally H_2 with N_2, CO_2, and H_2O also present. These data indicate that release of sorbed gases in fuel elements may be increased by reactor radiation.

Acceleration of gas release rates was also achieved by applying a high frequency (400 kc) induction field to the UO_2 sample. Desorption at slightly above room temperature was equivalent to 25% of the gas released by vacuum extraction at 1000 C.

Evaluation of UO_2 Analyses - H. J. Anderson

The reliability of purity values reported for commercially fused UO_2 was evaluated in a study of analytical techniques. Determination of density, stoichiometry, and carbon and nitrogen content were checked against the vendor's values on 15 samples representing 1500 pounds of recently purchased fused UO_2. Density, stoichiometry and carbon values were in good agreement, but nitrogen values disagreed by as much as a factor of two. A new dissolution technique for Kjeldahl analysis that was devised will be evaluated also by the vendor.

Determination of Pore Size Distribution in UO_2 - H. J. Anderson

A contact angle of 111 degrees between mercury and UO_2 (single crystal) was determined by capillary depression techniques. In the determination of pore size distribution by mercury porosimetry, this angle has been generally assumed to be 135 degrees (the same as that between mercury and glass).

UO_2 Specimens for Basic Research - H. J. Anderson

Standardized uranium dioxide specimens were prepared for distribution as indicated in the following table.

TABLE 2.3

STANDARD UO_2 SPECIMENS

Recipient	Specimen
Cornell University	Two precharacterized single crystals
National Bureau of Standards	Ten 1-gram single crystal spheres
Hahn-Meitner Institute (Berlin)	Fifty single crystal spheres, 1-5 mm diameter
Commissariat a l'Energie Atomique	Fifty single crystal spheres

The samples being sent to Europe (through Euratom) will be used for fission gas diffusion measurements.

High-Temperature Electron Microscopy - J. O. McPartland

Reflection electron microscopy specimens were heated to temperatures greater than 1400 C with an auxiliary electron gun. A 5 kv, low-energy electron gun was used to minimize microscope modification and interference with routine microscopy operations.

Modifications being made in the gun focus will lead to higher temperatures through selected area heating.

FUELS DEVELOPMENT

Impaction of UO_2-PuO_2 - D. W. Brite, K. R. Sump, W. T. Ross, and L. G. Merker

Mixed UO_2–2.5 wt% PuO_2 was impacted at 1200 C and 145,000 psi to demonstrate the feasibility of preparing plutonium-bearing fuels by this method. Complete containment of the fuel within the capsule during heating and impaction was achieved by using a double-canning technique. A hood over the impact machine (Figure 3.1) provided secondary protection. Figure 3.2 shows the capsule assembly components, the impacted UO_2-PuO_2 capsule, and a macrosection through a similarly impacted UO_2 capsule.

The UO_2-PuO_2 fuel was a mechanically blended mixture of PuO_2 (from calcined plutonium oxalate) and UO_2 powder (specific surface area, 1.2 m^2/g) produced by ball-milling scrap sintered and crushed UO_2. The mixture was pressed at 6000 psi into the inner can and closed with porous stainless steel disc. The capsule was enclosed in a second can and heated in vacuum at 1200 C immediately before impaction.

After impaction, no plutonium was detectable on the capsule or in the impact machine.

Planned experiments involve impaction of UO_2-PuO_2 mixtures at pressures 400,000 psi to prepare high-density fuel materials for fuel fabrication.

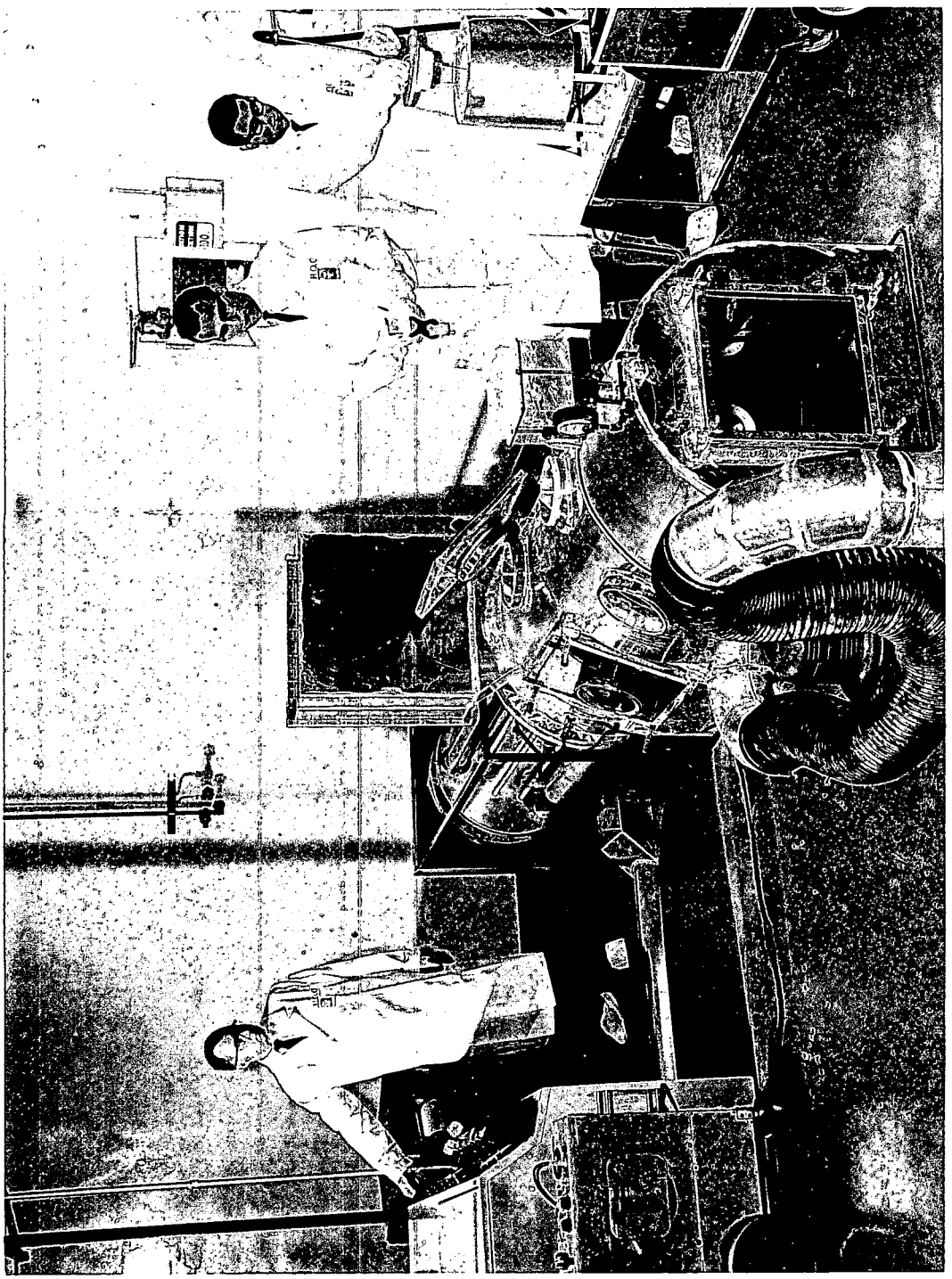

FIGURE 3.1
Impaction of UO_2-PuO_2

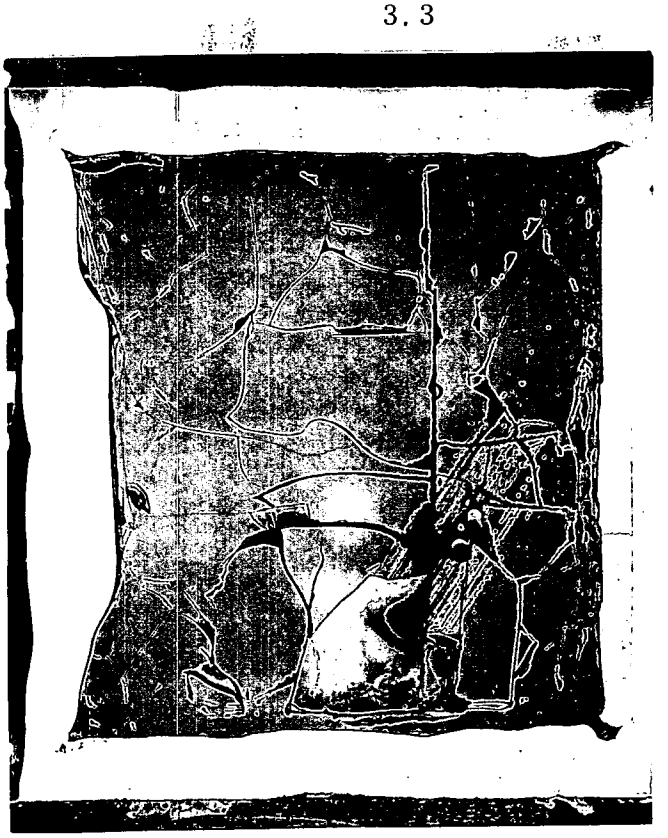

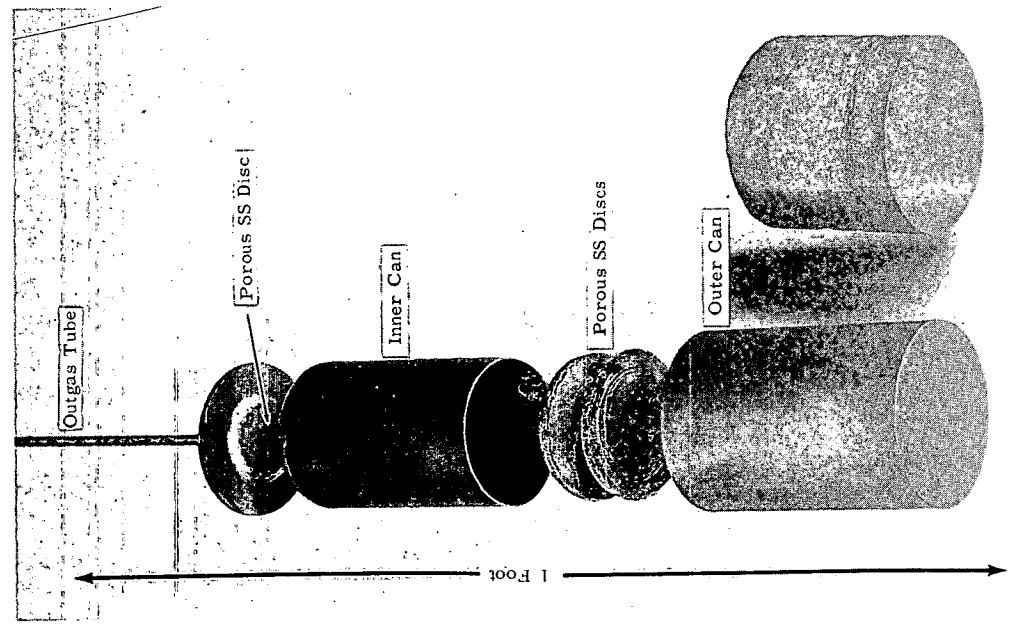

FIGURE 3.2
Capsule Assembly and Impacted Can Containing PuO_2-UO_2 (Left) and Axial Cross Section of Impacted Can (Right)

Fuel Element Rejuvenation - R. C. Smith

A fuel element, Figure 3.3, designed to test the feasibility of fuel rejuvenation was fabricated and sent to the NRTS (National Reactor Testing Station) for irradiation.(1) "Fuel rejuvenation" is defined as re-enrichment of the fuel without total reprocessing.

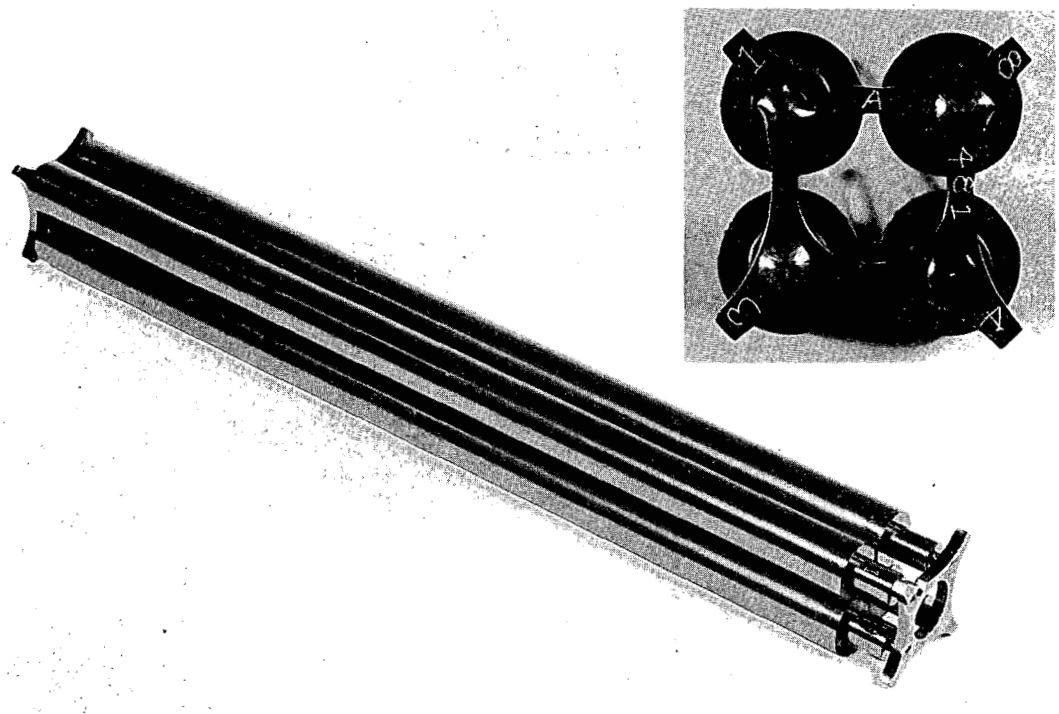

FIGURE 3.3

Fuel Rejuvenation Test Element

0622293

(1) Horn, G. R. and R. C. Smith. Irradiation Proposal -- A Fuel Element Rejuvenation Experiment: GEH-4-81, HW-75783 RD. December 7, 1962.

After irradiation the element will be re-enriched by opening each rod and inserting PuO_2 or enriched UO_2 into a concentric, 1/8-inch ID ZrO_2 tube (Figure 3.4). The fuel element will then be returned to the MTR (Materials Testing Reactor) for a second irradiation. A series of re-irradiations may be possible.

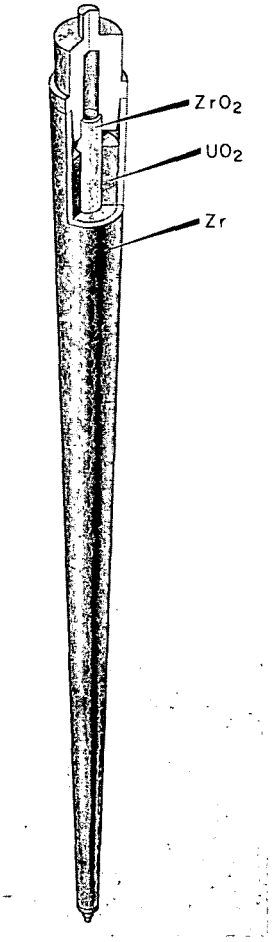

FIGURE 3.4
Rejuvenation Fuel Rod

The relatively high expense of cladding and fabrication for a fuel element and the high cost of reprocessing for fuel recycle provides an incentive for rejuvenating fuel elements for re-enrichment. The cost of sufficient enrichment material to overcome fission product poisons left in partially burned-out fuel elements, added to that necessary to re-enrich the fuel back to time zero reactivity, may be considerably less than fuel reprocessing and refabricating costs.

The irradiation and remote handling experience to be derived from this initial experiment will be applicable to a series of rejuvenation techniques.

Hot Isostatic Pressing - J. J. Hauth

UO_2 rods clad in thin-wall stainless steel were fabricated by swaging and hot isostatic pressing as part of a joint program with Battelle Memorial Institute (BMI).[1] Mixtures comprising 70 wt% fused UO_2 and 30 wt% micronized UO_2 were partially predensified by swaging to 80–85% TD in AISI 304L SS cladding (0.010-inch wall thickness), then hot isostatically pressed (1000 C, 10,000 psi) at BMI. The results for typical mixtures are shown in Table 3.1 and in Figures 3.5A to 3.5D.

TABLE 3.1

Fused UO_2 Mesh Size	Fabrication Method	Swaged Density, % TD	Final Average Density, % TD	O/U (average)
-100 +200	hot swaging (800C)	83	94.2	2.011
- 65 +100	hot swaging	85	93.7	2.010
- 35 + 65	cold swaging	81	93.6	2.004
- 20	hot swaging	83	96.3	2.009

Hot isostatically pressed fuel elements having high density core material and thin cladding of high integrity appear to be feasible. The principal problem is the agglomeration of the active, micronized UO_2 (Figures 26B and 26C). One possible solution is to use micronized powder which has been compacted at room temperature by high-energy-rate impaction

(1) Cadwell, J. J. Fuels Development Operation Quarterly Progress Report, January, February, March, 1962, HW-72347. April, 1962. SECRET

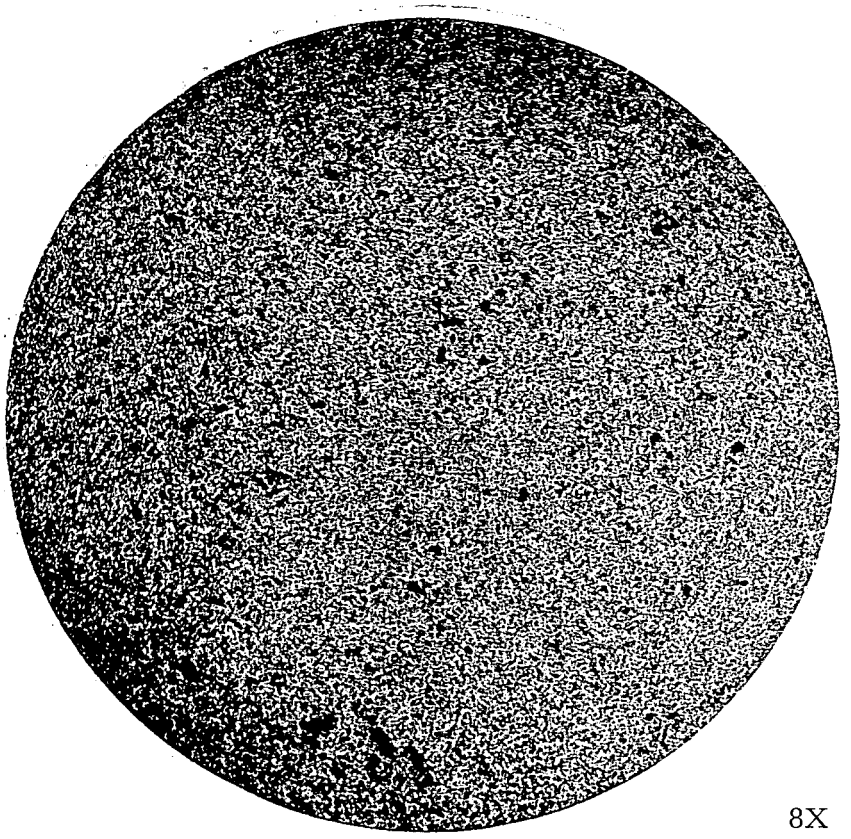

8X

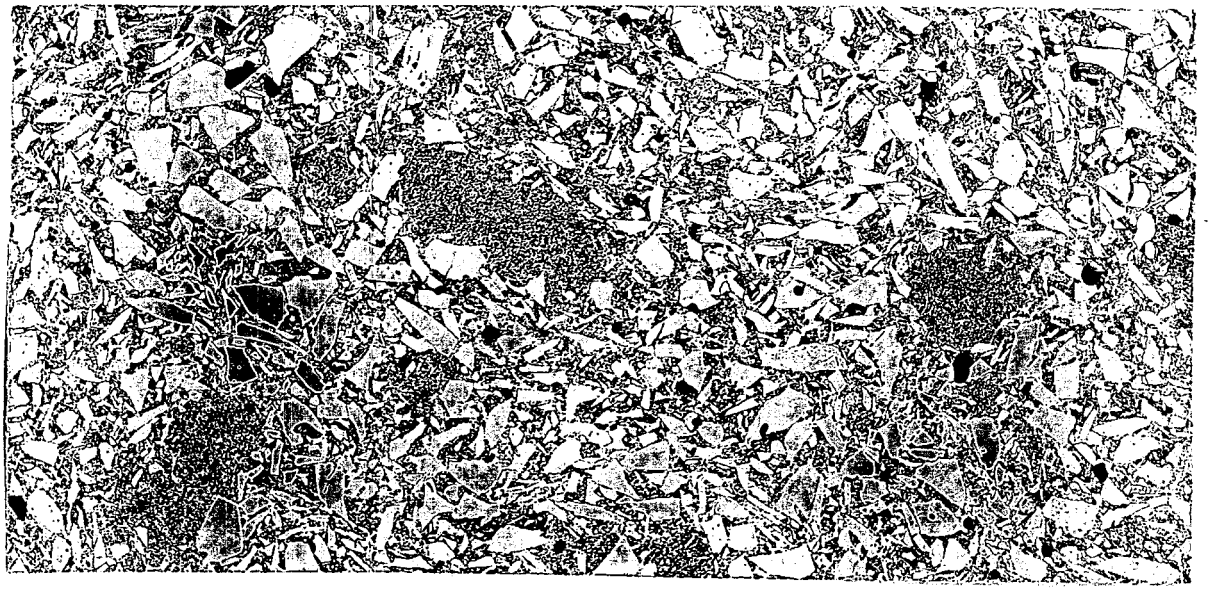

100X

FIGURE 3.5A

Hot Isostatically Pressed UO_2:
70 wt% Fused (-100 +200 mesh), 30 wt% Micronized
5K91C; 5K91B
AEC-GE RICHLAND, WASH.

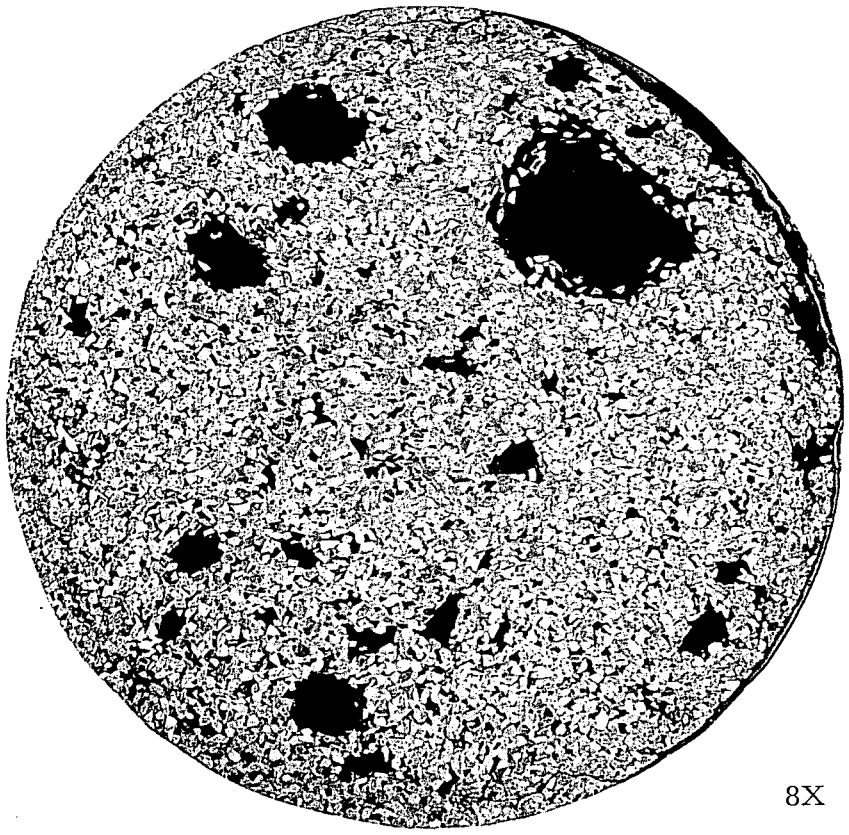

8X

100X

FIGURE 3.5B

Hot Isostatically Pressed UO_2:
70 wt% Fused (-65 +100 mesh), 30 wt% Micronized

5K87D; 5K87C
AEC-GE RICHLAND, WASH.

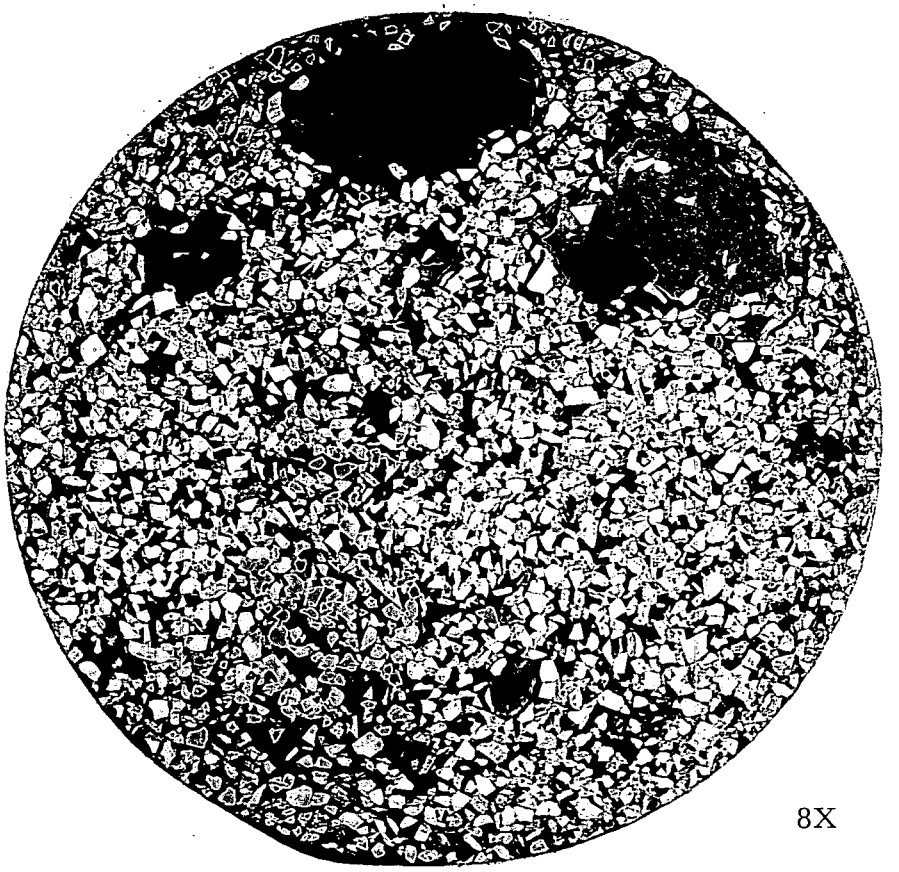

8X

100X

FIGURE 3.5C

Hot Isostatically Pressed UO_2:
70 wt% Fused (-35 +65 mesh), 30 wt% Micronized
5K88C; 5K88B

AEC-GE RICHLAND, WASH.

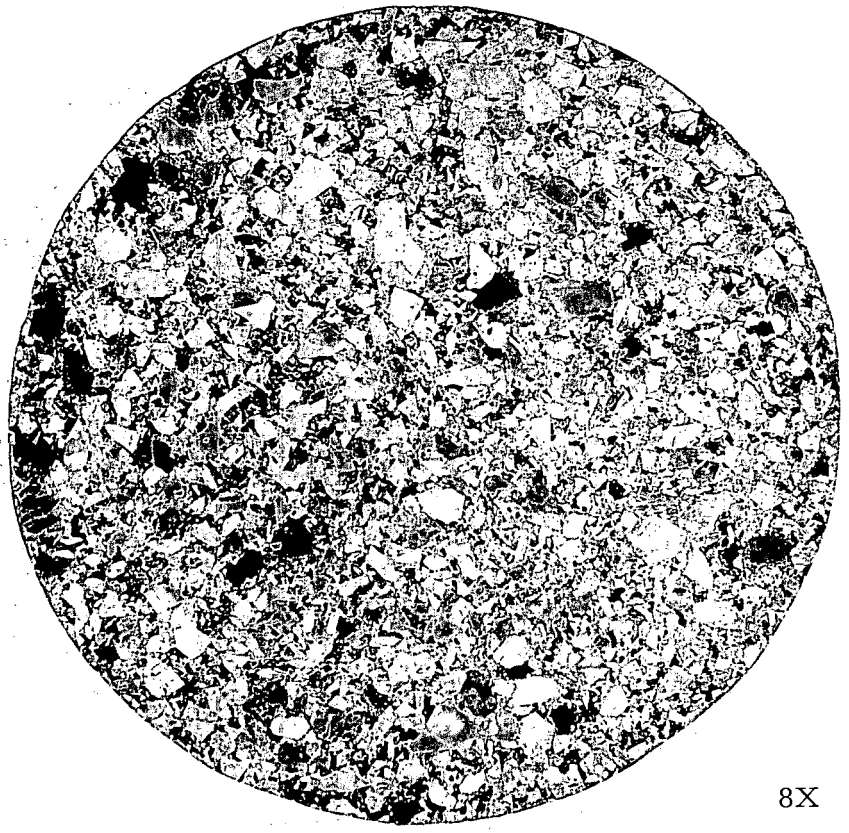

8X

100X

FIGURE 3.5D

Hot Isostatically Pressed UO_2:
70 wt% Fused (-20 mesh), 30 wt% Micronized

5K86D; 5K86C
AEC-GE RICHLAND, WASH.

and then pulverized. Rods comprising mixtures of this material with fused or high-energy-rate impacted, 99% dense particles are being fabricated.

Vibrational Compaction Studies - J. J. Hauth

A new method of vibrational compaction, involving transverse excitation of cladding suspended vertically from a horizontal bar, was investigated for use in fabricating fuel elements comprising plutonium-bearing or other fuels clad in aluminum alloys or thin-wall stainless steel. A 5000 pound force vibrator was modified for horizontal operation. The fuel cladding was coupled to the vibrator through a horizontal steel bar (Figure 3.6).

Transverse excitation simplifies the transmission of vibrational energy through the wall of a shielded facility. Stresses in the cladding at the point of coupling are minimized, so that simpler coupling devices can be used than those required for vertical excitation. Thus, eight-foot-long UO_2 rods clad in SAP (0.551-inch OD, 0.022-inch wall thickness) or stainless steel (0.56-inch OD, 0.010-inch wall thickness) withstood prolonged transverse vibration at accelerations greater than 50 gravities, at frequencies that were varied continuously between 180 and 2500 cps. Compaction efficiencies of 91% were achieved in eight-foot-long fuel rods containing fused UO_2.

Hot Vibrational Compaction - J. J. Hauth and D. R. Burroughs

Hot vibrational compaction of fuels clad in aluminum alloys or stainless steel may increase bulk fuel densities and reduce fabrication time. An undetermined amount of sintering would also increase fuel conductivity. A rapid density increase of 2.5% TD was obtained by resistance heating a previously compacted, SAP-clad UO_2 rod to ~150 C during transverse vibration (Figure 3.6). No distortion of the cladding was apparent.

Resistance heating Zircaloy-clad rods to 850–900 C during transverse vibration caused only a minor increase in density. Loading and compaction of fused UO_2 in thin-wall (0.010 inch) stainless steel and in Inconel tubes at 800–900 C resulted in a very slight, uniform distortion of the cladding as it cooled and contracted around the coarse (6 mesh) UO_2 grains. The ability to achieve higher density is directly related to the thermal expansion characteristics of the cladding and core materials.

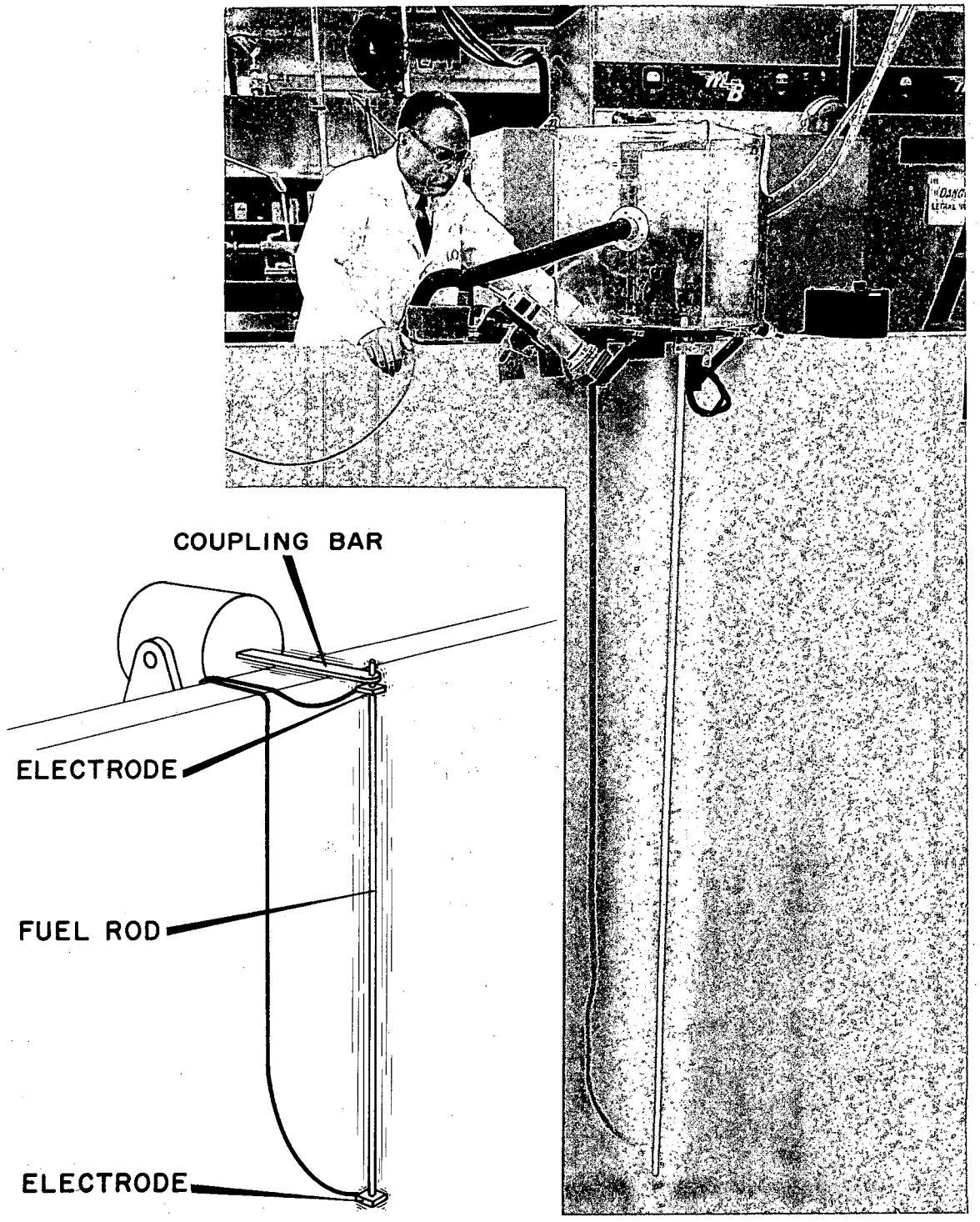

FIGURE 3.6

Hot Vibrational Compaction by Transverse Excitation

PRTR Fuel Fabrication - C. H. Bloomster

Conversion of the Plutonium Recycle Test Reactor (PRTR) fuel loading to uniformly enriched, mixed-oxide fuel elements is approximately 40% complete. Forty-two UO_2-PuO_2 19-rod cluster fuel elements (26 swaged and 16 vibrationally compacted) have been fabricated. These are being charged at the rate of about six per month. The mixed-oxide elements have been operated successfully to a maximum exposure of 600 Mwd/ton and at a maximum fuel element power of 1150 kw. Fabrication of the remaining elements is ahead of schedule.

Plutonium Distribution in Incrementally Loaded PRTR Fuel Rods - R. E. Bardsley and C. H. Bloomster

The uniformity of plutonium distribution in incrementally loaded, UO_2-PuO_2 PRTR Fuel rods was improved by addition of the plutonium-containing fuel in 150 increments rather than 80, as shown by autoradiographs reproduced in Figure 3.7.

To supplement loading studies, preliminary investigation was made of nondestructive tests for determining plutonium concentration variations in a fuel rod. Although autoradiography results can be related empirically to chemical analyses, the technique inherently has neither the sensitivity nor capacity for routine testing of large numbers of fuel rods. Tests based on eddy current, gamma attenuation, neutron activation, and neutron attenuation principles appear more promising.

Areas of plutonium segregation in a rod were well defined by eddy current tests (Figure 3.8).

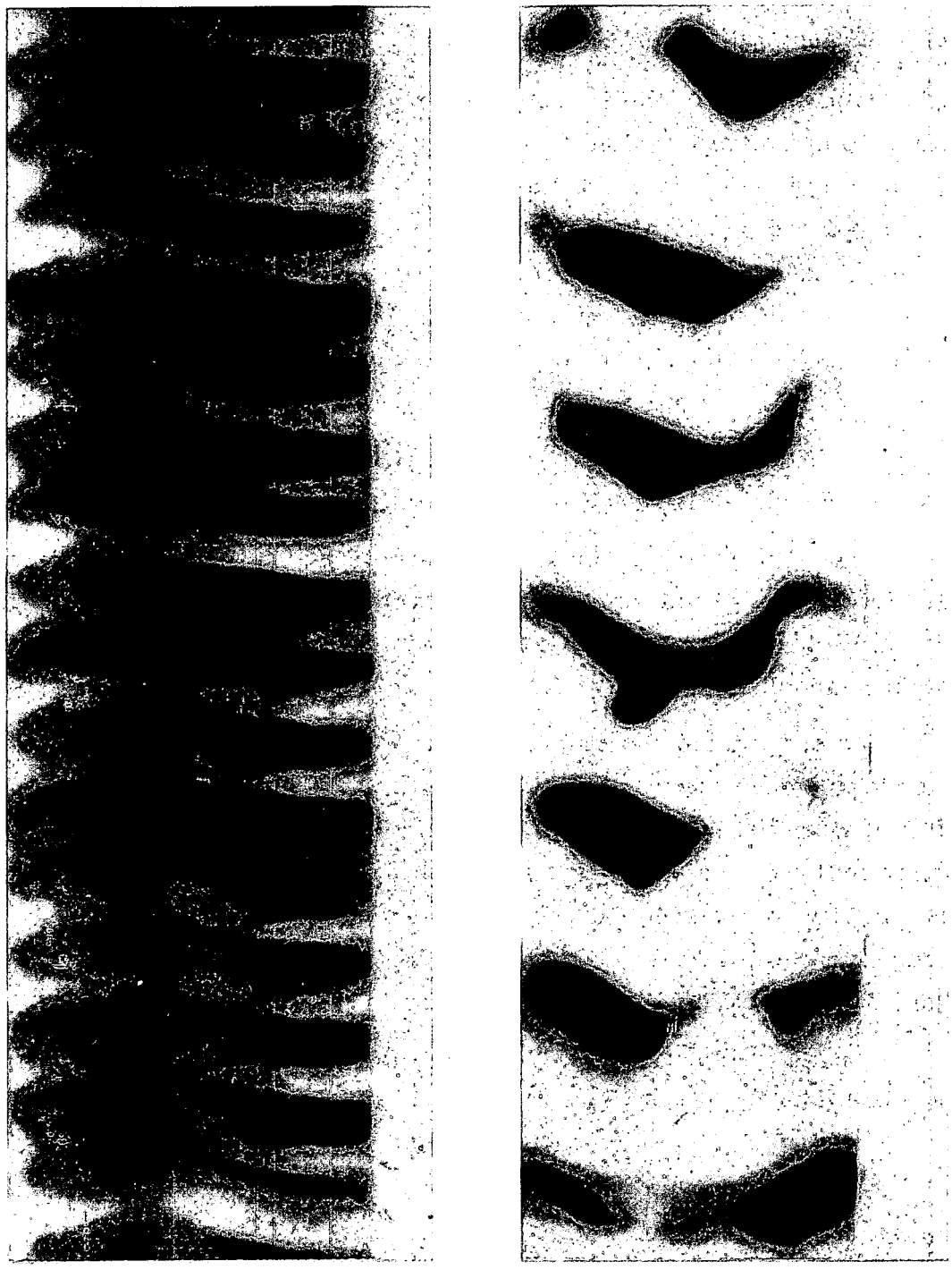

FIGURE 3.7

Comparative Autoradiographs
Left: 150-Increment Rod Vibrated Continuously During Loading
Right: 80-Increment Rod Loaded Without Vibration

0630094-2
AEC-GE RICHLAND, WASH.

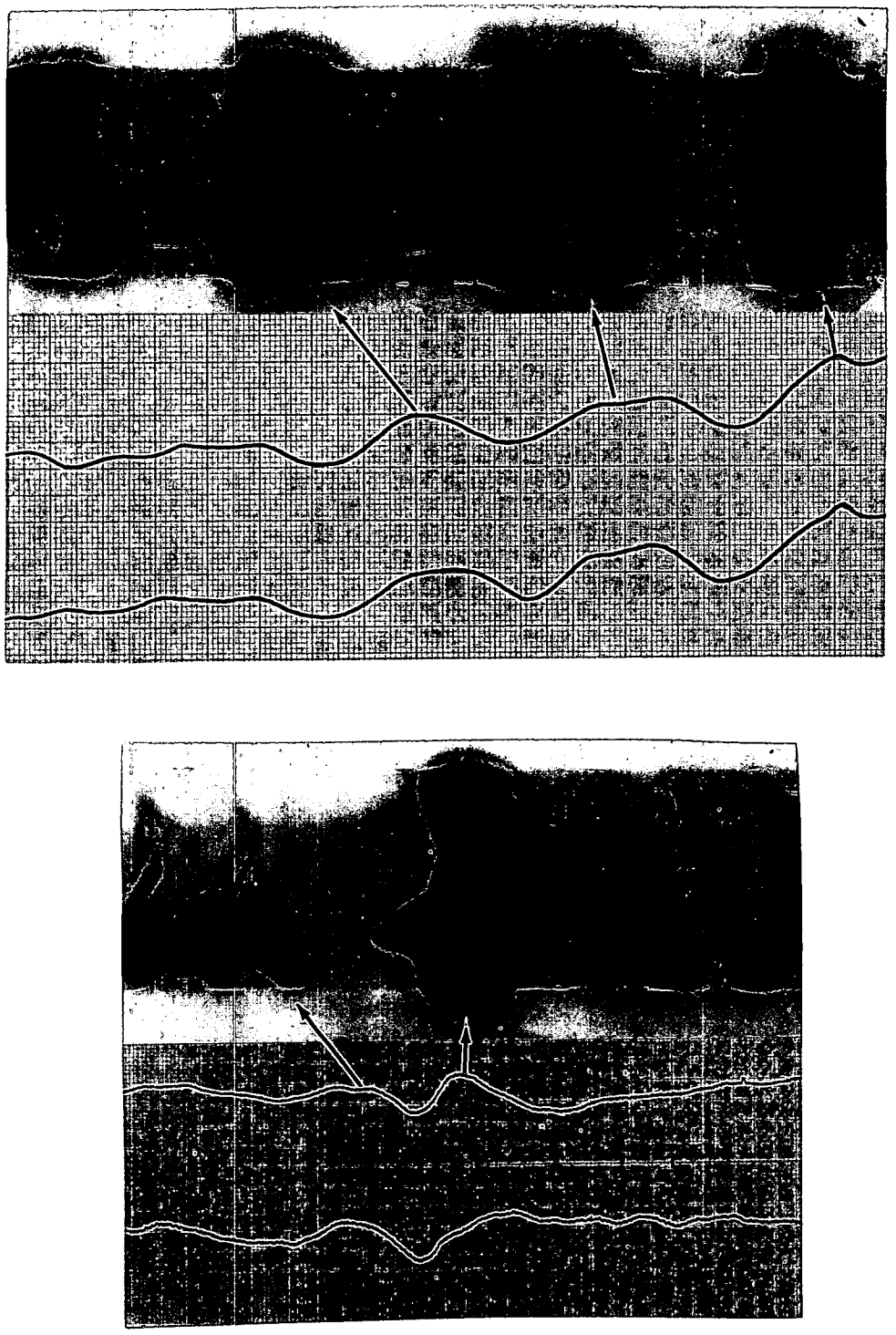

FIGURE 3.8

Autoradiographs and Eddy Current Test Results for Incrementally Loaded PuO_2-UO_2 Fuel Rods

0630094-3; 0630094-1

AEC-GE RICHLAND, WASH.

EBWR Plutonium Fuel Loading - R. E. Sharp

A joint Hanford Laboratories - Argonne National Laboratory program for irradiation of plutonium fuel elements in the Experimental Boiling Water Reactor (EBWR) is in progress.

Basic criteria for the first fuel loading were established as shown in Table 3.2. Rods for the 42 fuel assemblies will be fabricated by vibrational compaction.

TABLE 3.2

Reactor Loading

Central Core Region - Plutonium Fuel - 36 Fuel Assemblies in 6 x 6 array
Outer Core Region - UO_2 Fuel - 148 Fuel Assemblies

Total No. of Plutonium Assemblies - 42 (6 spares)

No. of Rods per Assembly - 36 (6 x 6 geometry)

Core Composition - UO_2-2.5 PuO_2;
UO_2-Depleted (0.2% U^{235})
PuO_2- High Exposure (8% Pu^{240})

Core Length - 48.5 inches

Core Weight - 830 grams

Core Density - 86–89% Theoretical Density

Cladding - Zircaloy-2 tubing
0.372-inch ID
0.025-inch wall thickness

Procurement of cladding material, design of a vibrational compaction facility, and modification of loading and compaction equipment are in progress. Sixty kilograms of unclassified plutonium was procured, and specifications for fusion of depleted UO_2 were prepared.

Extended Surface Plutonium Fuels - C. H. Bloomster

A process was developed to produce Zircaloy-clad, Pu-Zr core fuel element plates by roll-cladding (Figure 3.9). These fuel elements have potential application (1) in low cost spike elements, (2) as a means of keeping added plutonium enrichment separate from generated plutonium, and (3) rejuvenating partially spent fuel elements.

Previously reported difficulties with external contamination on the finished plate were eliminated by modifying the design of the Zircaloy sandwich. The core was placed in a recessed slot and a close fitting cover was placed on top of the core.

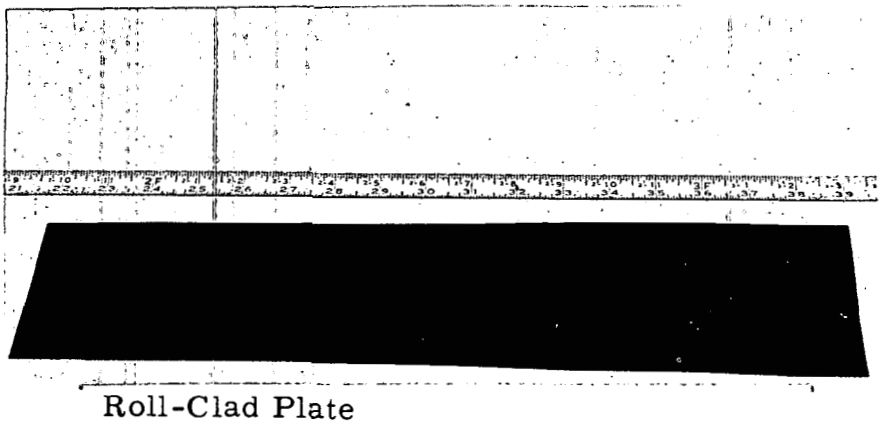

Roll-Clad Plate
840 C 12:1 Reduction Ratio
Zircaloy-Clad Pu-Zr Alloy Metallurgically Bonded and Autoclaved

FIGURE 3.9

Roll-Clad, Zircaloy-Clad, Zr-Pu Fuel Plate

0630063-7

Special Fuel Element Fabrication - C. H. Bloomster, L. C. Lemon, and W. T. Ross

Fabrication of 219 high exposure Pu-Al fuel rods of various shapes and sizes (Figure 3.10) and 40 flux monitor foils (Figure 3.11) was completed. These elements will be used in physics research activities at the Physical Constants Test Reactor (PCTR).

Fabrication was approximately 33% completed of 1000 high exposure Pu-Al fuel elements, shown in Figure 3.12, for physics experiments in the Plutonium Recycle Program Critical Facility (PRP-CF). Two hundred of the 3-foot extruded and clad elements (0.5-inch diameter) were shipped and another 200 are scheduled to be shipped early in January, 1963.

A process was developed to produce UO_2-PuO_2 pellet fuel elements for physics experiments in the PCTR. Approximately 16,000 pellets (1/2-inch diameter, 1/2-inch long) containing 0.90 wt% PuO_2 in depleted UO_2 are required. Low surface area (1.99 m^2/g) of the depleted UO_2 required a high green density of 6.6 to 7.2 g/cc to obtain a sintered density of 91 to 94% of theoretical. A new hydrogen atmosphere, batch sintering furnace with a capacity of 700 pellets/3 days was activated. Initial problems in maintaining uniform furnace temperatures were eliminated by redesign of the control circuit.

A coextrusion process was developed to produce 40 Pu-Al fuel elements (1-inch diameter, 5-inches long) for aluminum corrosion test purposes (Figure 3.13). Casting of the required 14 Al-8 wt% Pu-2 wt% Ni billets was completed, and three were extruded. Development of machining decontamination, and closure techniques remains to be done to complete fabrication

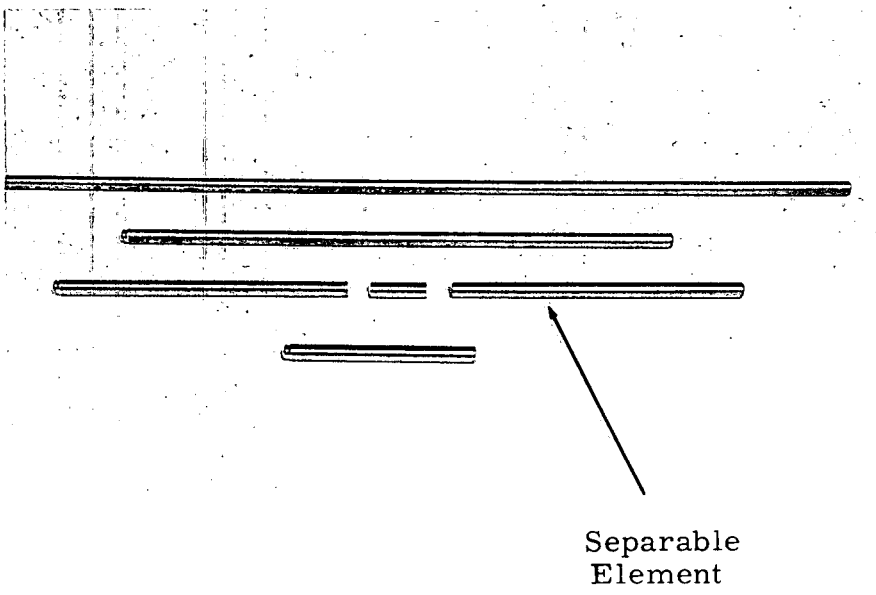

FIGURE 3.10

High Exposure Aluminum-Plutonium Elements (0.563-Inch OD) for PCTR

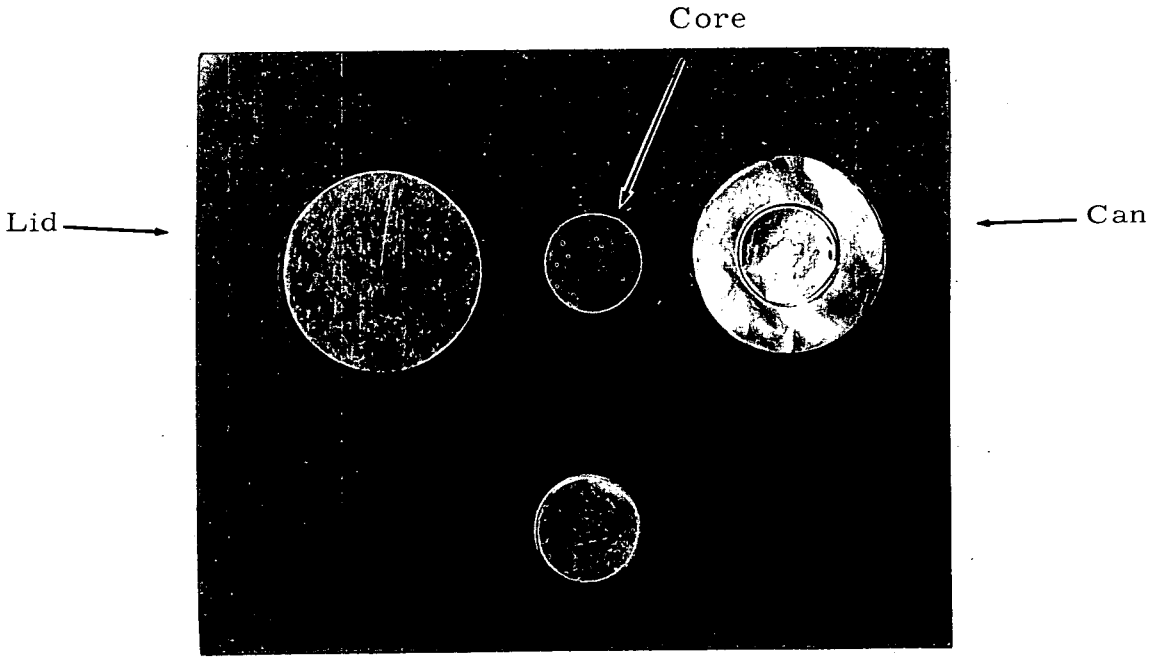

FIGURE 3.11

Flux Monitor Foil for PCTR

0630063-1; 17813-1

AEC-GE RICHLAND, WASH.

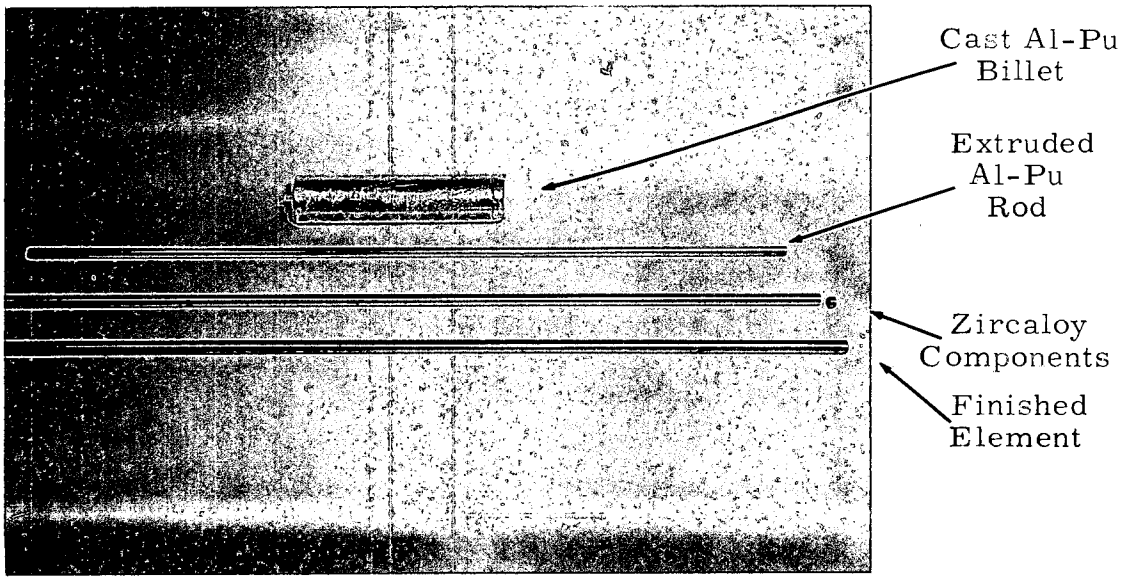

FIGURE 3.12

Aluminum-Plutonium Fuel Elements
for Light-Water Experiments in the PRP-CF

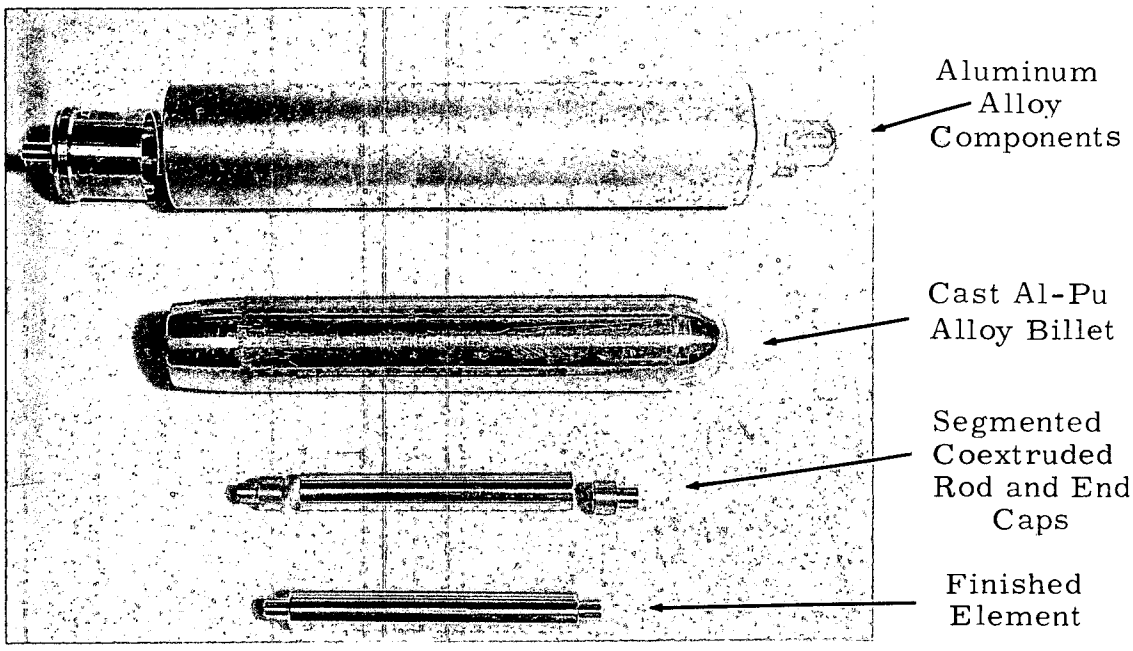

FIGURE 3.13

Plutonium Fuel Elements for Aluminum Alloy Corrosion Tests
0630063-8; 0630063-4

Seventy-one aluminum-clad, coextruded, thin-walled tubular elements were completed. Forty contain Al-Pu and Al-U^{235} alloy cores of various concentrations, and the remainder contain Al-U^{233}-Li, Al-U^{235}-Li, and Al-Pu-Li alloy cores of various concentrations. These elements have a nominal 0.80-inch OD and are four inches long.(1)

No difficulties were encountered during the final phase of the fabrication except for two bond test rejects. These were the first rejects of this type to occur since the process techniques were developed. They were attributed to incomplete outgassing of the coextursion billet. As anticipated, there were no significant differences in the extrusion flow characteristics of aluminum alloyed with U^{233}, U^{235} or plutonium of approximately the same concentrations within the limits of 3 to 13 wt% uranium or plutonium.

Fuel Preparation Facilities - L. P. Murphy

UO_2 powder preparation capacity was increased by installing a new disc pulverizer and two screeners (Figure 3.14). Procedures were developed utilizing the new equipment to crush and screen desired quantities of any desired sizes of material between 4 and 325 mesh.

Facility Hazards Analysis - W. J. Bailey, J. B. Burnham, and L. G. Merker

A rough draft of the Facility Hazards Analysis for the Plutonium Fabrication Pilot Plant (308 Building) was completed and issued. The final draft is being assembled for reproduction.

---

(1) Wick, O. J. Quarterly Progress Report, Plutonium Metallurgy Operation, July, August, September, 1962. HW-74718. October 15, 1962. (SECRET)

FIGURE 3.14

Equipment for Powder Preparation

FUELS TESTING AND ANALYSIS

Irradiation of a Large Diameter Fuel Rod - G. R. Horn, M. K. Millhollen, and W. J. Flaherty

A large diameter (2.33-inch OD) UO_2 fuel rod, irradiated in the ETR to study the effect of variations in startup rate on fuel structure changes, ruptured at low reactor power during initial startup. As previously reported,[1] preliminary examination revealed a bulge and split in the cladding, and circumferential ridges or ripples (maximum height, 0.003 inch) over the entire rod.

Examination of the fuel revealed an eccentric heat affected zone approximately 17 inches long. The shape and position of this zone (Figure 4.1) suggest that a severe transverse neutron flux gradient caused the rod to bow. The resulting coolant blockage would cause overheating and subsequent failure of the cladding.

The ripples in the cladding, which possibly reflect slight variations in the fuel bulk density, may have been caused by thermal expansion of the UO_2. Although the element was subjected to a series of excessively severe pressure cycles during its pre-startup residence, in-reactor and out-of-reactor tests with a similar non-irradiated element showed that the pressure cycling probably had no adverse effect on the cladding.

The top of the end of the test element included a 6-inch-long plenum to accommodate gases released during irradiation. Uranium dioxide was excluded from the plenum by perforated tungsten and MgO plates. Post-irradiation examination revealed no evidence of migration of vaporized UO_2 into the plenum. As shown in Figure 4.2, the MgO plate cracked (but did not break up) during or after irradiation. The tungsten plate remained intact. This appears to be a reliable method for providing a large plenum in ceramic fuel elements.

---

(1) Cadwell, J. J. Fuels Development Operation Quarterly Progress Report, July, August, September, 1962. HW-74378, p. 5.47. (SECRET)

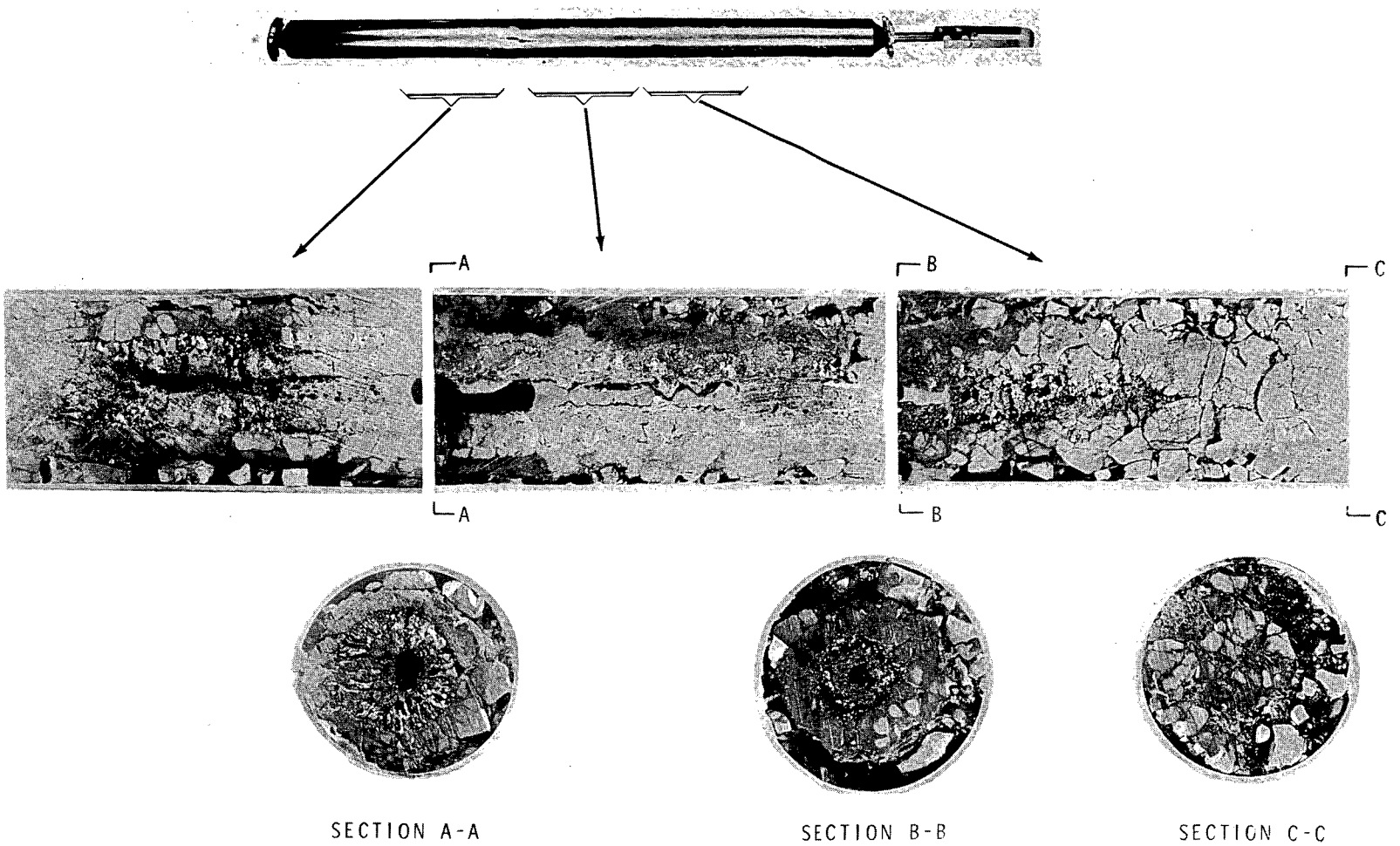

FIGURE 4.1

Sections of Irradiated Large Diameter (2.33-Inch OD) UO_2 Fuel Rod

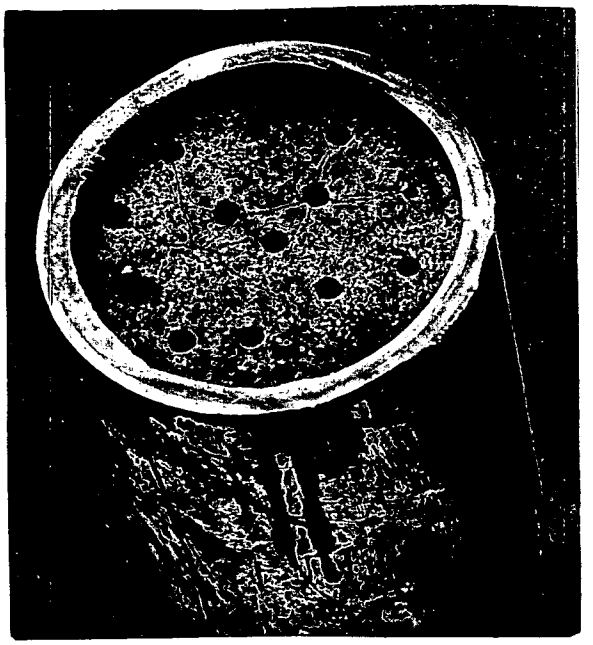

MgO Plate

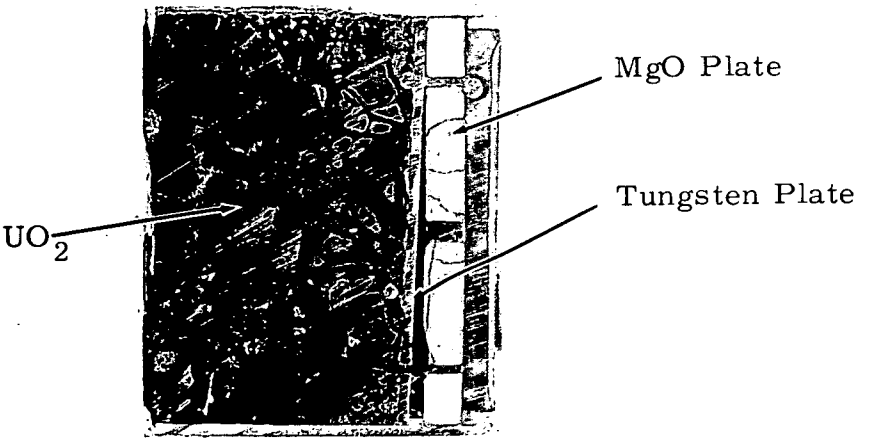

Cross Section Through Tungsten and MgO Plates

B-3592, B-3524

FIGURE 4.2

Separator Plates Between Gas Plenum and Fuel in Irradiated 2.33-Inch-Diameter Fuel Rod

High Temperature Irradiation Testing of UO_2-Tungsten Cermet - G. R. Horn, W. J. Flaherty, and D. W. Brite

Impaction of metal-ceramic mixtures produces a solid body with a large ceramic-metal interface area suitable for studying high temperature solid state reactions that occur during irradiation. Initial tests were begun.

A scheduled two-hour irradiation of a 50 wt% UO_2-tungsten cermet was completed in the MTR VH-4 (Rabbit) Facility. The 0.2-inch-diameter by 3-inch-long tungsten clad fuel was contained in an evacuated test assembly designed to allow a cladding surface temperature of ~2400 C. Figure 4.3 illustrates the microstructure of the fuel before irradiation. Figure 4.4 shows the details of the test assembly. The appearance of the capsule after irradiation is shown in Figure 4.5.

A second, similar cermet capsule was successfully irradiated one hour in a Hanford reactor under conditions which allowed a surface temperature greater than 2100 C (confirmed by post-irradiation examination). A photomosaic of the fuel cross section is shown in Figure 4.6. Surface UO_2, unprotected by the tungsten matrix, sublimed at the high operating temperature and re-deposited on the inner surface of the cladding. High temperature pretreatment of fuel pellets probably would prevent such relocation. Photomicrographs of the cermet before and after irradiation are shown in Figure 4.7, with a comparison micrograph of a non-irradiated sample heated to 2100 C.

The cermet fuel in both capsules was fabricated by impaction of a mixture of -325 mesh tungsten powder and -60 +200 mesh fused UO_2 particles, to 96% TD.

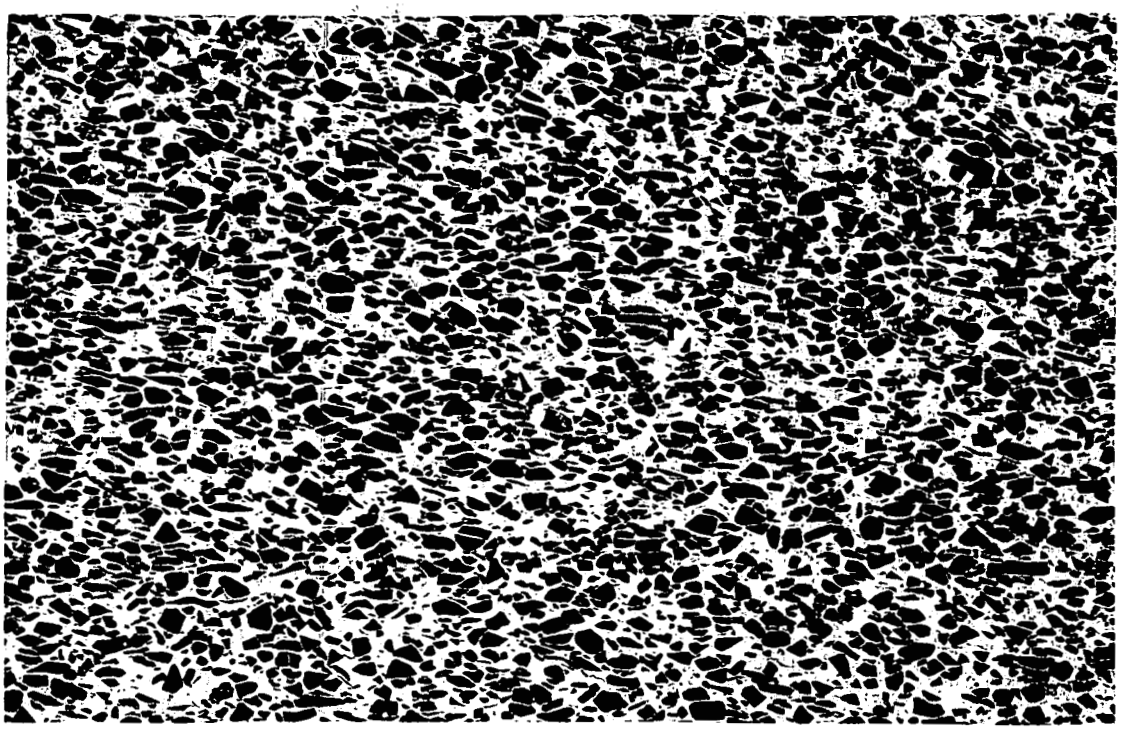

15X

500X

100X

0621983

FIGURE 4.3

Microstructure of Impacted UO_2 – 50 wt% Tungsten Cermet Before Irradiation

AEC-GE RICHLAND, WASH.

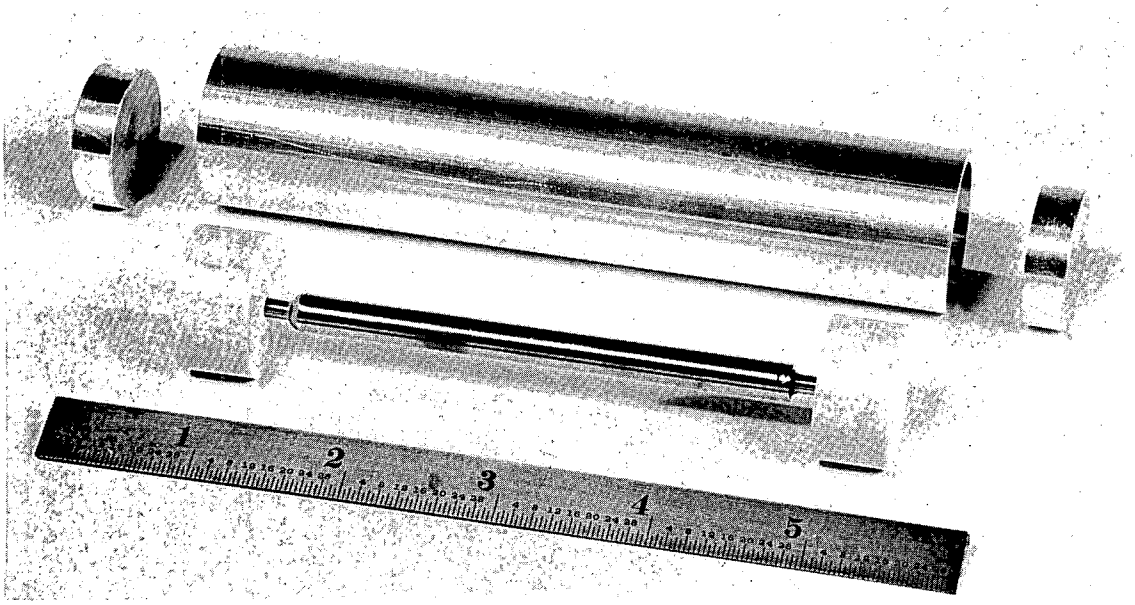

FIGURE 4.4

Components of Tungsten Clad, UO_2–Tungsten Cermet Irradiation Capsule

0621974

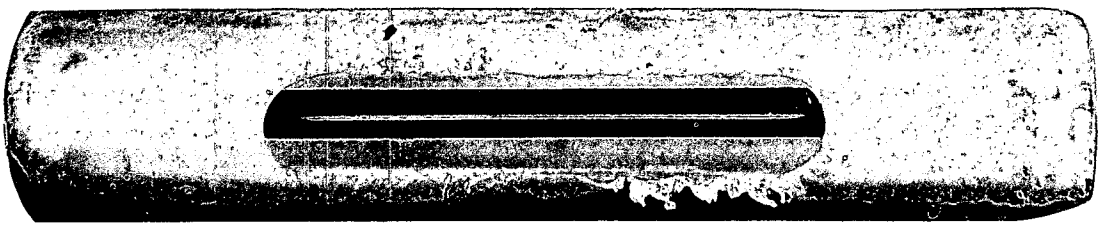

View of Capsule Through Slot Milled in Outer Aluminum Sheath

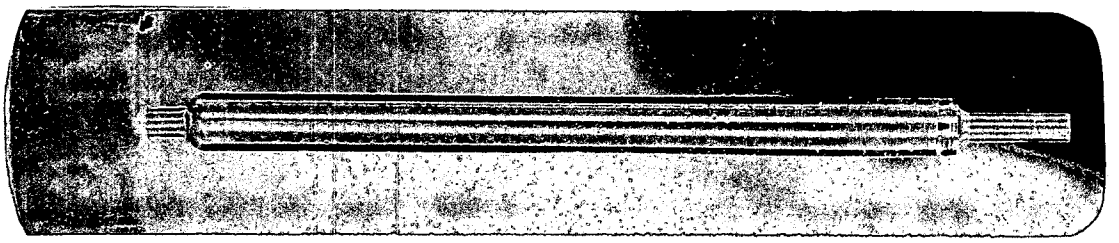

Capsule after Removal from Outer Aluminum Sheath

FIGURE 4.5

UO_2–Tungsten Cermet Test Capsule after Irradiation

B-3747, B-3753

AEC-GE RICHLAND, WASH.

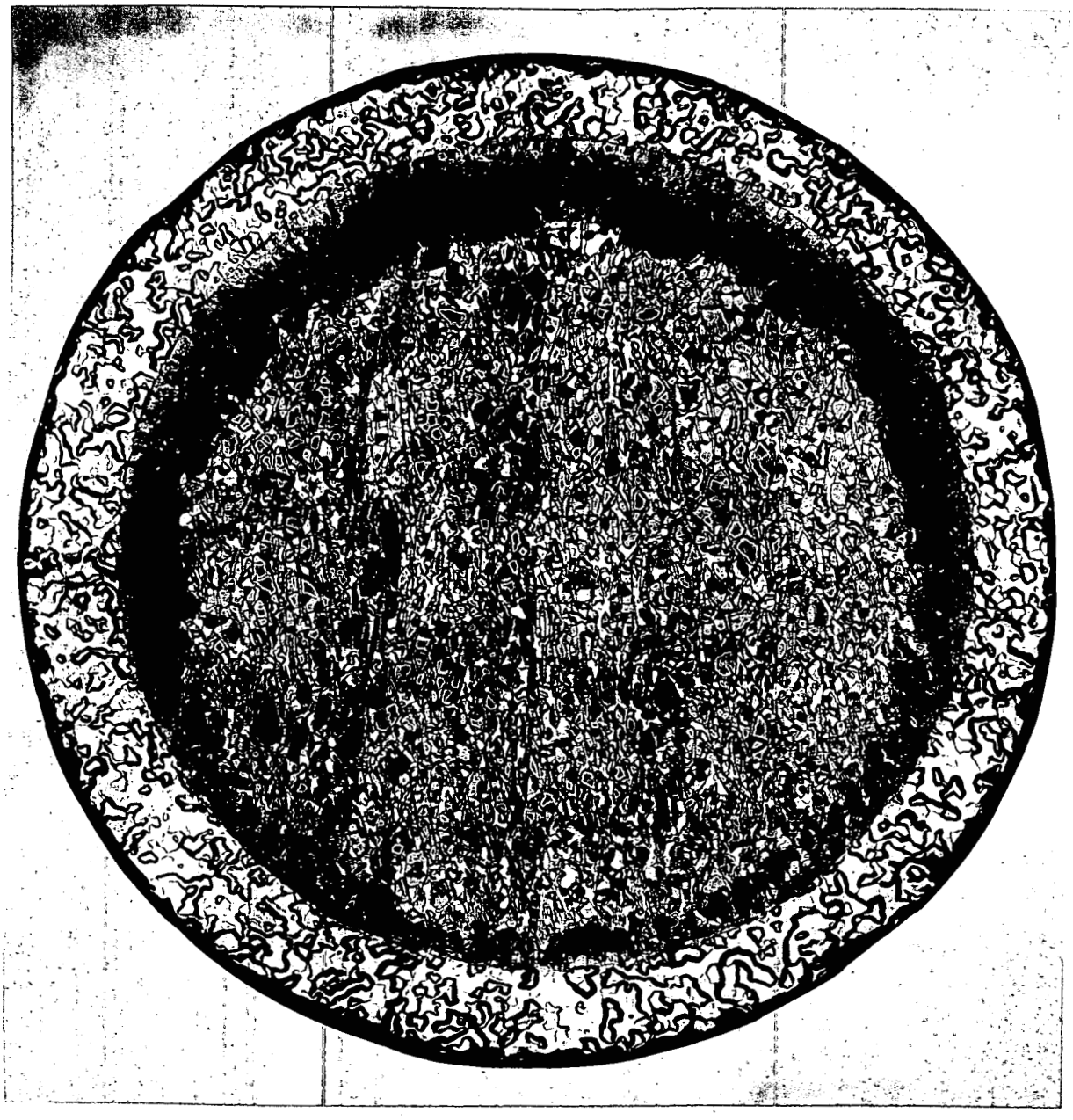

0622147

FIGURE 4.6

Cross Section of Irradiated, Tungsten Clad UO_2–Tungsten Cermet

AEC-GE RICHLAND, WASH.

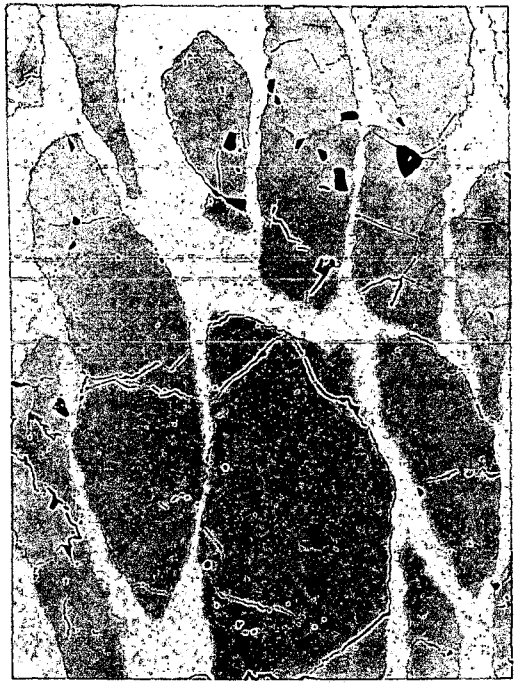

Before Irradiation

(average W grain diameter ≤ 4μ)

4J 1720B

After Irradiation

(average W grain diameter ~ 20μ)

B-3170

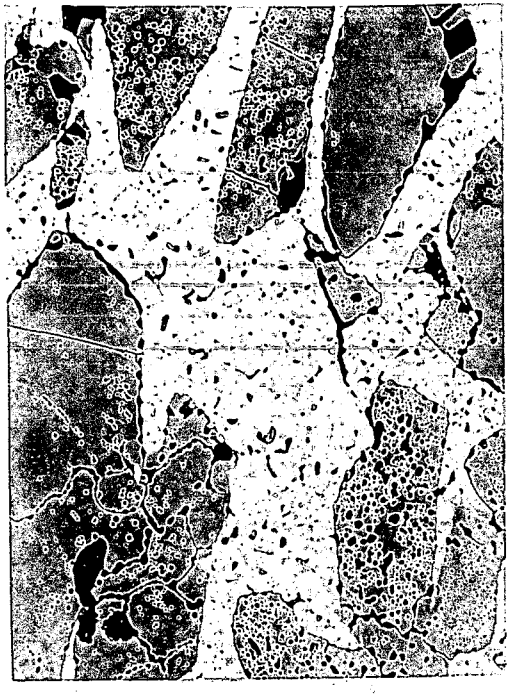

Nonirradiated; Heated to 2100 C
(average W grain diameter ~ 20μ)

4J 1653B

FIGURE 4.7

Microstructure of UO_2–50 wt% Tungsten Cermet (250X)

Irradiation of UO_2 Single Crystal Pellets - G. R. Horn

Preliminary postirradiation examination of a single crystal UO_2 pellet showed that no gross structural changes, other than cracking, resulted from irradiation at a cladding surface heat flux of 640,000 Btu/(hr)(ft^2). The lack of structure alteration indicates high thermal conductivity of large grains of UO_2. Small crystal UO_2, as in sintered pellets, would have exhibited evidence of initial center melting under similar irradiation conditions.

The test capsule contained one 0.500-inch-diameter, 3/4-inch-long single crystal pellet plus several 0.500-inch-diameter bi- and tri-crystal pellets. Cross sections through two of these pellets are shown in Figure 4.8. Previous investigations[1] demonstrated that cracks in fused UO_2 are sources of voids that produce columnar grains. This effect was not observed in in these cross sections, probably because temperatures were not sufficiently high to cause extensive void migration.

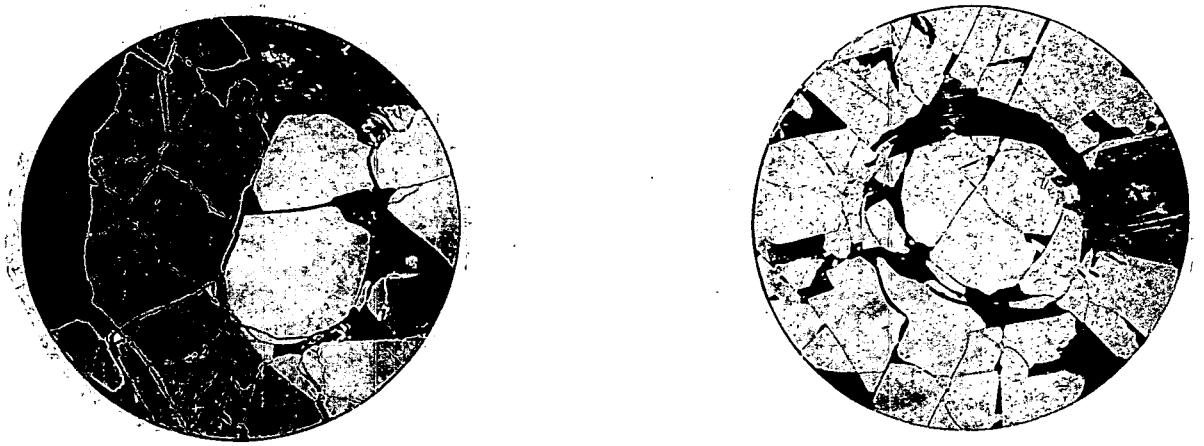

Tri-Crystal B-3904

Single Crystal B-3902

FIGURE 4.8
Irradiated High Density UO_2 Pellets

(1) Roake, W. E. Irradiation Alteration of Uranium Dioxide, HW-73072. March, 1962.

Low Temperature Irradiation Sintering of Swaged UO_2 - W. J. Flaherty

Ceramographic examination of cold swaged UO_2 revealed that sintering, Figure 4.9, occurred during irradiation at remarkably low bulk UO_2 temperatures (300-400 C). In earlier reports it was hypothesized that stressed point contacts between fuel particles were bonded as a result of localized transient high temperatures in the regions of individual fission events. That phenomenon would contribute to thermal conductivity increases noted during irradiation of a thermocoupled, swaged UO_2 fuel element in the PRTR.

Because much of the volume of fuel in an element operates at relatively low temperatures, this discovery has important implications with respect to erosion resistance in the event of cladding failure.

In an effort to separate thermal effects from irradiation effects, a series of out-of-reactor heat-and-hold tests is being conducted. Similar in- and out-of-reactor tests are planned, using vibrationally compacted UO_2 to determine the effect of compaction method on in-reactor sintering.

Burst Tests of Cold-Swaged PRTR Fuel Rods - W. J. Flaherty and L. E. Mills

Pressures of 7820 and 7880 psi were required to burst one-foot-long sections of cold-swaged PRTR fuel rods at 550 F. These pressures are more than three times the maximum internal pressure ($\sim$ 2500 psi) calculated to exist in a PRTR fuel rod irradiated to 10,000 Mwd/ton. Burst rods are shown in Figure 4.10.

These tests, at simulated PRTR fuel element cladding temperatures, indicated that the limiting stress conditions that might be caused by internal gas pressure or waterlogging should be calculated from the tensile strength rather than from the yield strength. Failure was caused by excessive longitudinal stress at the rod ends as evidenced by the complete removal of one end cap. There was no indication that failure was induced by roughening of the internal cladding surface during swaging.

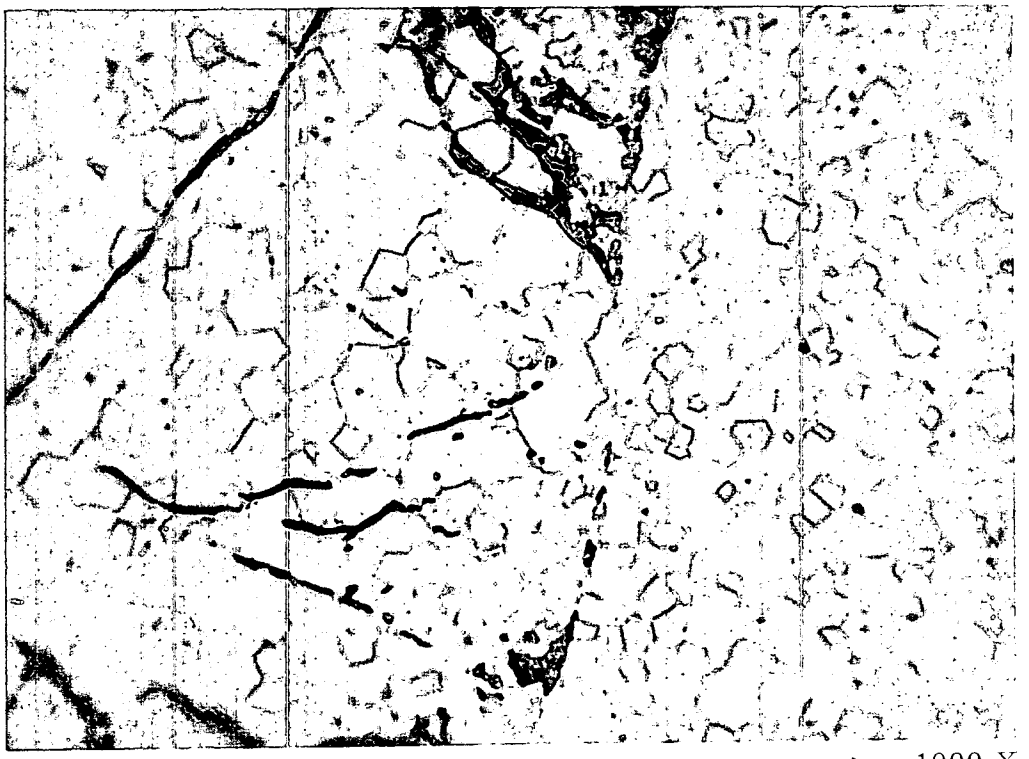

B-2316 1000 X

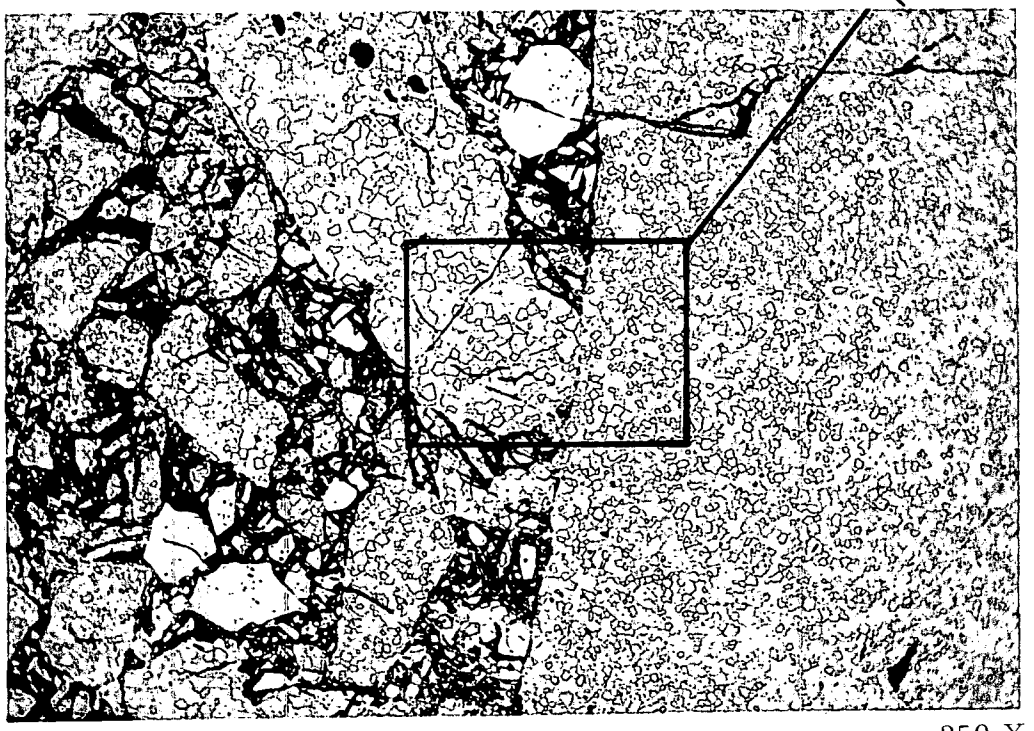

B-2311 250 X

FIGURE 4.9

Low Temperature, In-Reactor Sintering of Swaged UO_2

AEC-GE RICHLAND, WASH.

The test procedure included a 16-hour hold period at 450 F and 1450 psi and a subsequent 1/2-hour hold period at 450 F and 4000 psi to assure equalization of hydraulic pressure throughout the rods. One rod failed at the hydraulic connection end and the other at the opposite end. Heat affected zones adjacent to the welds bulged before failure conditions were reached.

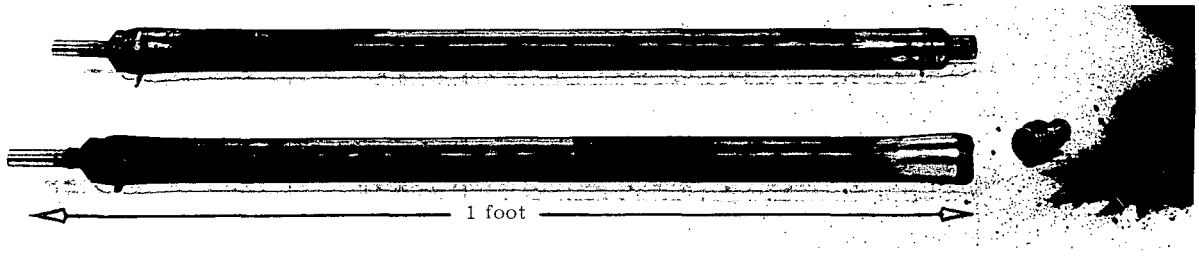

FIGURE 4.10
PRTR Fuel Rod Burst Test Specimens

Phoenix Fuel Experiment - M. D. Freshley

A plutonium burn-up experiment* designed to show the effect of exposure on the reactivity of plutonium was previously reported.(1) Aluminum-plutonium alloy specimens were irradiated in the MTR and the resulting reactivity changes were measured in the Advanced Reactivity Measurement Facility (ARMF). Reactivity effects now being computed will be reported later.

Three Al-Pu specimens containing plutonium of differing isotopic compositions were irradiated at a power generation of 40 kw/ft and an associated surface heat flux of approximately 1,000,000 Btu/(hr)(ft^2). One Al-Pu specimen, made from plutonium that initially contained 16.33%

---

* in cooperation with L. C. Schmid, Physics Laboratories

(1) O. J. Wick. Quarterly Progress Report, Plutonium Metallurgy Operation, July, August, September, 1962. HW-74718. October 15, 1962. (SECRET)

Pu^{240}, is being irradiated for its 7th (last) cycle in the MTR. This will complete the irradiation phase of this experiment. (The other 2 specimens of the series containing 6.33 and 27.17% Pu^{240} were also irradiated seven cycles). After a suitable decay period, reactivity measurements will be made in the ARMF. The samples will be returned to Hanford for burnup and isotope analyses.

Irradiations of Prototypic UO_2-PuO_2 Fuel Elements - M. D. Freshley

Heat generation rate ordinarily is not uniform along a nuclear reactor fuel element because of axial variations of the neutron flux to which it is exposed. Hence, the maximum point heat transfer rate of the element and the maximum exposure of the fuel are significantly greater than the average. One method of raising the average closer to the maximum (and often limiting) quantities is to vary the fissionable isotope enrichment inversely to the expected axial neutron flux pattern. This method is particularly adaptable to incrementally loaded, swaged or vibrationally compacted fuel elements. Two swage compacted UO_2-PuO_2, 7-rod cluster test elements were irradiated in a pressurized water loop in the ETR to compare the two methods of enrichment.

Zircaloy clad elements were fabricated by incrementally loading arc-fused UO_2 and calcined PuO_2 into the tubes. The ratio of PuO_2 and UO_2 was held constant along the 42-inch length of one element (GEH-11-7) and was varied axially, in a cosine pattern, in the other element (GEH-11-8) to achieve a constant axial heat generation rate in the nonuniform neutron flux. The elements were irradiated approximately 25 days under PRTR coolant conditions.

More xenon was collected from the rods of the cosine-enriched fuel element than from the uniformly enriched element, because more fission events occurred in the former. Also, more xenon was collected from those rods which reached higher exposures and fuel temperatures as a result of being closer to the center of the reactor. These data are related to the position of each rod in Figure 4.11. Rods 1 and 6 were closer to the center of the reactor, whereas 3 and 4 were further from the reactor center during irradiation. Gas release data from the center rods are not included.

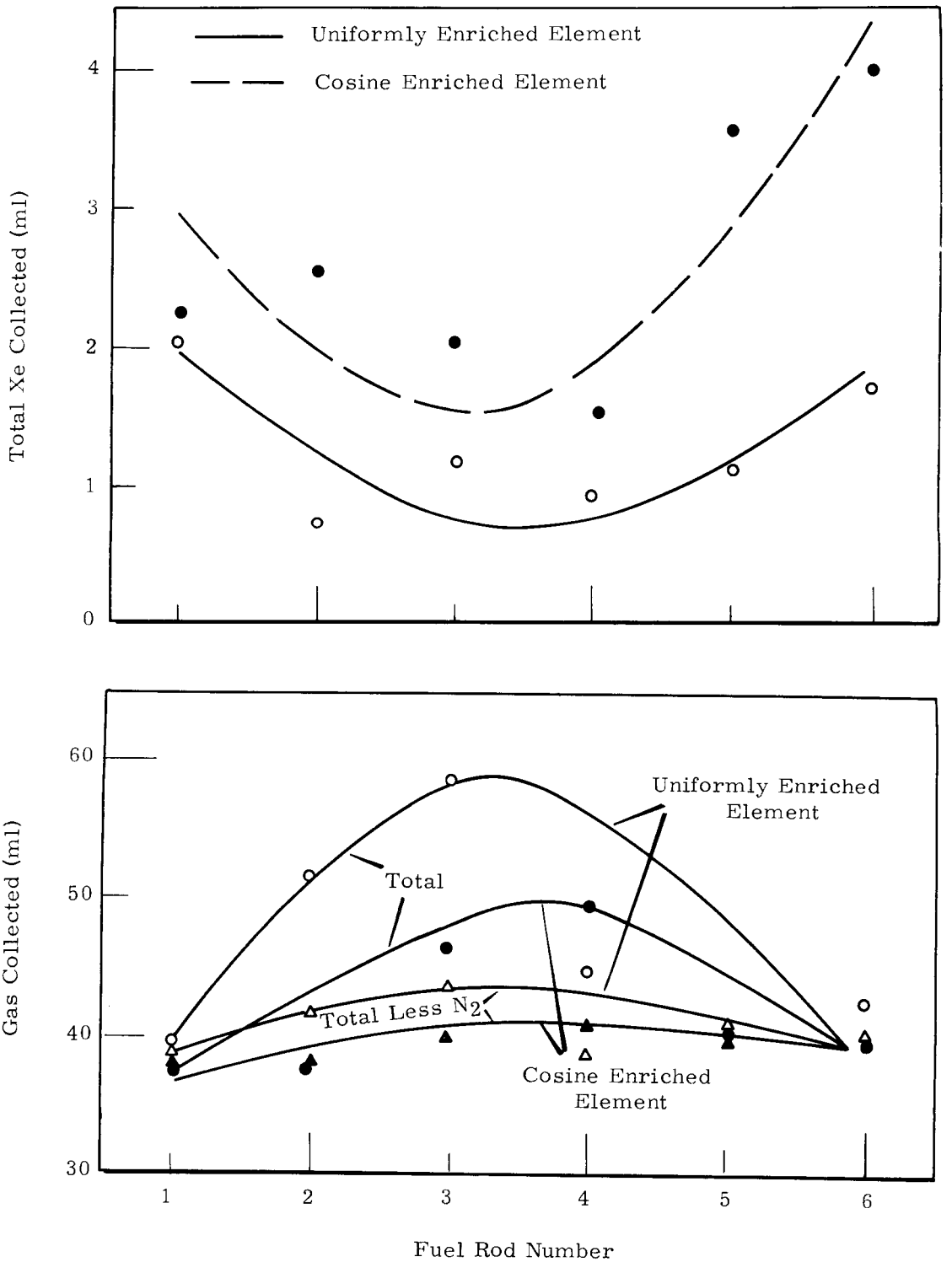

FIGURE 4.11

Gas Release from Irradiated Swage-Compacted UO_2-PuO_2

The test results can be interpreted to show that nitrogen released from the fuel during irradiation was dissolved in the Zircaloy cladding. The total gas curves (Figure 4.11) are inversely related to the total xenon curves. The fuel rods from the cosine enriched element (which had the higher average fuel temperatures) yielded less total gas than did the rods from the uniformly enriched element and, within each element, less total gas was collected from the rods that had operated at higher temperatures. The out-gassing treatment of the UO_2 (heating at 1000 C in vacuum for two hrs) carried out during fabrication of some of the rods of the uniformly enriched element had no apparent effect on the total gas collected. Most of the gas collected from the rods was helium introduced during welding. However, some of the gas samples contained as much as 25% nitrogen, presumably from nitride impurities in the UO_2. If the nitrogen content is subtracted from the total gas collected, the remaining gas curves closely approach a straight line. The nitrogen possibly was dissolved in the Zircaloy cladding on the hotter fuel rods. If the backfill gas in all the rods was initially the same, more nitrogen was dissolved by the Zircaloy cladding in the cosine enriched element which had higher average cladding and fuel temperatures. The nitrogen content of the Zircaloy cladding will be determined.

With the nitrogen content subtracted, less total gas was collected from those fuel rods which operated at the higher temperatures. This apparent anomaly could be caused by entrapment of gas in the greater number of closed pores formed in the hotter rods.

Irradiation Performance of MgO-PuO_2 and ZrO_2-PuO_2 Fuels -
M. D. Freshley and D. F. Carroll

Eight Zircaloy-clad capsules (1/2-inch diameter by 4-inches long) containing MgO-PuO_2 high density pellets and eight capsules containing ZrO_2-PuO_2 pellets were irradiated in the ETR to evaluate fuel materials of interest for ceramic, plutonium spike fuel element applications. Magnesium oxide and PuO_2 are completely immiscible. The ZrO_2-PuO_2 compositions being studied exist in a two-phase region, monoclinic ZrO_2 and a cubic ZrO_2-PuO_2 solid solution. Small PuO_2 additions dimensionally stabilize ZrO_2 by eliminating the severe tetragonal-to-monoclinic transformation.

The requested irradiation conditions for the capsules are summarized in Table 4.1. Actual operating conditions have not been sufficiently defined for inclusion in this report. Because $MgO-PuO_2$ has a greater thermal conductivity than ZrO_2-PuO_2, the former capsules were irradiated at higher heat ratings to obtain comparable fuel temperatures.

TABLE 4.1

REQUESTED IRRADIATION CONDITIONS
FOR $MgO-PuO_2$ AND ZrO_2-PuO_2 FUEL CAPSULES

Fuel	$MgO-3.05$ wt% PuO_2 and $MgO-13.52$ wt% PuO_2	$ZrO_2-2.2$ wt% PuO_2 and ZrO_2 10.4 wt% PuO_2
Number of Capsules	4 of each composition	4 of each composition
Power Generation (kw/ft)	29 & 50 ($\int kd\theta$ = 77 and 130 watts/cm)	17 & 22 ($\int kd\theta$ = 45 and 58 watts/cm)
Maximum Heat Flux [Btu/(hr)(ft^2)]	665,000 and 1,150,000	400,000 and 500,000
Maximum Core Temperature (C)	1700 and 2200	1700 and 2800
Requested Exposure	0.5×10^{20} and 1.0×10^{20}	0.5×10^{20} and 1.0×10^{20}

Postirradiation examination of the $MgO-PuO_2$ specimens revealed general cracking of the fuel in those samples which operated at the lower heat ratings and in which no recrystallization or grain growth took place. Center voids and columnar grains were observed in the specimens which had operated at the higher heat ratings.

The general appearance of specimens which operated under comparable conditions is about the same. Because of its better thermal conductivity, and reduced thermal gradients, MgO-PuO_2 does not crack as extensively as UO_2 during irradiation. The PuO_2 second phase is randomly distributed throughout the MgO matrix in the equiaxed grain growth regions as well as in regions of extensive recrystallization and columnar grain growth. The distribution of PuO_2 was not affected by gross structural changes in the surrounding MgO matrix, as shown in Figures 4.12, 4.13 and 4.14. However, the average PuO_2 particle size increased slightly in the columnar grain growth region, indicating that temperatures were sufficiently high to cause agglomeration or sintering of smaller PuO_2 particles. The fact that the distribution of the PuO_2 particles was unaffected by columnar grain growth in the surrounding MgO matrix, suggests that the columnar grains were formed in the solid state or by deposition from the vapor phase.

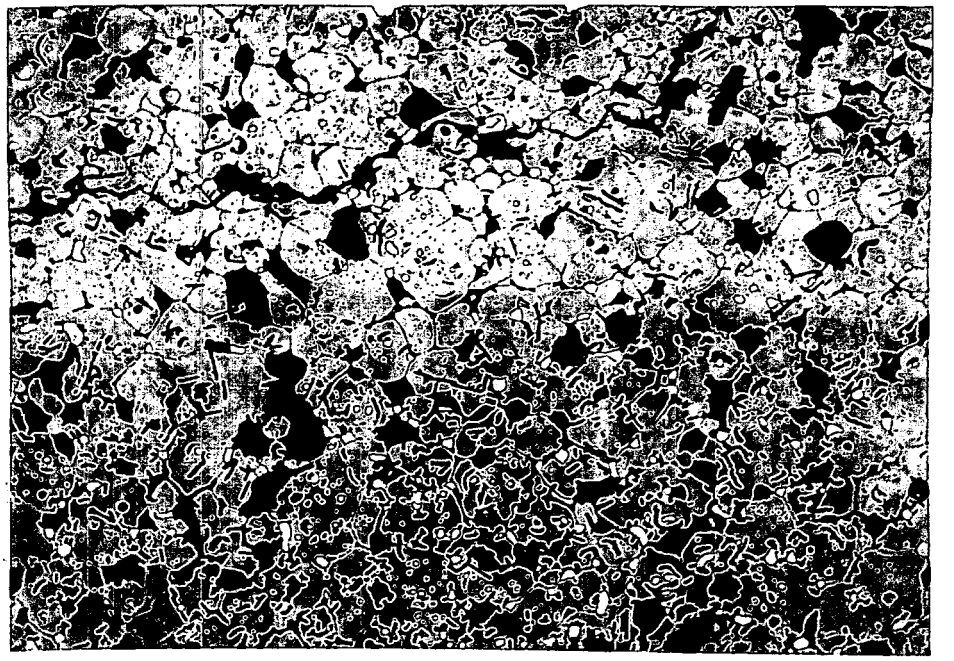

RM-B2032 (250 X)

FIGURE 4.12

Irradiated MgO-13.5 wt% PuO_2 Sintered Pellet Showing Uniform Distribution of PuO_2 (white particles) in Unrecrystallized Region Near the Surface of the Sample

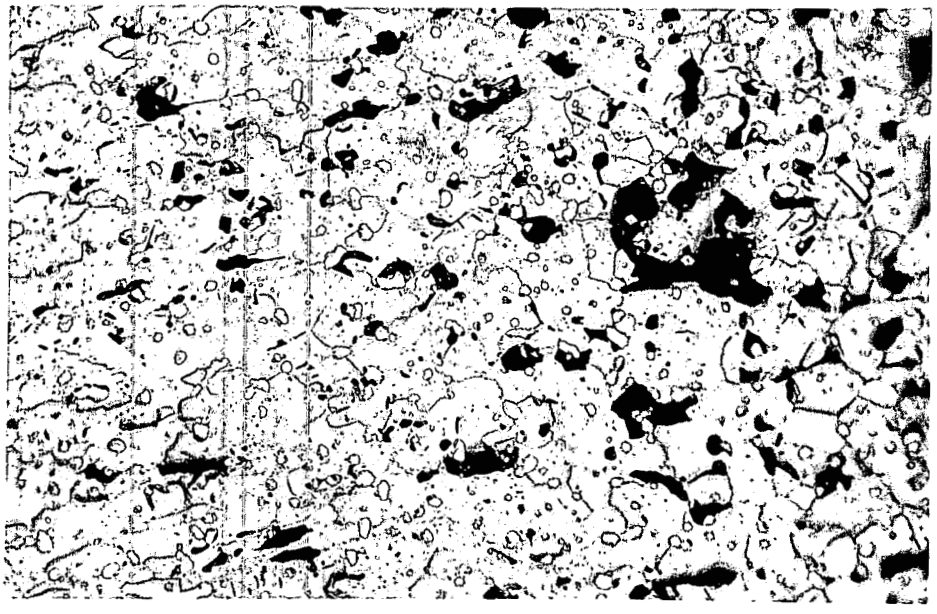

RM-B2032 (250 X)

FIGURE 4.13

Irradiated MgO-13.5 wt% PuO_2 Sintered Pellet Showing Uniform Distribution of PuO_2 (white particles) in the Equiaxed-to-Columnar Grain Transition Region

RM-B2040 (250 X)

FIGURE 4.14

Irradiated MgO-13.5 wt% PuO_2 Sintered Pellet Showing Uniform Distribution of PuO_2 (white particles) in the Columnar Grain Growth Region of the MgO Matrix

AEC-GE RICHLAND, WASH.

Microstructural features different from those normally observed in many other irradiated ceramic fuels were seen in the irradiated ZrO_2-10.4 wt% PuO_2 (solid-solution sintered pellets). Five distinct microstructural zones were observed (Figure 4.15a). The second zone from the cladding appeared white. The width of the white band increased with increasing exposure and/or temperature. The innermost (or, in some cases, the next to innermost) zone was essentially free of voids and had no apparent grain structure. This zone was not present in the higher exposure samples (Figure 4.15b).

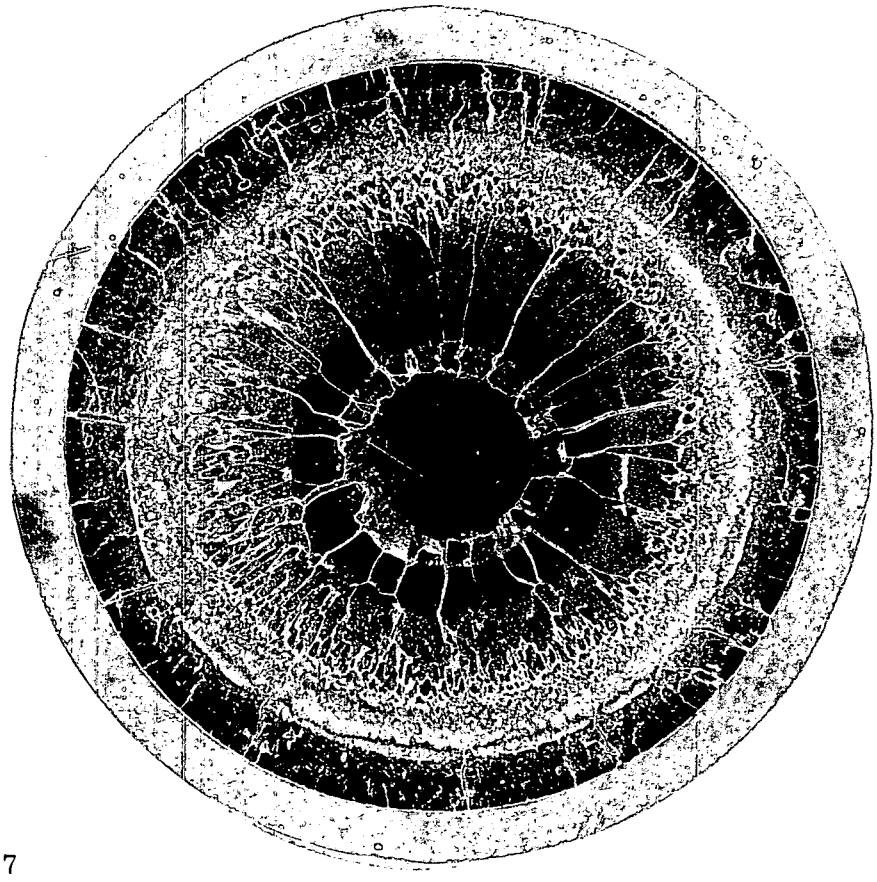

15587 (8 X)

2800 C Calculated Core Temperature;
Approximate Exposure, 0.5×10^{20} fissions/cm^3 (GEH-14-3441)

FIGURE 4.15a

Irradiated ZrO_2 - 10.4 wt% PuO_2 High Density
(91% TD) Sintered Pellets

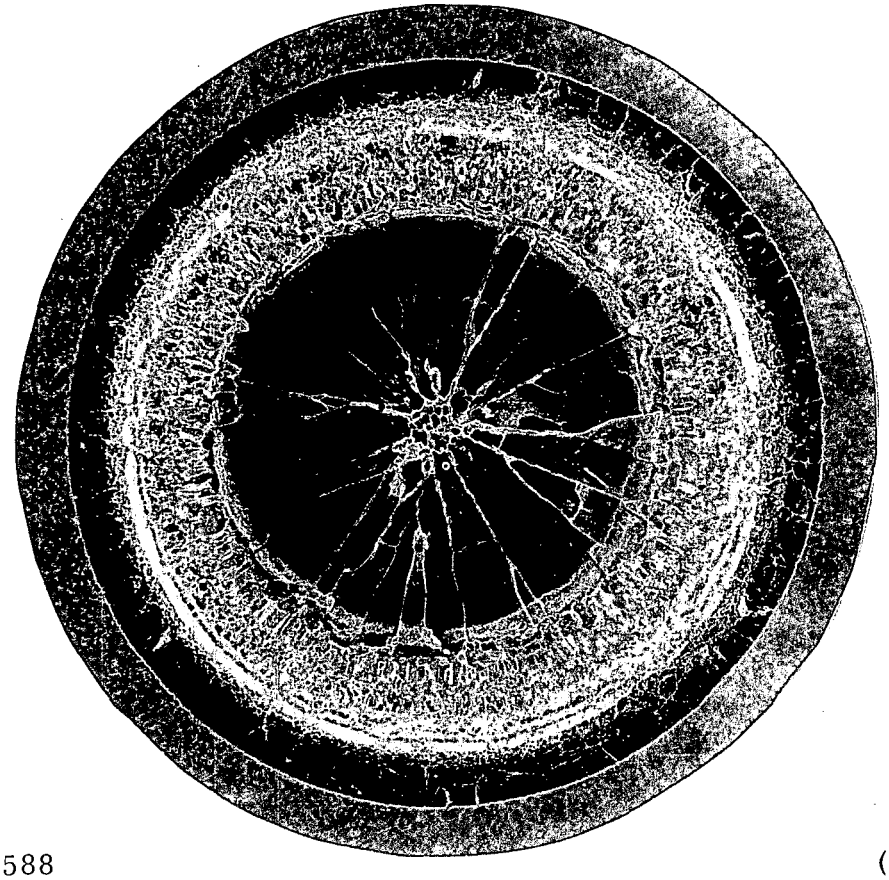

15588 (8 X)

2800 C Calculated Core Temperature;
Approximate Exposure, 1.0×10^{20} fissions/cm^3 (GEH-14-345)

FIGURE 4.15b

Irradiated ZrO_2 - 10.4 wt% PuO_2 High Density (91% TD) Sintered Pellets

PuO_2 Segregation in Incrementally Loaded PRTR Fuel Rods - M. D. Freshley

Two irradiated fuel rods from an incrementally loaded, swage compacted UO_2- PuO_2 fuel element (#5096) were destructively examined to determine the effects of PuO_2 segregation on heat transfer as revealed by fuel structure. One rod contained 80 one-inch-long increments of UO_2-PuO_2 (old process) and the other contained 160 one-half-inch-long increments (present process). Segregation of the PuO_2 within each increment is revealed by autoradiographs, Figure 4.16. Approximately the same amount of in-reactor sintering was observed in each rod; i.e., equiaxed grain growth was observed only in the PuO_2-rich regions, as shown in Figure 4.17a and 4.17b. Similar fuel structures (Figure 4.17c) were observed earlier in UO_2-PuO_2

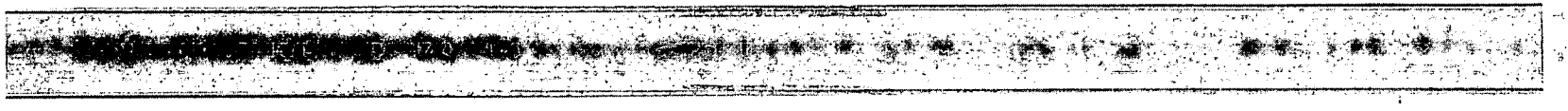

160-Increment Rod

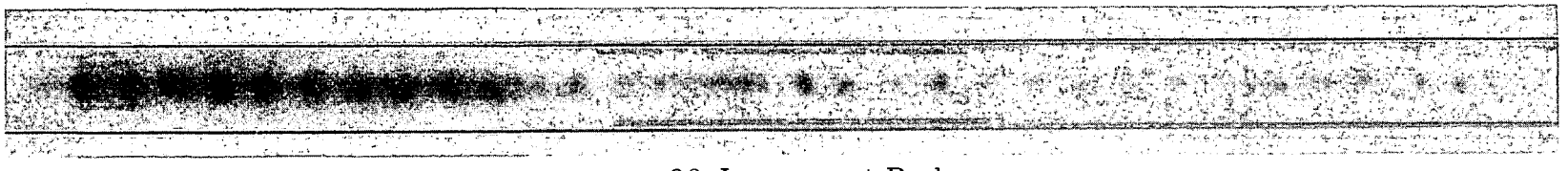

80-Increment Rod

0622257

FIGURE 4.16

Autoradiographs of Segments of Irradiated, Incrementally Loaded, and Swage-Compacted UO_2-PuO_2 PRTR Fuel Rods

RM-B3893 a. 80-Increment Rod (PRTR) (4.5 X)

RM-B3656 b. 160-Increment Rod (PRTR) (4.5 X)

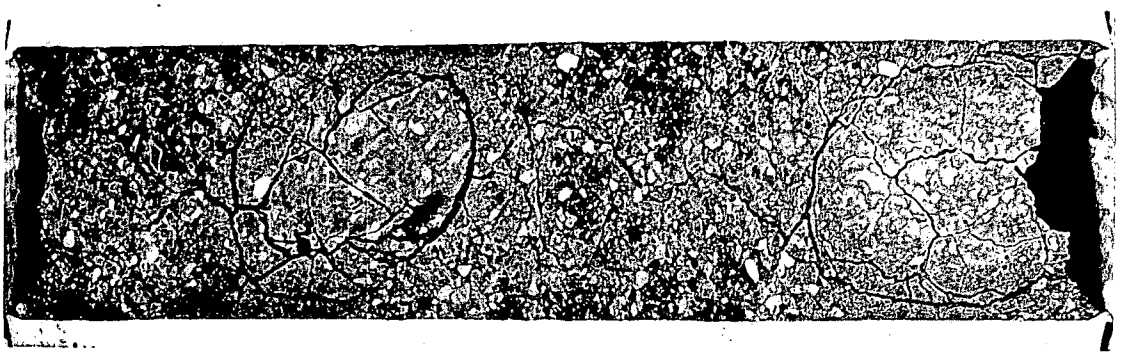

062855-1 c. 1/2-Inch-Increment Rod (ETR)
(Autoradiograph of polished surface shows areas of high fission product concentration due to PuO_2 segregation.)

FIGURE 4.17

Longitudinal Sections of Irradiated, Swage-Compacted UO_2-PuO_2 Fuel Rods

AEC-GE RICHLAND, WASH.

test elements which had been irradiated in the ETR under approximate PRTR conditions. The fuel structure is typically developed during operation at surface heat fluxes in the range of 300,000 to 400,000 Btu/(hr)(ft^2), an empirical observation that agrees well with the heat transfer analyses made by Thermal Hydraulics Operation. A limited reaction layer (less than 0.0005-inch thick) of unknown composition was seen on the inner surface of the cladding of the 160 increment rod only. No zirconium hydride was found in the cladding of either rod.

Extended Surface, PRTR Fuel Element Wear Pads - W. J. Flaherty, M. D. Freshley, M. K. Millhollen, and R. E. Sharp

Several instances of accelerated wear or fretting corrosion have been observed where 1/16-inch-wide fuel element end fixture pads contact PRTR process tubes. This can be reduced by increasing the contact area. Extended surface, clip-on wear pads (Figure 4.18) for irradiated, 19-rod cluster fuel elements are being tested under PRTR conditions (550 F water flowing at 80 gpm) in the out-of-reactor TF-7 loop. After four weeks' operation of a test element utilizing the new pads, contact areas on the wear pads and on a simulated PRTR process tube were worn only slightly (less than 0.001 inch). The test section was mechanically vibrated during this experiment (1.8 mils deflection at 85 cps) to accelerate wear and fretting corrosion. Each of the three pads on each end bracket has a wear surface 1/4 x 1/2 inch.

Pads were remotely attached to three irradiated UO_2-PuO_2 elements which previously had caused excessive PRTR process tube wear. Inspection of these elements and the process tubes after several weeks' additional operation revealed no measurable wear or fretting corrosion. Clip-on pads will be remotely installed on nine additional irradiated UO_2-PuO_2 elements.

0622051-2

FIGURE 4.18

Extended Surface, Clip-on Wear Pads (Insert)
Installed on PRTR Mark I Fuel Element

Postirradiation Examination of a $MgO-PuO_2$ PRTR Fuel Element - M. D. Freshley

A full-size, Zircaloy-2 clad, swage compacted $MgO-PuO_2$ 19-rod cluster element was irradiated in the PRTR. The PuO_2 (calcined, -325 mesh) and arc-fused MgO (-6 mesh) were incrementally loaded into low nickel Zircaloy-2 tubes (0.565-inch OD, 0.030-inch wall thickness). A 900 C maximum fuel temperature was anticipated. Individual process tube coolant activity records suggest that the fuel element failed approximately three hours after the PRTR achieved 60 Mw operation. The test was continued for approximately 8 Mwd (about eight days operation), at which time it was discharged because of excessive coolant activity observed following a reactor shutdown. Postirradiation examination revealed a longitudinal split (1-1/2-inches long and 1/4-inch wide) in the cladding of one rod, and washout of approximately 9 inches of fuel material. There is no nonuniform discoloration of the cladding that would indicate overheating.

Plutonium segregation, with a periodicity of about 1/2 inch, occurred as a result of the mechanics of the incremental loading technique. However, postirradiation autoradiographs revealed additional unexplained higher concentrations of fission products approximately every six inches in the failed rod. There is evidence that one such region of high plutonium concentration coincided with the point of failure. Fuel temperatures in regions of anomalously high PuO_2 content were sufficient to cause columnar grain growth and center void formation (Figure 4.19a). The PuO_2 second phase is uniformly distributed thoughout the columnar grain region except in a layer of PuO_2 (0.002 to 0.003 inch thick) on the fuel surface defining the center void (Figure 4.19b). MgO has a higher vapor pressure than PuO_2 in the assumed temperature range, and the MgO appears to have preferentially relocated outward by vaporization and deposition.

The cladding split began as a brittle failure, associated with a massive hydride deposit (Figures 4.19a, 4.20) and propagated in a ductile manner. Radial cracks (0.010-inch maximum length) in the hydride layer were presumably initiated by circumferential stresses caused by fuel swelling

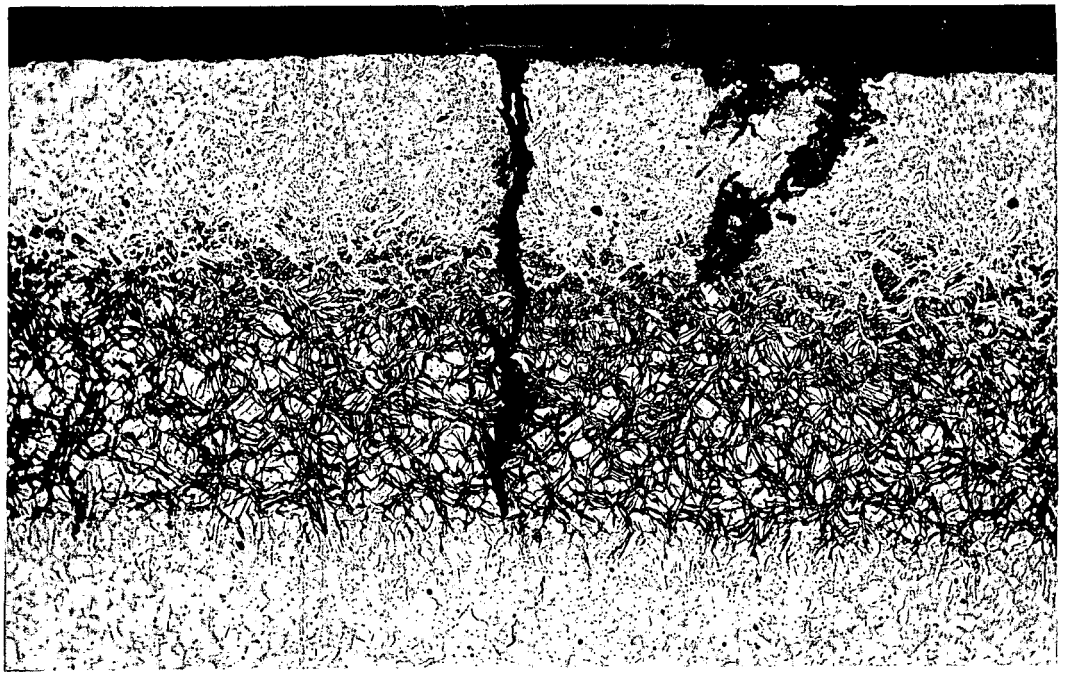

RM-B2632 (250 X)

a. Radial Crack Through Zirconium Hydride Layer on the Outer Surface of the Cladding

RM-B2631 (250 X)

b. Severely Corroded Inner Suface of the Zircaloy Cladding in the Rupture Area

FIGURE 4.19

Cross Sections of Cladding from $MgO-PuO_2$ PRTR Fuel Element

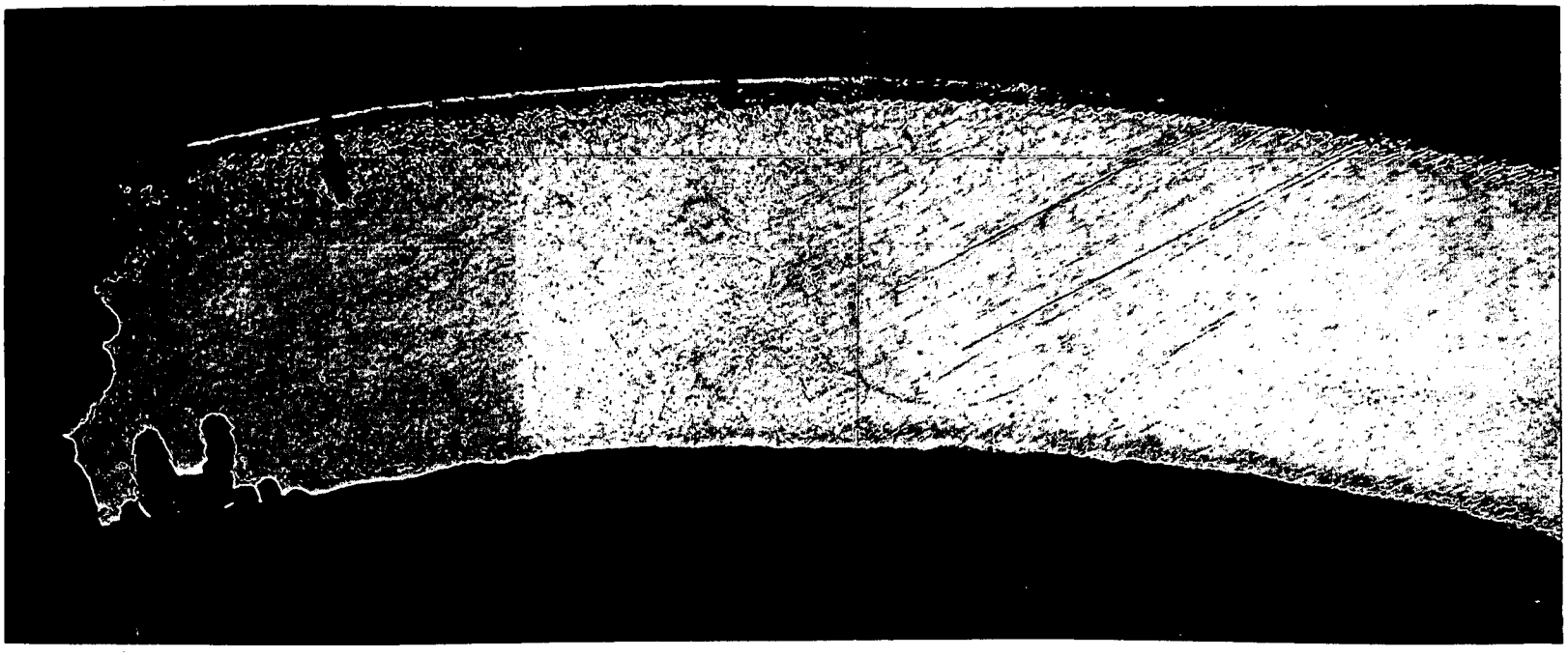

RM-B2433

(75 X)

FIGURE 4.20

Polished Cross Section of Zircaloy Cladding from $MgO-PuO_2$ Fuel Element. Hydride Layer on the Outer Surface is Thickest at the Point of Failure. Radial Cracks Penetrate the Hydride Layer. Severe Local Corrosion is Evident on the Inner Surface.

in the failure region. Although preirradiation autoclave tests of deliberately defected fuel rods containing the same fuel mixture did not cause fuel swelling, later tests showed a strong dependence on defect shape. Swelling occurred with slit defects but not with round holes through the cladding!

The inner surface of the cladding was severely and locally corroded particularly at the point of failure (Figure 4.19b). Corrosion and surface hydriding were observed in other regions of high PuO_2 concentration.

If residual fluoride ions from the etching process remained trapped in internal cladding defects, a tentative failure mechanism could be hypothesized, involving the 0.2 wt% water found in the fused MgO. Reaction between the water, Zircaloy and fluoride ions would produce the observed corrosion and hydride layers, leading to initial, brittle failure. Waterlogging and/or a slow volume increase of the fuel as a result of the hydration of MgO would induce ductile propagation of the original split. Continued irradiation of the element and attendant thermal and pressure cycling would cause washout of the nonsintered fuel until other localized areas of sintered, high PuO_2 concentration were encountered.

Inspection of PRTR Fuel Elements - M. K. Millhollen, W. J. Flaherty and M. D. Freshley

All PRTR fuel elements were ultrasonically decontaminated* in a detergent solution after contamination by $MgO-PuO_2$ fuel that was released into the coolant stream by a fuel element failure.(1) After decontamination, all fuel elements were visually examined before being recharged into the reactor. Three UO_2 elements had broken spacer wires, and bands on one Al-Pu fuel bundle were loose or missing. These four fuel elements were removed from service. Two UO_2 fuel elements were temporarily removed from service. Two UO_2 fuel elements were temporarily removed from service for further inspection when the PRTR Fuel Element Examination Facility (FEEF) is available. Hanger pins of some of the elements had been bent and these were replaced.

---

* By PRTR Operation personnel.

(1) Cadwell, J. J. Fuels Development Operation, Quarterly Progress Report, July, August, September, 1962. HW-74378. October 15, 1962. (SECRET)

Irradiation of Uranium-Plutonium Oxide - W. J. Bailey and T. D. Chikalla

A series of test capsules was irradiated with the objectives of (a) determining the effect of PuO_2 content on the irradiation stability of the fuel, (b) comparing the in-reactor performance of fuel pellets prepared from mixtures of UO_2 and PuO_2 and from mixtures of UO_2 and (U, Pu)O_2 (from calcination of $Pu(OH)_4$ and $(NH_4)_2U_2O_7$ coprecipitated from hot ammonium hydroxide), and (c) investigating the in-reactor sintering of low density (63 – 65% TD) uranium-plutonium oxide pellets. Structure changes and fission gas release appeared more extensive in low density specimens, particularly those containing lower concentrations of plutonium added as mixed crystal oxide. Six pairs, each of high density and low density fuel capsules (Table 4.2), were irradiated in the MTR.

The high density oxide capsules were designed to generate 19 kw/ft with a surface heat flux of 440,000 Btu/(hr)(ft^2). One capsule of each pair was irradiated to approximately 30 x 10^{18} fissions/cm^3 and one to approximately 150 x 10^{18} fissions/cm^3. One exception, a capsule fueled with 2.57 mole % PuO_2, was irradiated to 296 x 10^{18} fissions/cm^3 or 10,000 Mwd/ton of UO_2-PuO_2.

The low density oxide capsules were designed to generate 12 kw/ft with an associated surface heat flux of 275,000 Btu/(hr)(ft^2). The capsule pairs were irradiated to the same exposure levels as the high density ones.

Burnup analyses of the irradiated fuel are being performed by mass spectrometry. These analyses will allow computation of capsule rod power for comparison with values estimated from flux-monitoring wire data.

Figure 4.21 shows the fuel structure developed in a low density, 0.0259 mole % PuO_2 specimen. Both capsules in this set exhibit long, narrow columnar grains and central voids. After irradiation the lower exposure specimen was about 0.030 inch smaller in diameter than the cladding ID. The external appearance and longitudinal sections were similar for both capsules.

TABLE 4.1

UO_2-PuO_2 CAPSULE IRRADIATION TESTS

Capsule Data

UO_2-PuO_2 Pellets	1/2 inch diameter
Diametral Gap	0.001 – 0.003 inch
Cladding	Zircaloy-2, 0.031 inch thick
Atmosphere	Helium
Size	9/16 inch OD x 2-1/2 inch long

High Density Pellet Capsules (6 pairs)

Identity Number	GEH-14-19, -20, -85 through -91
PuO_2 Content	0.0259 to 5.67 mole %
PuO_2 Type*	4 MCO, 8 MM
Sintering Conditions	1600 C in H_2, to 11 hours
Density	90 – 93% TD

Low Density Pellet Capsules (6 pairs)

Identity Number	GEH-14-21, -22, -65 through -74
PuO_2 Content	0.0259 to 7.45 mole %
PuO_2 Type*	2 MCO, 10 MM
Heating Conditions	1000 C in H_2
Density	63 – 65% TD

* MCO – mixed crystal oxide, UO_2/PuO_2 = 5/1
MM – mechanical mixture UO_2(natural) and PuO_2

A low density oxide specimen with 0.187 mole % PuO_2 (Figure 4.22) shows evidence of central melting. Note the small columnar grains, the large high density columnar grains, the rough inner surface, and the porous spongy mass in the central region.

The higher exposure companion to the preceding capsule is shown in Figure 4.23. Note the relatively uniform coloration of the capsule exterior. The longitudinal sections reveal a hard oxidation-resistant sphere (0.1 inch in diameter), an unusual microstructure, a tear-drop shaped central void, and a marked core-cap reaction zone. Knoop hardness measurements (500 gram load) of the various regions are: the fuel, 723; the sphere, 543; the fuel-cap interaction zone, 198; and the Zircaloy-2 cap, 225. The sphere is believed to be a compound, rather than an alloy, of uranium,

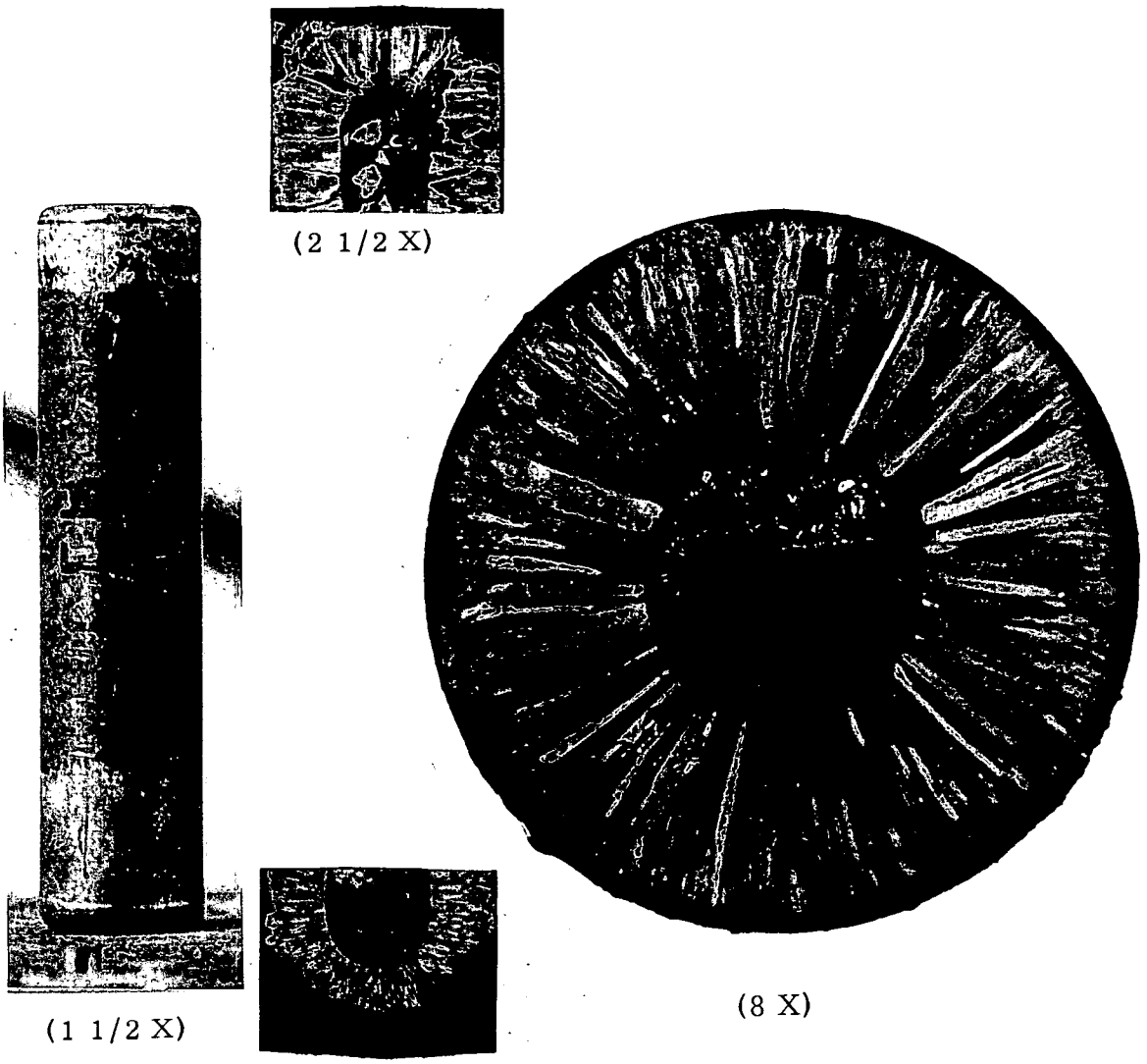

062 2107-4

FIGURE 4.21

Irradiated UO_2-0.0259 mole % PuO_2 (GEH-14-22). Specimen Impregnated with Plastic to Retain Fuel in Position During Examination. Capsule Data: Initial Fuel Density, 65% TD; Exposure, 72 x 10^{18} fissions/cc.

AEC-GE RICHLAND, WASH.

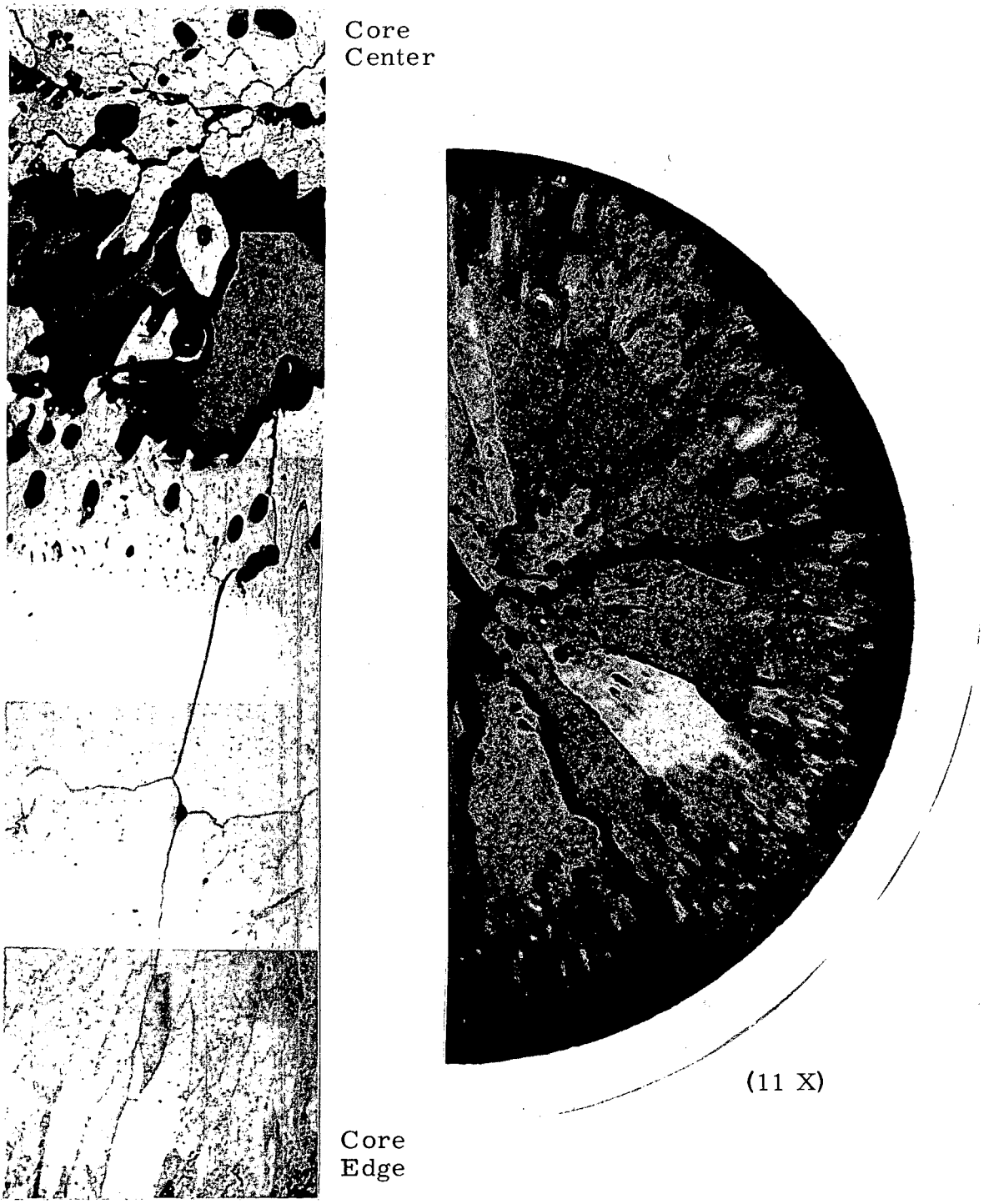

062 2107-12

FIGURE 4.22

Irradiated UO_2-0.187 mole % PuO_2 (GEH-14-65)
Capsule Data: Initial Density–65% TD; Exposure, 36 x 10^{18} fissions/cc

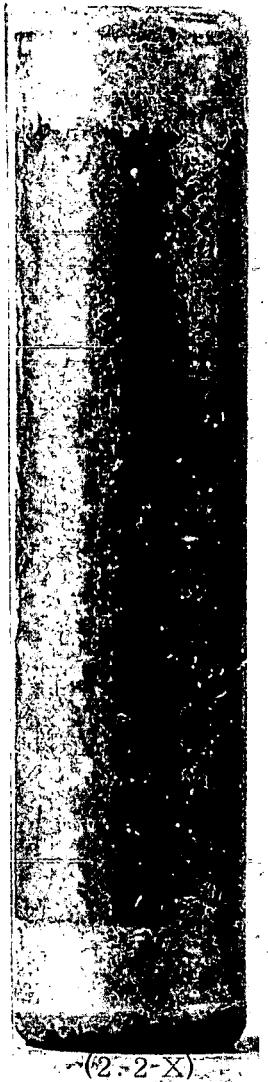

(2-2-X)

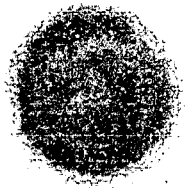

(1.7 X)

Autoradiograph of

(4 X)

(3 X)

Autoradiograph of

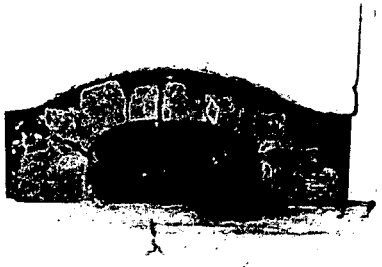

(3.4 X)

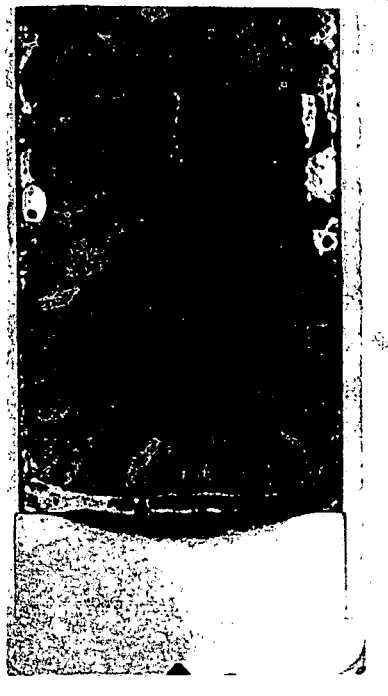

FIGURE 4.23

Irradiated UO_2-0.187 mole % PuO_2 (GEH-14-66)
Note 0.1-inch Diameter Sphere
Capsule Data: Initial Density, 65% TD;
Exposure, 79 x 10^{18} fissions/cc

062 2107-5

plutonium, and/or zirconium plus fission products. Autoradiographs show the sphere to be significantly more radioactive than the surrounding fuel. X-ray diffraction studies yielded no conclusive results. The sphere is being chemically analyzed.

Figure 4.24 shows the characteristic appearance of most of the irradiated low density oxide specimens. Slight sintering has occurred. The grain size was not markedly changed and relatively few cracks developed.

Equiaxed grains are present in the central region of the fuel in the capsule of Figure 4.25 and in its companion capsule. The high density fuel contains 0.0259 mole % PuO_2 added as mixed crystal material. Note the increase in grain size from edge to center and the relatively uniform fission product distribution shown by the autoradiograph.

Columnar grains were formed in the high density oxide sample (Figure 4.26) containing 0.0259 mole % PuO_2. In contrast to the preceding capsule, the fuel in this specimen was prepared by sintering mechanical mixtures of UO_2 and PuO_2. Note the fission product distribution revealed by the autoradiograph.

The high density 2.57 mole % PuO_2 specimen shown in Figure 4.27 was irradiated to a maximum of 296×10^{18} fissions/cm^3 or 10,000 Mwd/ton of UO_2-PuO_2. From reactor data, the average exposure was estimated to be 9100 Mwd/ton UO_2-PuO_2. Very long, narrow columnar grains and a central void were formed. Note the nonuniform fission product distribution shown in the autoradiograph. The microstructure near the cladding exhibits evidence of nonuniform PuO_2 distribution, and enhanced porosity in the large-grain boundary material. The photomicrograph of the columnar grain region shows the accumulation of voids along the grain and sub-grain boundaries. Thirty percent of the krypton and 31% of the xenon were released.

The fuel shown in Figure 4.28 is the only specimen thus far examined that exhibits equiaxed grains at the core center surrounded, in turn, by large and small columnar grains. The high density fuel contains 4.13 mole % PuO_2. Note the markedly nonuniform fission product distribution revealed

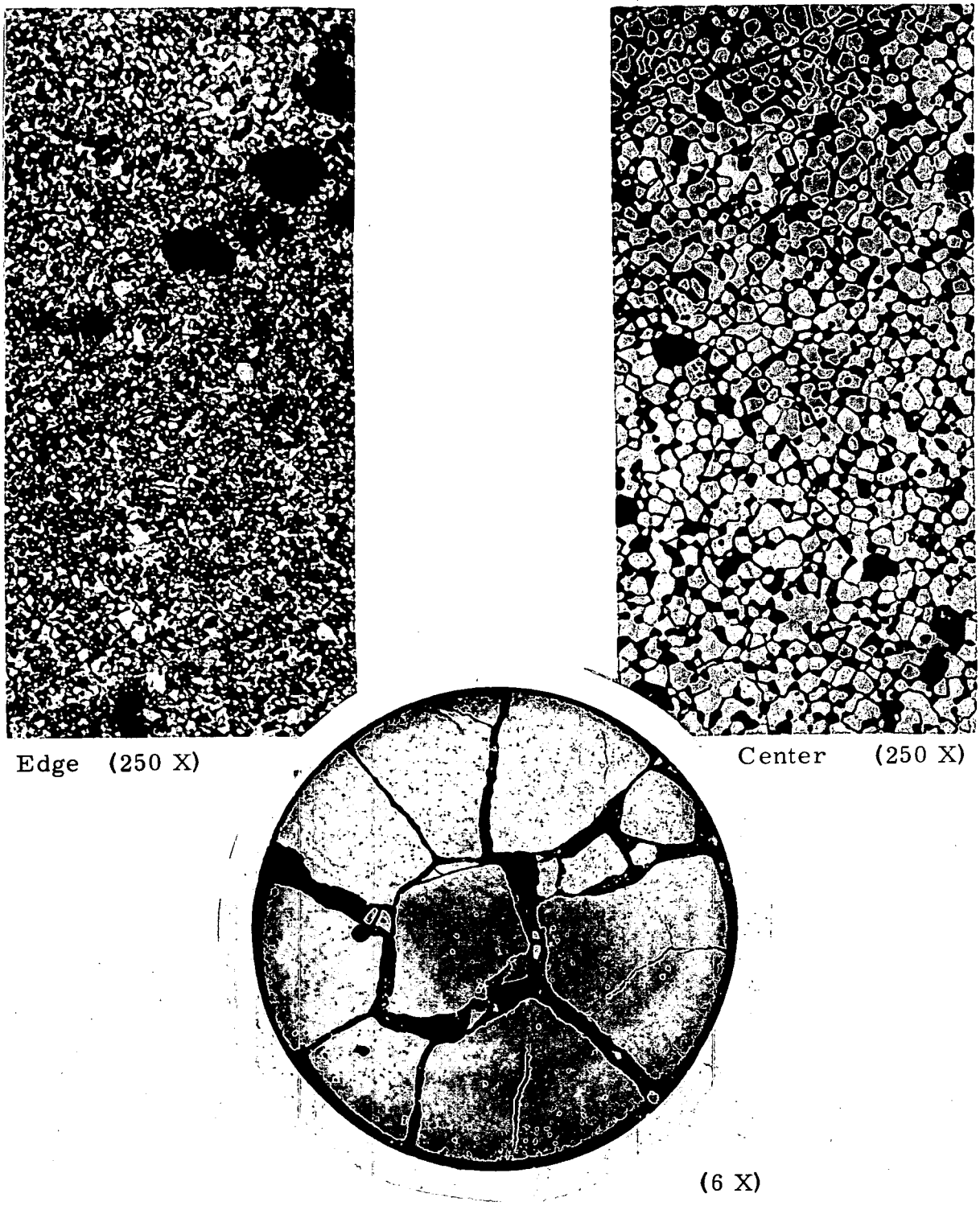

FIGURE 4.24

Irradiated UO_2-1.46 mole % PuO_2 (GEH-14-68)
Capsule Data: Initial Density, 65% TD; Exposure, 110 x 10^{18} fissions/cc
062 2107-9
AEC-GE RICHLAND, WASH.

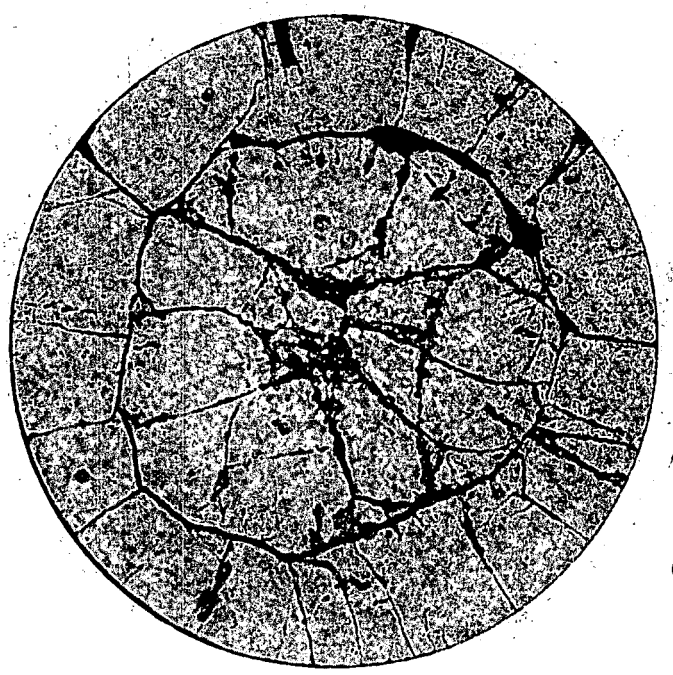

(7 X)

Edge (250 X)

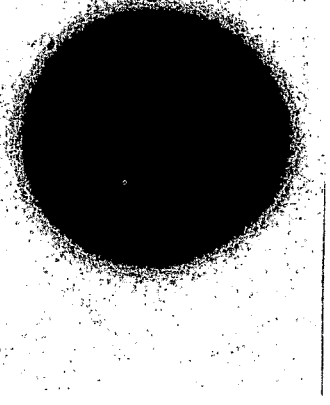

Autoradiograph (3 X)

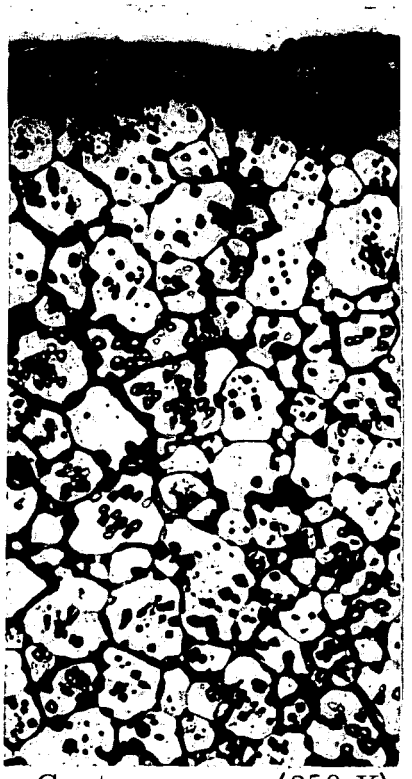

Center (250 X)

FIGURE 4.25

Irradiated UO_2-0.0259 mole % PuO_2 (GEH-14-20)
Capsule Data: Initial Density, 90% TD; Exposure, 84 x 10^{18} fissions/cc
0622107-6

AEC-GE RICHLAND, WASH.

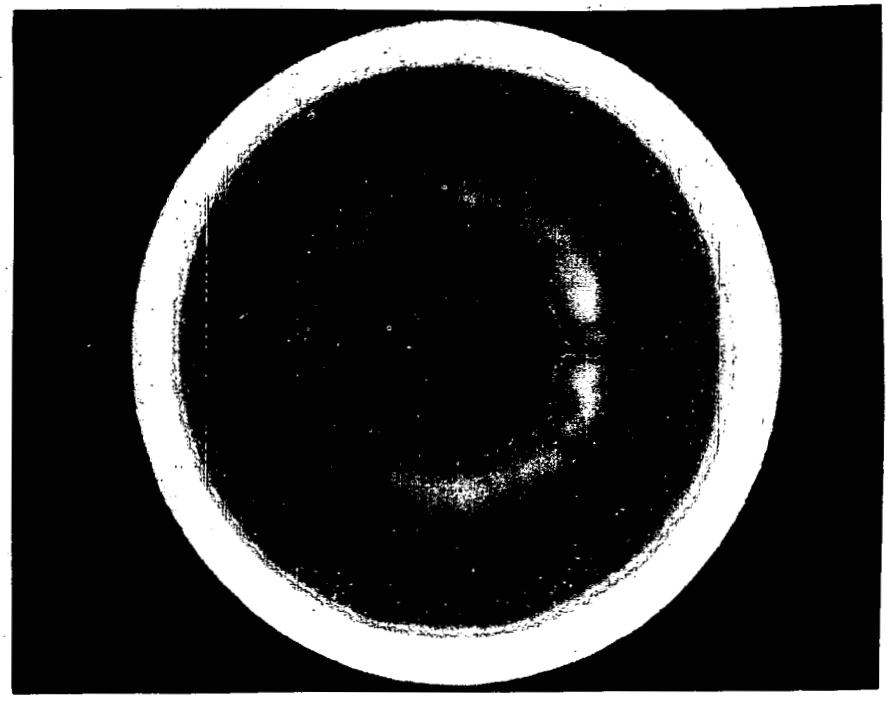

(6 X)

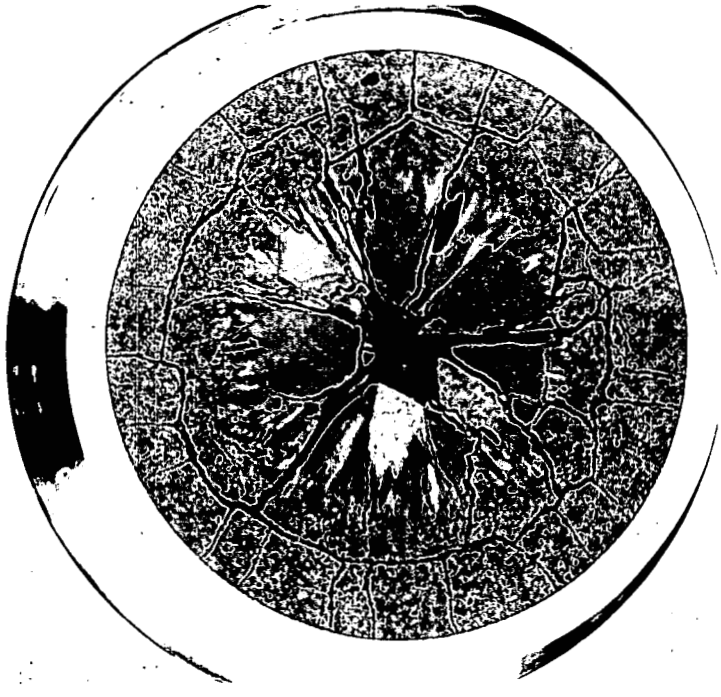

(6 X)

FIGURE 4.26

Irradiated UO_2-0.0259 mole % PuO_2 (GEH-14-91)
Capsule Data: Initial Density, 90% TD; Exposure, 104 x 10^{18} fissions/cc
062 2107-10

AEC-GE RICHLAND, WASH.

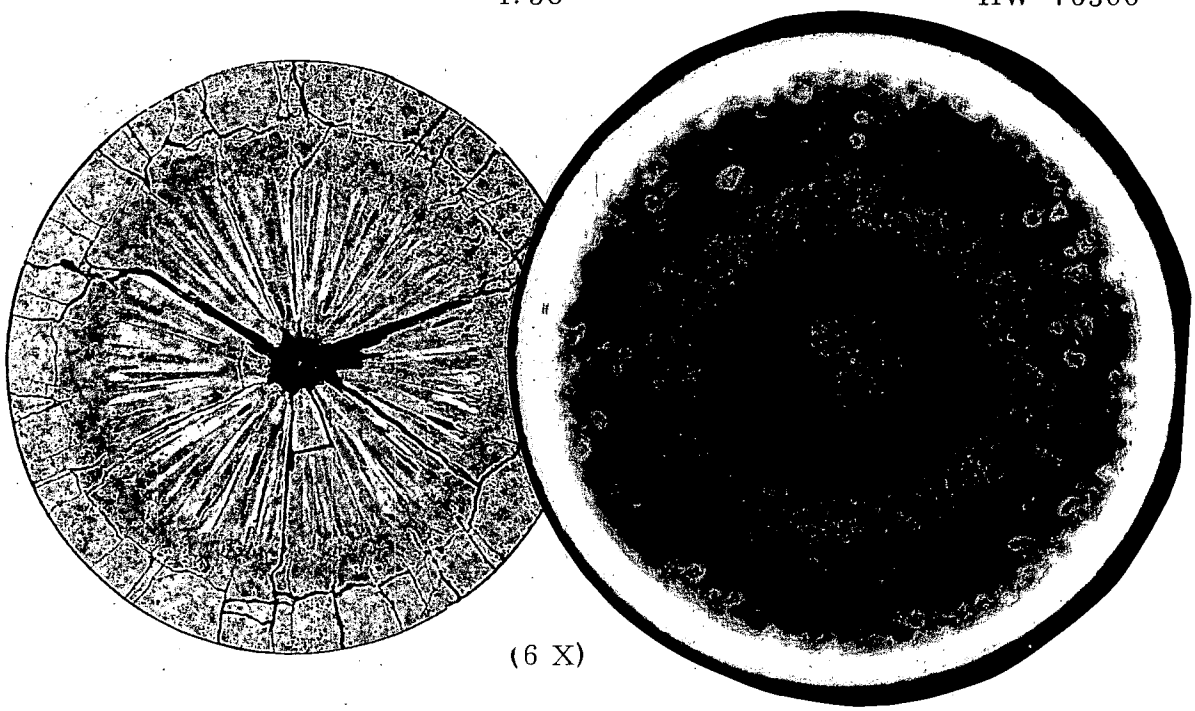

(6 X)

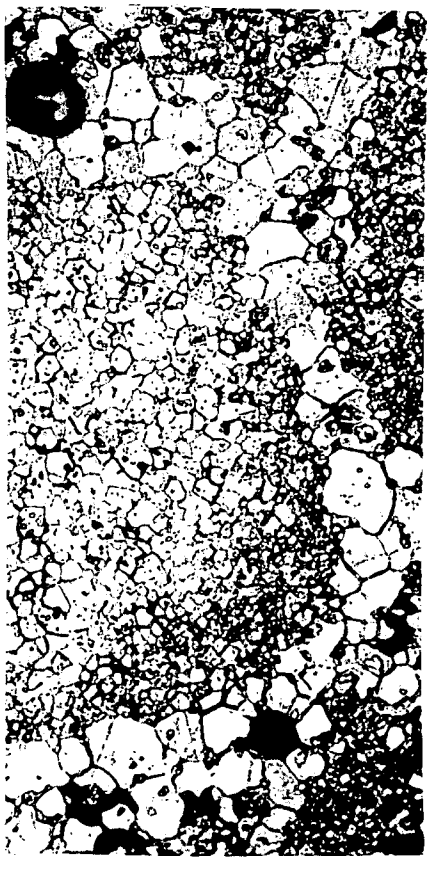

FIGURE 4.27

Irradiated UO_2-2.57 mole % PuO_2 (GEH-14-85)
Capsule Data: Initial Density, 91% TD; Exposure, 296 x 10^{18} fissions/cc

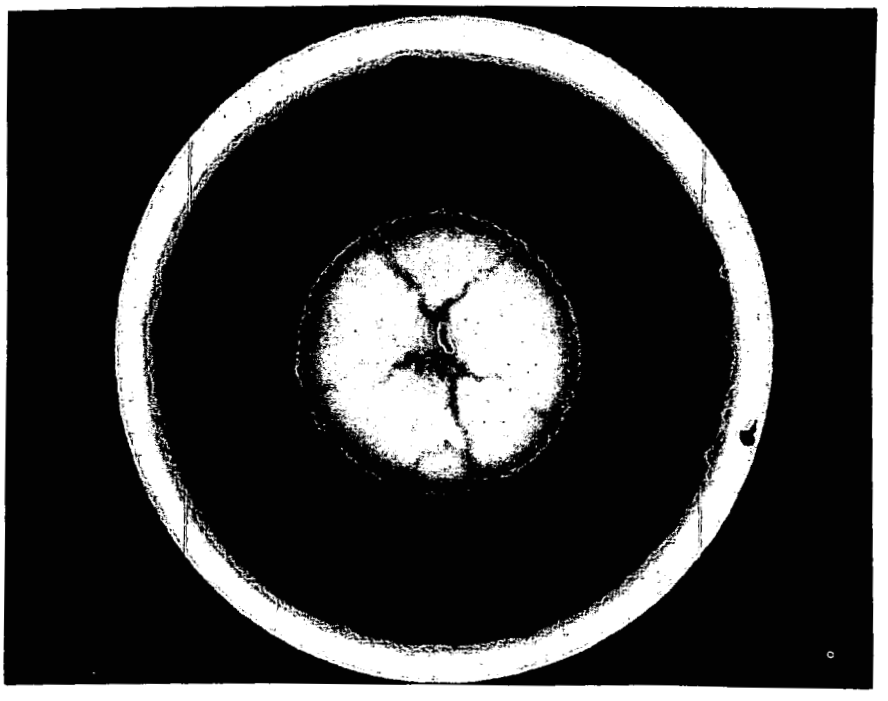

(6 X)

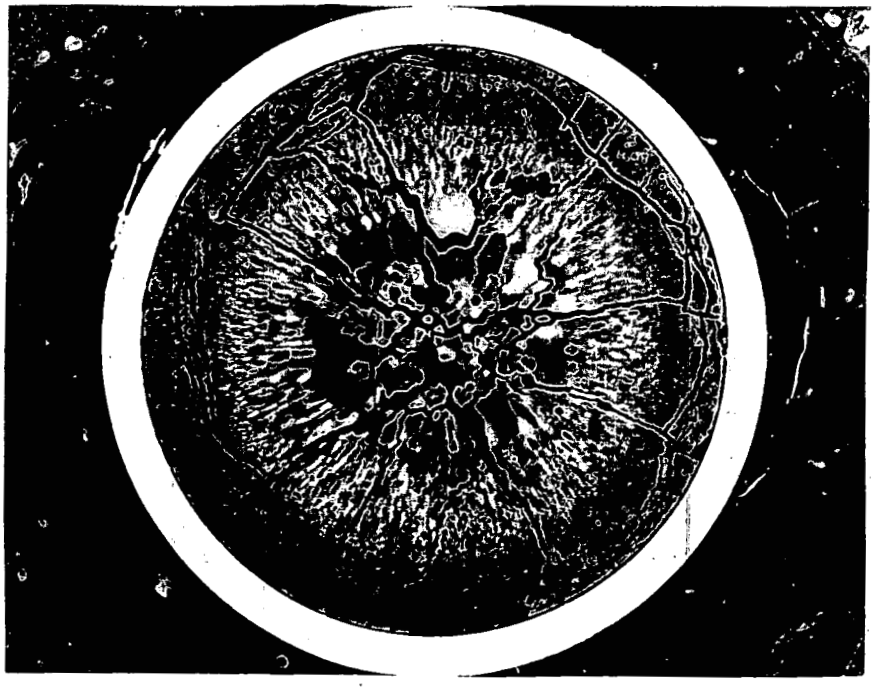

(6 X)

FIGURE 4.28

Irradiated UO_2-4.13 mole % PuO_2 (GEH-14-86)
Capsule Data: Initial Density, 91% TD; Exposure, 166 x 10^{18} fissions/cc

062 2107-11
AEC-GE RICHLAND, WASH.

by the autoradiograph. A probable cause of the unusual grain formation is the excessive heat generation rate that occurred when the capsule was inadvertently exposed to double the requested neutron flux during its last cycle of irradiation.

One capsule in the series of 24 failed during an inadvertent exposure to thermal neutron flux 11 times greater than specified. The capsule was irradiated six days, generating an initial surface heat flux of 4,000,000 Btu/(hr)(ft^2). Increased coolant activity, noted on the second day, continued to rise until the capsule was discharged. None of the high density, 5.67 mole % PuO_2 fuel remained in the capsule after discharge. An extensive core-cap reaction had occurred. Hydriding and gross cracking of the cladding at the rupture site were observed.

Hardness measurements on several specimens allowed the estimation of the postirradiation density (see Table 4.3). Marked density increases occurred in the low density fuel during irradiation.

As anticipated, gross radial cracking and some circumferential cracking were encountered. However, low exposure specimens, regardless of density, exhibited a lesser tendency for cracking at higher plutonium contents.

Central cavity formation was observed in seven specimens, the majority of which had the lower plutonium concentrations. In the case of low density, mechanically mixed oxide specimens, it was found that the extent of in-reactor sintering and density increase were generally less at the higher PuO_2 concentrations. A similar density change trend has been observed in out-of-reactor sintering studies with UO_2-PuO_2 mechanical mixtures. The most significant structure changes in low density specimens occurred when the PuO_2 concentration was less than 0.2 mole percent.

Metallic inclusions were noted in the microstructures of nearly all specimens which had formed central voids.

From the autoradiographs it was observed that gross segregation of the fission products occurred only in specimens exhibiting columnar grains.

TABLE 4.3

MICROHARDNESS AND DENSITY DATA FOR IRRADIATED UO_2-PuO_2

Capsule No. (GEH-14-)	UO_2-PuO_2 (mole % PuO_2)	Average Exposure* (fissions $cm^{-3} \times 10^{-18}$)	Approximate Hardness** (KHN, 500 gram)		Density, (% TD)		
			Center	Average	Measured Pre	Estimated from Hardness Pre	Estimated from Hardness Post
20	0.0259	84	477	437	90		89-92
91	0.0259	104	595	536	90		92-96
82	1.02	160	627	570	93		96-98
88	5.67	16	618	638	91	93-94	94-97
22	0.0259	72		681	65		98-100
66	0.187	79		723	65		98-100
68	1.46	110		503	65		91-93
69	3.47	116		443	64		88-90
71	5.46	104		420	63		87-89
73	7.45	113		500	63		91-93
66	sphere			543			
	core-cap interface			198			
	Zircaloy-2 cap			225			

* From flux-monitoring wire data

** Center, average of three values; Average, average of 13 to 19 values

External dimensional changes on the capsules were negligible except for four high density oxide capsules. Three with central voids had maximum cladding diameter increases of 0.008 – 0.014 inches (1.4 to 2.4%). The ruptured capsule showed a fairly uniform 9 – 10% increase in diameter.

Excellent X-ray diffraction patterns of the low exposure fuel showed well defined peak broadening and strong evidence of preferred orientation. Weak patterns were obtained from the high exposure specimens. On one low density oxide capsule with 5.46 mole % PuO_2 and an exposure of 104 x 10^{18} fissions/cm^3, a lattice constant of $a_o = 5.476 \pm 0.001$ A was obtained. The theoretical value for this composition is 5.464 A, so irradiation damage is evident.

Nonuniform plutonium distribution was noted in both high and low density UO_2-PuO_2 specimens not exhibiting marked grain growth. It is believed that there are numerous small alternately UO_2-rich and PuO_2-rich regions. Greater porosity is observed in one type of region, believed to be PuO_2-rich because the majority of the fissions occur in the plutonium atoms in specimens containing more than one mole % PuO_2.

High density pellets prepared from mixed crystal (U, Pu)O_2 and from UO_2-PuO_2 mechanical mixtures performed comparably. However, the samples made from mixed crystal oxide tend to show more grain growth and higher fission gas release. Of the high exposure specimens, the mixed crystal oxide pellets released 12% of the Kr and 14% of the Xe while the pellets made from mechanically mixed oxides released 2% of the Kr and 4% of the Xe. PuO_2 concentration in these pellets was 0.0259 mole percent.

Assuming exposure and gas release data are correct, the fission gas volume released per gram of low density UO_2-PuO_2 tends to decrease, for comparable exposures, with increasing plutonium concentration. New data from high density UO_2-PuO_2 specimens show the above trend to be very slight or nonexistent.

From this series of irradiation tests (assuming comparable exposures) the following conclusions were drawn:

(1) The PuO_2 concentration has a marked effect on the irradiation behavior of low density fuel. The more drastic microstructural changes and higher fission gas releases occurred when the PuO_2 content was very low. The PuO_2 concentration in high density UO_2-PuO_2 has relatively little effect on structure change and fission gas release.

(2) High density pellets prepared with additions of mixed crystal fuel material revealed more grain growth and higher fission gas release than pellets made from mechanically mixed UO_2 and PuO_2. Low density fuel, attractive because of the ease of fabrication, sintered to high density in the reactor and revealed relatively high fission gas release values for the exposures studied. (The release rate may decrease at high exposures because of the sintering which occurred during earlier stages of the irradiation.)

(3) Low density fuel capsules operated satisfactorily to 5000 Mwd/ton of UO_2-PuO_2, although gross fuel structure changes occurred in some of them. A more complete understanding of the irradiation behavior is desirable before initiating large scale application of the low density fuels to full-size reactor elements. Nonuniform distribution of plutonium which can exist in both low and high density UO_2-PuO_2 is significantly reduced during irradiation only in regions where marked grain growth occurs. Gross fission product migration occurs in areas of columnar grain growth.

(4) Irradiation of fueled capsules indicates that UO_2-PuO_2 will perform adequately to at least 5000 Mwd/ton of UO_2-PuO_2. One capsule performed satisfactorily to 10,000 Mwd/ton UO_2-PuO_2.

Short Duration Irradiations of UO_2 and UO_2-PuO_2 - W. J. Bailey and T. D. Chikalla

Four specimens, each containing high density pellets of UO_2-0.154 mole % PuO_2 and of UO_2 (1.00 mole % U^{235}), were irradiated in the VH-4 Hydraulic Rabbit Facility of the MTR. The objective of the experiment was to obtain a better understanding of the phenomenon of in-reactor sintering and of the effect of increased Pu content on the stability of UO_2 during irradiation. During in-reactor sintering, fuel material properties that change and affect fuel performance include fission gas release rates, thermal conductivity, and solid solution formation.

The capsules were in the active zone of the Hydraulic Rabbit Facility (VH-4) for various times.

Capsule Number	In-Reactor Time (min)	Irradiation Date	Radioactivity (β and γ)
GEH-21-13	3	10/7/62	10/18/62, 35 mrad/hr at 3 ft in air
GEH-21-14	5	10/29/62	12/19/62, 900 mrad/hr at surface in air*
GEH-21-15	15	11/19/62	12/19/62, 9 rad/hr at surface in air
GEH-21-16	60	12/10/62	

* Approximately this same radioactivity was observed on same date from GEH-21-13.

Attempts to obtain autoradiographs on glass of the first three capsules were unsuccessful. Using high-resolution film, a faint autoradiograph was obtained from Capsule GEH-21-15 with a 27-hour exposure. A 25-hour exposure with film produced no image of either Capsule GEH-21-13 or GEH-21-14.

The cobalt and Al-Co alloy flux-monitoring wires on GEH-21-16 are being measured at the MTR. Postirradiation destructive examination of the fuel will begin early in 1963.

Fission Fragment Migration in UO_2 - J. L. Bates, J. A. Christensen and W. E. Roake

Drilled samples taken along the diameter of an irradiated UO_2 fuel core confirmed earlier measurements of gross fission fragment relocation during irradiation.[1, 2, 3] Samples were obtained with vibrating tungsten carbide tools at radial intervals of 0.090 inch. Previously, samples were obtained by scribing the polished surface of a fuel element cross-section and retrieving the resulting powder on strips of adhesive which were subsequently sectioned into small pieces, each representing a portion of the fuel radius. Drilling is more time consuming than scratch sampling but provides larger samples of unquestionable origin.

Results of both drilling and scratch sampling techniques applied to the same cross-section are shown in Figure 4.29. Both sets of results have the same significant features, in particular, the gross depletion of fission products in the high density columnar grain region. The scratch samples indicated a possible Pu redistribution; however, this is not supported by results from the drilled samples, which are considered more accurate. The differences in isotopic concentration in the two sets of samples reflects the longer decay time (approximately one year later) applied to the drilled samples. The autoradiograph is included in Figure 4.29 to illustrate the gross concentration distribution of δ- and β-active fission fragments across the fuel diameter.

In-Reactor Testing Devices - W. J. Bailey and S. H. Woodcock

Three novel in-reactor testing devices are being designed and evaluated. These are shown in Figures 4.30, 4.31 and 4.32.

---

(1) Cadwell, J. J. Fuels Development Operation Quarterly Progress Report, July, August, September, 1962. HW-74378, October, 1962. (SECRET)

(2) Cadwell, J. J. Fuels Development Operation Quarterly Progress Report, January, February, March, 1962. HW-72347, April, 1962. (SECRET)

(3) Bates, J. L., Christensen, J. A., Roake, W. E. "Fission Products and Plutonium Migrate in Uranium Dioxide Fuel," Nucleonics 24, No. 3: 88-90.

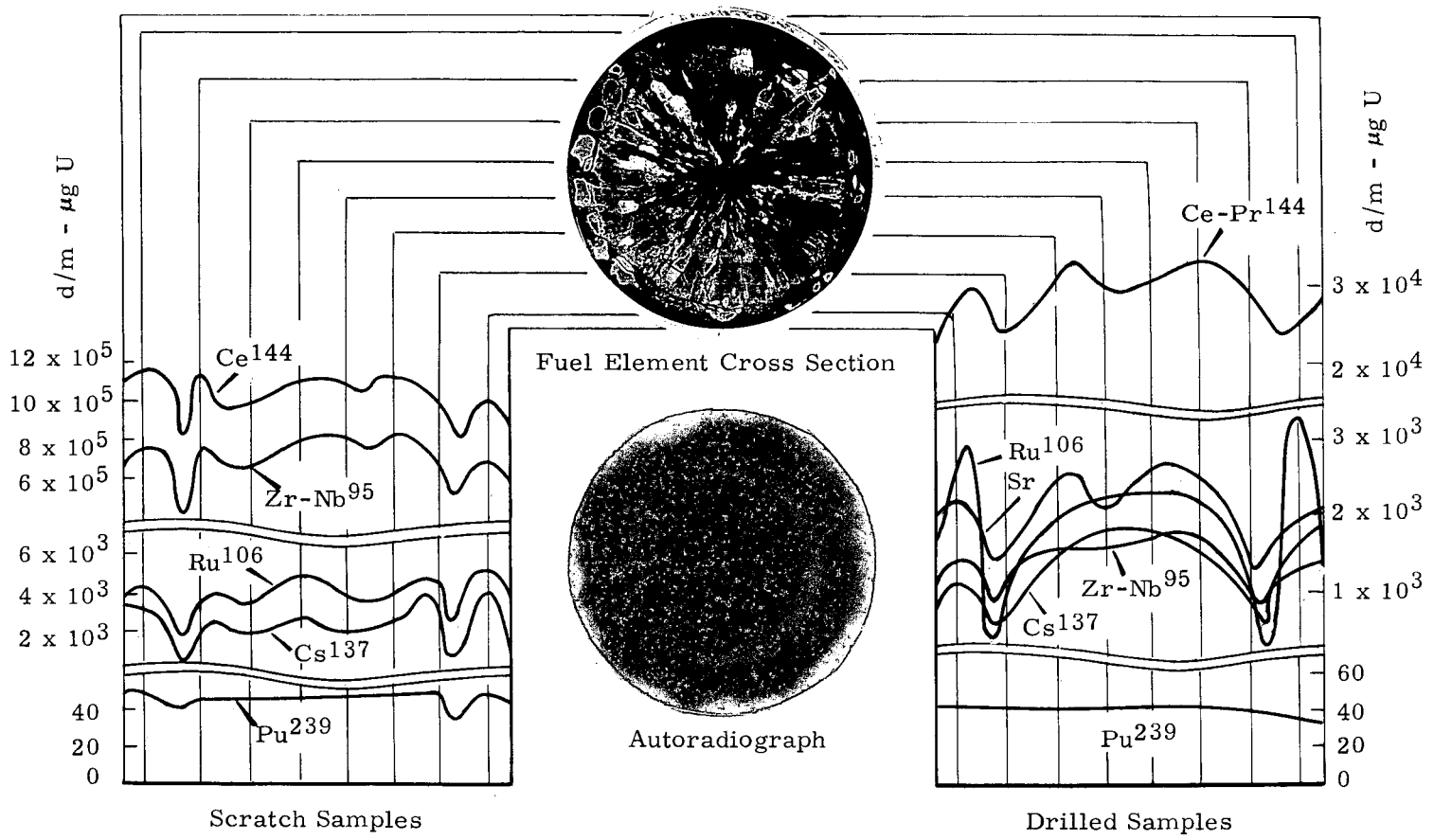

FIGURE 4.29

Fission Fragment Distribution in Irradiated UO_2;
Comparison of Scratch Sampling with Drill Sampling

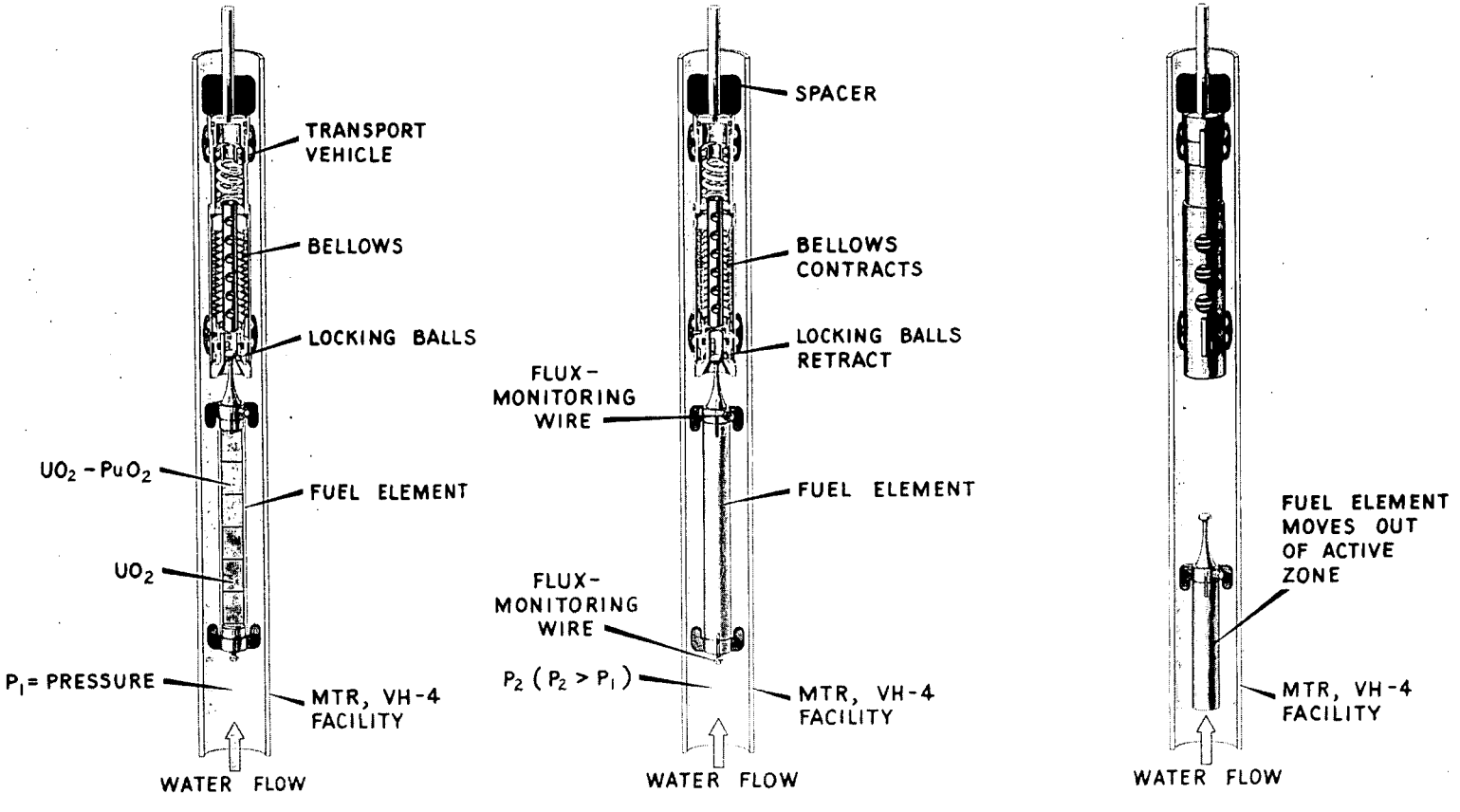

FIGURE 4.30

Proposed Equipment to Operate Fuel Elements at High Specific Power and Discharge Them During Reactor Operation Without Reducing Coolant Flow ("Icarus" Experiment)

29170-1

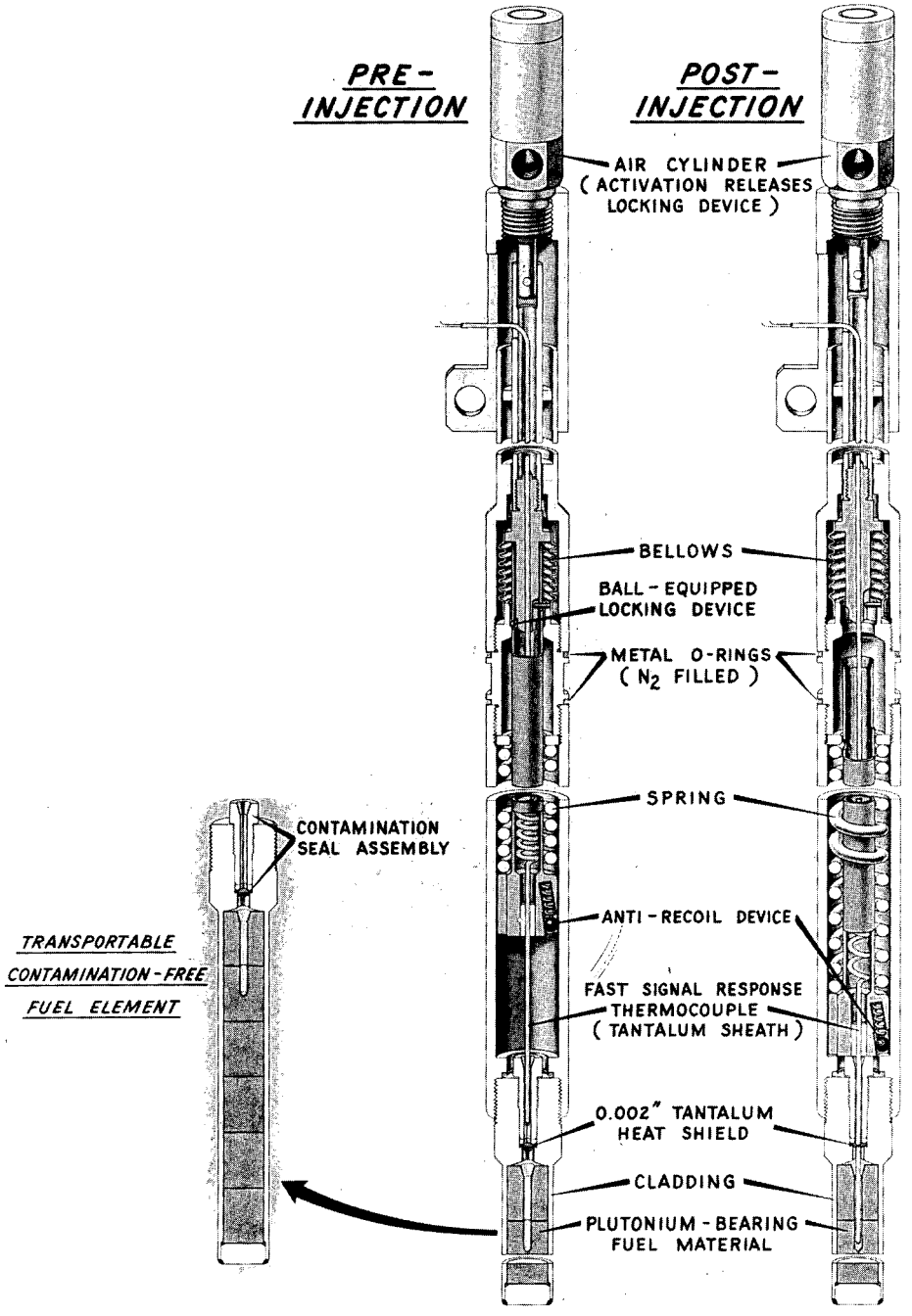

FIGURE 4.31

Proposed Equipment for Measurement of High Temperatures in an Operating Fuel Element ("Helios" Experiment)

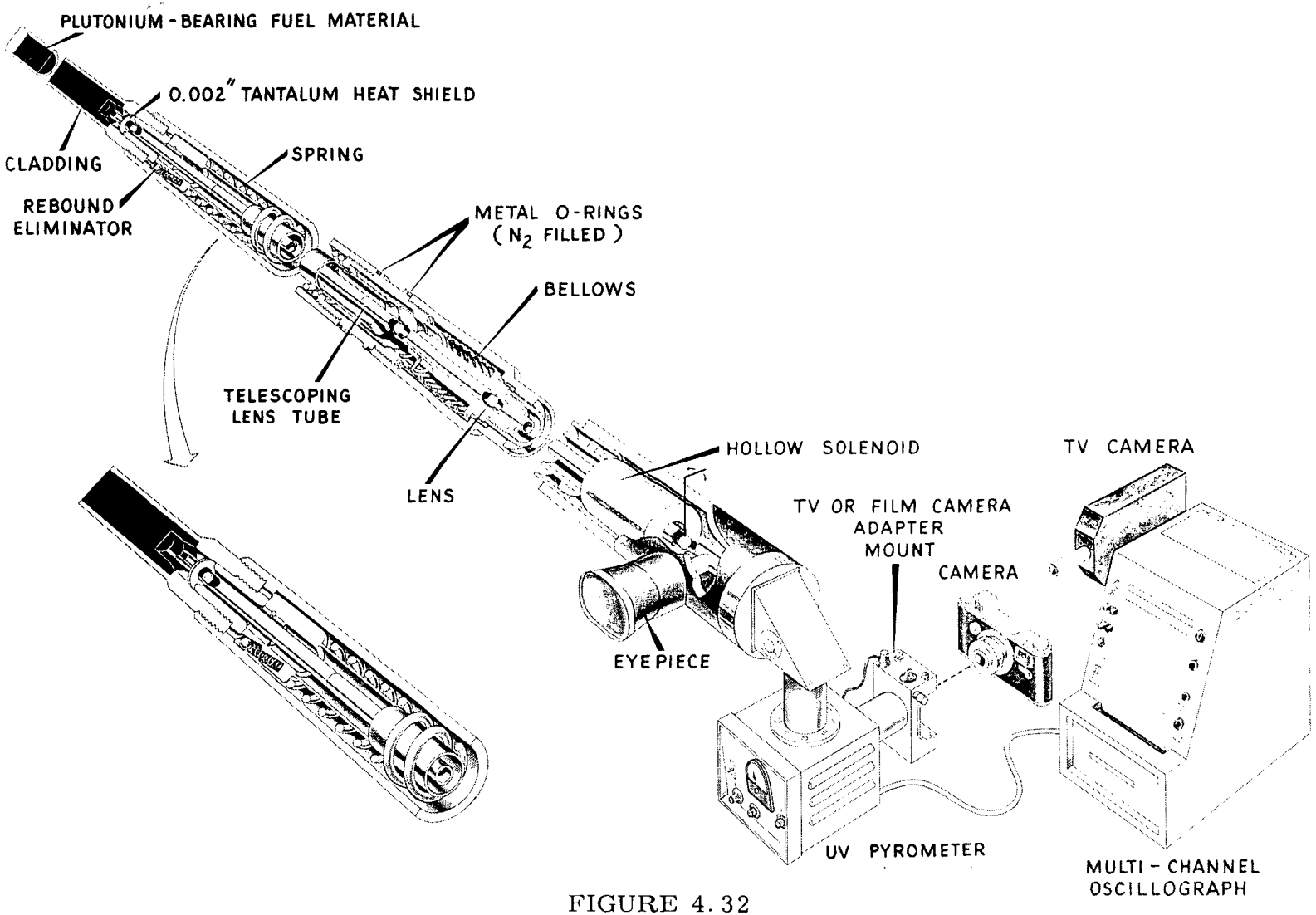

FIGURE 4.32

Proposed Equipment for Visual Observation and Recording of High Temperature Fuel Region of an Operating Fuel Element ("Argus" Experiment)

0630196